

Biodegradation of Organophosphates: Studies on horizontal gene transfer (HGT) of organophosphate degrading (*opd*) gene cluster and functional analysis of *mfhA* found in plasmid-borne integrative mobilizable element (IME) of *Sphingobium fuliginis* ATCC 27551



**Thesis submitted for the Award of
Doctor of Philosophy
In
Animal Sciences**

**By
Deviprasanna Chakka**

**Supervisor
Prof. Dayananda Siddavattam**

**Dept. of Animal Sciences
School of Life Sciences
University of Hyderabad
Hyderabad – 500046, India**

July, 2013

Enrolment No. 05LAPH12



UNIVERSITY OF HYDERABAD

(Central University established in 1974 by an act of Parliament)

Hyderabad-500046, INDIA

DECLARATION

I hereby declare that the work embodied in this thesis entitled "**Biodegradation of Organophosphates: Studies on horizontal gene transfer (HGT) of organophosphate degrading (*opd*) gene cluster and functional analysis of *mfhA* found in plasmid borne integrative mobilizable element (IME) of *Sphingobium fuliginis* ATCC 27551**" has been carried out by me under the supervision of Prof. S. Dayananda and this has not been submitted for any degree or diploma of any other university earlier.

Date:

Deviprasanna Chakka
(Research scholar)

Prof. Dayananda Siddavattam
(Research Supervisor)



UNIVERSITY OF HYDERABAD

(Central University established in 1974 by an act of Parliament)

Hyderabad-500046, INDIA

CERTIFICATE

This is to certify that **Mrs. Deviprasanna Chakka** has carried out the research work embodied in the present thesis under my supervision and guidance for a full period prescribed under the Ph.D. ordinance of this University. We recommend her thesis entitled "**Biodegradation of Organophosphates: Studies on horizontal gene transfer (HGT) of organophosphate degrading (*opd*) gene cluster and functional analysis of *mfhA* found in plasmid borne integrative mobilizable element (IME) of *Sphingobium fuliginis* ATCC 27551**" for submission for the degree of Doctor of Philosophy in Life Sciences of this University.

Head
Department of Animal Sciences

Research Supervisor
Prof. Dayananda Siddavattam

Dean
School of Life Sciences

Dedicated

to



my parents

Sri Anjaneyulu Chakka

Smt Niranjani Chakka

Acknowledgements

At the outset I would like to thank **Almighty** for giving me all the strength and health to complete this endeavour without whose blessings this success cannot be achieved.

I would like to acknowledge my sincere thanks and heartfelt gratitude to my supervisor **Prof. Dayananda Siddavattam** for his guidance, constant encouragement, patience and support throughout the course of my study.

I thank Dean **Prof. R. P. Sharma** and the former Deans **Prof. M. Ramanadham** and **Prof. A. S. Raghavendra** of School of Life Sciences for providing the school facilities.

My thanks to the Head, Department of Animal Sciences, **Prof. Senthil kumaran** and former Heads **Prof. Manjula Sritharan**, **Prof. S. Dayananda** and **Prof. Aparna Dutta Gupta** for allowing me to use the Department facilities.

I would like to thank my Doctoral Committee members **Prof. Aparna Dutta Gupta** and **Prof. Pallu Reddanna** for their valuable suggestions during the course of my study.

I thank **ICMR, NewDelhi** for giving me financial assistance as JRF and SRF during my Doctoral studies.

I thank **DST, DRDO, CSIR, UGC, DBT** and **Biological E. ltd, Hyderabad** for funding our laboratory and funding by **DST-FIST, UGC-CAS, DBT-CREEB** etc. to the School of Life Sciences is also highly acknowledged.

I would like to thank **Dr. Manjula Reddy, CCMB** for providing me E. coli K-12 mutant cultures.

I would like to thank **Prof. Utpal Nath, IISc** Bengaluru for helping me during microarray and qPCR experiments, and Mr. Mainak, Mr. Prem, and specially Mr. Shyam to make my stay in the IISc campus memorable.

I would like to thank **Dr. Sailu Yellaboina** and **Dr. P. Manimaran, CR Rao AIMSCS, Hyderabad** for helping me in microarray data analysis.

I also thank **Dr. K. Arun Kumar** for his suggestions and allowing me to use his lab facilities and **Mr. Surendra Kumar** and **Mr. Maruthi** for their help in Real time PCR experiments.

I would like to thank all the **faculty members** of School of Life Sciences for their help whenever needed.

I also thank my former colleagues **Dr. Suresh Pakala, Dr. Khazamohiddin, Dr. Pandey, Dr. Gopi krishna, Dr. Elisharaj, Dr. Purushotham, Dr. Aleem Basha, Dr. Vijay Paul, Dr. Toshisangba, Mr. Santhosh** and **Mr. Koteswar rao** for their help during my work.

I thank my current lab mates **Dr. Sujana, Mr. Venkateswar Reddy, Mrs. Swetha, Mr. Sunil, Mr. Ashok kumar, Mr. Udaykiran, Mr. Ram murthy, Mr. Akbar Pasha, Ms. Harshita, Ms. Aparna, Mr. Rajendra prasad** (Lab assistant) **Mr. Krishna** (Lab Attendant) and **Mr. Manohar** (Lab Attendant) for their help and constant support during my work.

I would also like to thank all the friends from **School of Life Sciences** for helping me whenever needed and all the friends from **University of Hyderabad** for all the memorable time I had.

Help of all the **non-teaching staff** is greatly acknowledged.

I am grateful for my parents **Sri. Anjaneyulu Chakka, Smt. Niranjani Chakka** and my sister **Mrs. Ramadevi Sangadi** for their love, help, caring, affection and inspiring me to carry out my studies.

My special thanks to my father-in-law **Mr. Simon Kamatham** for his support and patience, during my doctoral study.

Constant support from my husband **Dr. Samuel Kamatham** and our little son **Yasrith Niranjani Simon** is greatly acknowledged.

- **Deviprasanna Chakka**

Contents

Contents	i-x
1. Introduction	1-18
1.1 Horizontal gene transfer	3
1.2 Role of HGT in bacterial evolution.....	4
1.2.1 Phylogenetic approach.....	7
1.2.2 Parametric approach	7
1.3 HGT in xenobiotic compound degradation	9
1.3.1 Class I transposon	11
1.3.2 Class II transposon.....	11
1.3.3 Mobile genetic elements other than class I and II transposons	12
1.4 HGT of OP degradation genes	13
1.4.1 Organophosphate hydrolases (OPHs).....	13
1.4.2 Methyl parathion hydrolases (MPHs).....	15
1.4.1 Organophosphate acid anhydases (OPAAs).....	17
1.5 Objectives.....	18
2. Materials and Methods.....	19-60
2.1 Materials.....	20
2.1.1 Antibiotics	20
2.1.2 Chemicals	20
2.1.3 Restriction enzymes and DNA modifying enzymes.....	22
2.1.4 Bacterial strains	23
2.1.5 Plasmids.....	24
2.1.6 Preparation of Antibiotics or Chemical stocks	26
2.1.7 Substrates for growth/enzyme assays	28
2.1.7 Growth media	31
2.1.8 Preparation of Solutions	30
2.1.8.1 Solutions for plasmid Isolation	30
2.1.8.2 Solutions for Agarose gel electrophoresis.....	31
2.1.8.3 Solutions for Southern hybridization.....	32

2.1.8.4 Solutions for SDS-Polyacrylamide Gel electrophoresis.....	33
2.1.8.5 Protein estimation	34
2.1.8.6 Buffers and Solutions for Two-D electrophoresis	35
2.1.8.7 Solutions for Western blotting	36
2.1.8.8 Solutions for Protein purification and protein interaction studies ...	37
2.1.8.9 Solutions for LC-MS/MS chromatography	37
2.1.8.10 Reagents for β -galactosidase activity	38
2.2 Methodology	38
2.2.1 Isolation of cloning vectors by Alkaline Lysis method	38
2.2.2 Purification of plasmids using QIAGEN Mini preparation kit method	39
2.2.3 Isolation of Large indigenous plasmids	40
2.2.4 DNA manipulations	41
2.2.5 Agarose gel electrophoresis	41
2.2.6 Southern hybridization	41
2.2.6.1 Preparation of probe	41
2.2.6.2 Hybridization.....	42
2.2.7 Gene transfer methods	43
2.2.7.1 Transformation	43
2.2.7.2 Transduction.....	44
2.2.7.3 Conjugation	44
2.2.8 Expression of MfhA	45
2.2.9 Purification of MfhA _{N-GST} protein	46
2.2.9.1 Affinity chromatography.....	46
2.2.9.2 Gel exclusion chromatography	46
2.2.9.3 Thrombin cleavage.....	47
2.2.10 Purification of MfhA from inclusion bodies	47
2.2.11 Protein interaction studies	48
2.2.11.1 GST pull down assay	48
2.2.11.2 Western blotting	49
2.2.11.3 Subcellular localization of MfhA in <i>S.fuliginis</i>	49
2.2.12 Construction of pCMS1 library	50
2.2.13 Two-dimensional electrophoresis.....	50
2.2.13.1 Preparation of sample for TwoD electrophoresis.....	51

2.2.13.2 Isoelectric focussing.....	51
2.2.13.3 In-gel digestion.....	52
2.2.13.4 MALDI TOF/TOF	52
2.2.14 Esterase assay of MfhA	53
2.2.15 <i>p</i> -Nitrophenol supported growth in <i>E.coli</i> K-12 MG1655 (pSDP5)	53
2.2.16 Oxygraph studies	54
2.2.17 Nitrite estimation in the culture medium.....	54
2.2.18 Isolation and characterization of PNP degradation products.....	55
2.2.18.1 Resting cell assay	55
2.2.18.2 HPLC-MS/MS analysis of PNP metabolites.....	55
2.2.19 β -galactosidase assay	56
2.2.20 Isolation of RNA	57
2.2.21 Microarray	58
2.2.21.1 cDNA synthesis, labeling and microarray hybridization	58
2.2.21.2 <i>E. coli</i> K12 MG1655 gene-specific microarray and data normalization.....	58
2.2.22 Quantitative Real time PCR	59
2.2.22.1 Primer design and selection of target sequence for qPCR	59
2.2.22.2 Absolute quantification of target genes.....	59
Results and Discussion	61-130
3. Chapter 1	61-85
3.0 Background	62
3.1 Physical comparison of <i>opd</i> regions between pCMS1 and pPDL2	66
3.1.1 Construction and screening of fosmid library	67
3.1.2 Cloning of flanking region of <i>opd</i> cluster	68
3.2 Lateral transfer of the <i>opd</i> island from plasmid pPDL2 of <i>S. fuliginis</i>	71
3.2.1 Integration module	72
3.2.1.1 Prediction of <i>attP</i> sites	73
3.2.1.2 Construction of temperature sensitive plasmid with <i>attB</i> sequence	75
3.2.1.3 <i>in vivo</i> Integration assay.....	76
3.2.2 Degradation module	79
3.2.2.1 Construction of pPDL2KT	80

3.2.2.2 Transposition assay	82
4. Chapter 2	86-111
4.0 Background	87
4.1 The <i>mfhA</i> is an independent transcriptional unit.....	87
4.2 Heterologous expression of MfhA	91
4.2.1 Expression of MfhA with N-terminal affinity tag.....	91
4.2.2 Construction of pSDP5, pSDP6, pSDP7	92
4.2.3 Construction of pSDP9	93
4.3 Expression and purification of MfhA	94
4.4 <i>In vivo</i> studies	98
4.4.1 PNP metabolism in <i>E. coli</i> K-12 MG1655.....	100
4.4.1.1 Oxygraph studies.....	100
4.4.1.2 HPLC and LC-MS/MS analysis of PNP degradation products	103
4.4.1.3 Proteomic approach.....	105
4.5 OPH interacts with MfhA	108
4.5.1 Sub-cellular localization of MfhA _{N-6His} in <i>S. fuliginis</i>	111
5. Chapter 3	112-130
5.0 Background	113
5.1 MfhA dependent genome-wide expression profiling in <i>E. coli</i> K-12 MG1655	114
5.1.1 MfhA dependent upregulation of Phenyl propionate (PP) pathway	115
5.1.2 Quantification of PP and HPP transcripts in presence of MfhA	120
5.1.3 MfhA dependent promoter activity of MhpA.....	121
5.2 Is non-coding RNA responsible for metabolic diversion ?.....	129
6. Summary	131-133
7. Appendix.....	134-136
8. Bibliography.....	137-149

List of Figures

Fig 1-1 Evolution of genes and non-genetic factors that contribute to the generation of genetic variations	3
Fig 1-2 Horizontal gene transfer and its impact on the evolution of life	5
Fig 1-3 Transfer of DNA between bacterial cells	6
Fig 1-4 Physical map of plasmid pPDL2	15
Fig 1-5 Geographical distribution of identical <i>opd</i> or <i>mpd</i> genes among soil bacteria	16
Fig 1-6 Genetic organization of <i>mpd</i> genes	17
Fig 1-7 Phylogenetic tree of bacterial phosphotriesterases	18
Fig 2-1 Mobilization of pSDP5 into <i>Sphingobium fuliginis</i> ATCC 27551.....	45
Fig 2-2 Probes designed for microarray	59
Fig 3-1a Plasmid pCMS1 isolated from <i>B. diminuta</i>	66
Fig 3-1b Construction of fosmid library of pCMS1 isolated from <i>B. diminuta</i>	66
Fig 3-2 The restriction pattern of pCMS1	68
Fig 3-3 Schematic representation showing sub-cloning of <i>opd</i> flanking regions of pCMS1 in pBluescript KS II (-)	69
Fig 3-4 Comparison of physical map and organization of <i>opd</i> clusters of pCMS1 and pPDL2	71
Fig 3-5 Organization of integration modules of plasmid pPDL2	72
Fig 3-6 Serine tRNA sequence	74
Fig 3-7 Diagrammatic representation of pSDP7 and pSDP8 construction	75
Fig 3-8 Schematic representation of site-specific recombination between <i>attP</i> site of pPDL2 and artificial <i>attB</i> of pSDP8.....	77
Fig 3-9 Confirmation of co-integrate formation between pPDL2-K and pSDP8	77
Fig 3-10 Amplification of junction sites	78
Fig 3-11 Physical map of organophosphate degradation module identified on the pPDL2 plasmid	80

Fig 3-12 Construction of pPDL2-KT	81
Fig 3-13 Amplification of junction sites of <i>opd</i> island	83
Fig 4-1 Enzymatic hydrolysis of OP compound by OPH	87
Fig 4-2 Transcriptional organization of <i>mfhA</i> in pPDL2	88
Fig 4-3 Detection of <i>mfhA</i> promoter motif	89
Fig 4-4 Construction of expression plasmids coding MfhA with N-terminal affinity tag.....	91
Fig 4-5 Construction of broad host range mobilizable expression plasmid coding MfhA ...	93
Fig 4-6 Cloning strategy followed for expression of MfhA without any tag	94
Fig 4-7 Expression of MfhA _{N-6His} in <i>E. coli</i> BL21 DE3	95
Fig 4-8 Purification of MfhA _{N-GST}	96
Fig 4-9 Kinetic studies using purified MfhA and using the substrate PNP-Ac	97
Fig 4-10 Quantification of PNP in the culture medium	98
Fig 4-11 Growth studies of <i>E coli</i> K-12 MG1655 (pSDP5) expressing MfhA _{N-6His}	99
Fig 4-12 PNP dependent oxygen consumption in <i>E coli</i> K-12 MG1655 (pSDP5).....	102
Fig 4-13 Nitrite estimation in <i>E coli</i> K-12 MG1655 (pSDP5).....	102
Fig 4-14 RP-HPLC profile of PNP degradation products	103
Fig 4-15 Identification of PNP degradation products using stable PNP isotope	104
Fig 4-16 LC-MS analysis of PNP degradation products	104
Fig 4-17 Two dimensional electrophoresis of proteins extracted from <i>E. coli</i> K-12 MG1655 and <i>E coli</i> K-12 MG1655 (pSDP5).....	105
Fig 4-18 Proposed PNP degradation pathway in <i>E. coli</i> K-12 MG1655 (pSDP5).	107
Fig 4-19 Cloning strategy to indicate construction of expression plasmids to code OPH with C-terminal deletions.....	109
Fig 4-20 GST pull down assay showing interactions between OPH and MfhA _{N-GST}	110
Fig 4-21 Subcellular localization of MfhA _{N-6His} in <i>S. fuliginis</i> ATCC 27551 (pSDP5).	111
Fig 5-1 Genome-wide expression profile of <i>E.coli</i> K-12 MG1655 (pSDP5)-Heatmap showing differently and differentially expressed operons	116

Fig 5-2 Phenyl propionate (PP) and Hydroxy phenyl propionate (HPP) degradation pathways in <i>E. coli</i> K-12.....	117
Fig 5-3 Influence of MfhA influence on expression of four aromatic degradation pathway genes	118
Fig 5-4 <i>E. coli</i> K-12 MG1655 deletion mutants	119
Fig 5-5 Growth studies of <i>E coli</i> K-12 MG1655 (pSDP5) wild type and mutant strains in PNP supplemented minimal medium.....	120
Fig 5-6 Qunatitative PCR of PP pathway and HPP pathway genes in the presence of MfhA expression	121
Fig 5-7 Generation of <i>E.coli</i> K-12 MG1655 Δcrp	122
Fig 5-8 Assay of <i>mhpA</i> and <i>mhpR</i> promoter activity in the presence of MfhA	123
Fig 5-9 Influence of MfhA on certain key carbon metabolic pathways	124
Fig 5-10 Influence of MfhA on carbon metabolic pathways	125
Fig 5-11 MfhA dependent repression of glycolytic and TCA cycle genes.....	126
Fig 5-12 MfhA mediated changes on the carbon metabolism of <i>E coli</i> K-12 MG1655.....	128
Fig 5-13 Predicted interactions between <i>lpdA</i> mRNA and sRNA46.....	129
Fig 5-14 Influence of MfhA on the promoter activity of <i>srna46</i> gene	130

List of Tables

Table 2.1-1 Antibiotics	20
Table 2.1-2 Chemicals.	20
Table 2.1-3 Restriction enzymes and DNA modifying enzymes	22
Table 2.1-4 Bacterial Strains.....	23
Table 2.1-5 Plasmids.....	24
Table 3-1 The predicted <i>attP</i> sequences on plasmid pPDL2	73
Table 3-2 Primers used for the amplification of junction sites after transposition	82
Table 4-1 The 2D gel images in the region containing upregulated protein spots	106
Table A-1 PCR primers used for construction of expression plasmids or transcriptional fusions	135
Table A-2 PCR primers used to screen deletion mutants of <i>E. coli</i> K-12 MG 1655	135
Table A-3 PCR primers used for quantitative real time PCR.....	136

Abbreviations

ACN	: Acetonitrile
Aes	: Acetyl esterase
AKGDH	: α -keto glutarate dehydrogenase
ATCC	: American type culture collection
BT	: Benzene triol
Cfu	: colony forming unit
CIME	: Cis-integrative mobilizable element
<i>clc</i>	: chlorocatechol
D ⁴ -PNP	: 4-Nitrophenyl-2,3,5,6-d ₄
DHPP	: Dihydroxy phenyl propionate
GI	: Genomic island
HGT	: Horizontal gene transfer
HPP	: Hydroxyl phenyl propionate
ICE	: integrative conjugative element
IME	: Integrative mobilizable element
IPTG	: Isopropyl β -thiogalactoside
IS	: Insertion sequence
Kb	: Kilobase
KDa	: Kilo Dalton
LGT	: Lateral gene transfer
LipY	: Lipase Y
Lpd	: Lipoamide dehydrogenase
MfhA	: meta fission product hydrolase
MfhA _{N-6HIS}	: MfhA with N-terminal (His) ₆ tag
MfhA _{N-GST}	: MfhA with N-terminal GST tag
MGE	: Mobile genetic elements
MP	: Methyl parathion
MPH	: methyl parathion hydrolase
MW	: Molecular Weight
NC	: Nitrocatechol

ncRNA	: non-coding RNA
OP	: Organophosphate
OPAA	: organophosphate acid anhydrase
OPH	: organophosphate hydrolase
PA	: Phenyl acetate
PDH	: Pyruvate dehydrogenase
Pfu	: plaque forming unit
PNP	: p-Nitrophenol
PNP-Ac	: 4-Nitrophenyl acetate
PP	: Phenyl propionate
PTE	: Phosphotriesterase
qRT-PCR	: quantitative real time PCR
SDS	: Sodium dodecyl sulphate
<i>srna</i>	: small RNA
THB	: Trihydroxy benzene
Tn	: Transposon

Introduction

Xenobiotic compounds in a strict sense can be defined as man-made molecules that have never been exposed to any living organisms before their introduction into an environment. Broadly they are referred as chemicals that are present in significantly higher amounts than natural composition of an environment (TOP and SPRINGAEL 2003). As the chemical ligature found in these compounds are very new to the existing enzymes of living organisms (CASES and DE LORENZO 2001) most of them remain recalcitrant. However, because of the remarkable adaptive nature of the bacteria to extreme conditions of life, considerable numbers of anthropogenic compounds are found to be degradable. According to microbial genetists, three major strategies contribute for bacterial adaptation, rich biodiversity, long-lasting maintenance and development of life on earth (ARBER 2000) [Fig 1-1]. In the first strategy the small local gene sequence changes that occur during the development of a new process contribute for bacterial adaptation. However, in the absence of essential participation of natural selection development of a novel biological function is extremely rare (ARBER 1994). In the second strategy, recombination between related gene sequences results in DNA reshuffling which involves novel combination of existing capacities by the fusion of different functional domains. Third strategy is very efficient phenomenon of genetic variation in which, there is an exchange of evolutionary success between the micro-organisms. Due to such exchange micro-organisms can adapt to a sudden change in the surrounding conditions in a relatively short period of time (OCHMAN *et al.* 2000) (SPRINGAEL *et al.* 2002). This phenomenon of acquiring genetic material from neighbouring bacterial species is referred to as Horizontal (Lateral) gene transfer (HGT/LGT). In recent years, wide genome sequencing data available indicated the presence of identical metabolic pathways and enzymes for the degradation of xenobiotic compounds in phylogenetically unrelated bacterial strains isolated from

geographically distinct areas. Such results signifies the existence of similarities in the gene organizations and nucleotide sequences (SENTCHILO *et al.* 2000; SPRINGAEL *et al.* 2001) and supports for the of Arber's third strategy of inter-genomic acquisition (HACKER and CARNIEL 2001).

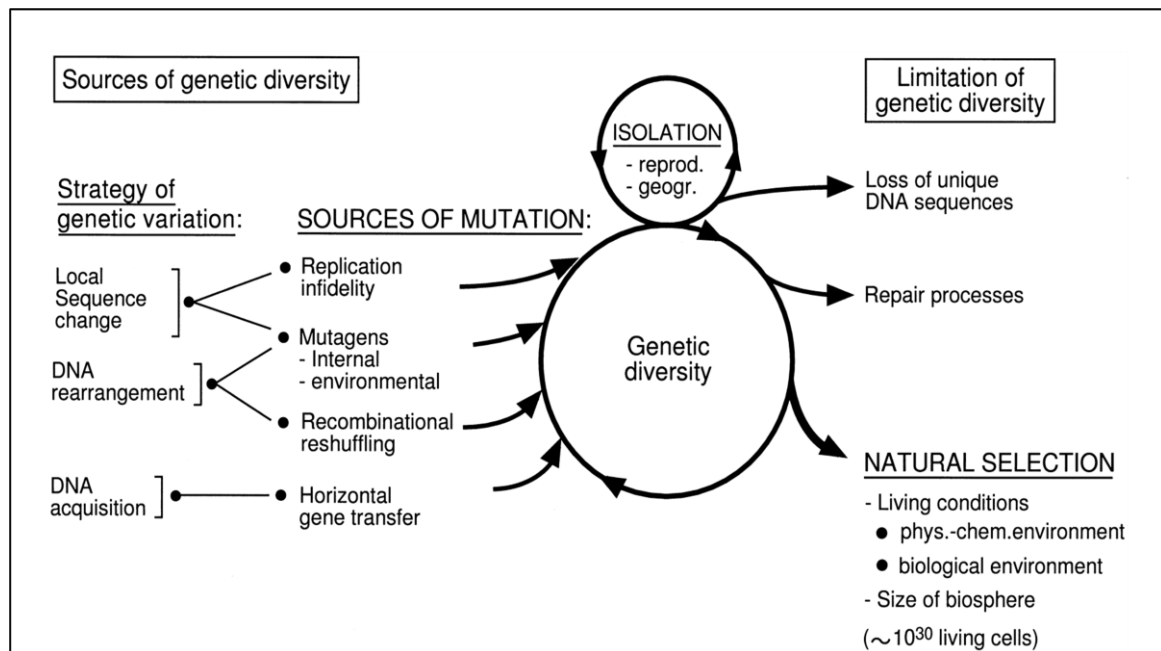


Fig 1-1 | Evolution of genes and non-genetic factors contribute to the generation of genetic variations (ARBER 2000).

1.1 Horizontal gene transfer:

Horizontal gene transfer is an important mechanism in evolution, that provides metabolic, physiological fitness, and enables the ecological exchange in most prokaryotes (RAGAN and BEIKO 2009). HGT is defined to be the movement of genetic material between bacteria other than by descent in which information travels through the generations as the cell divides. It is often regarded as a sexual process that requires a mechanism for the mobilization of chromosomal DNA among bacterial cells that encode adaptive traits that might be beneficial for bacteria under certain growth or environmental conditions. The five essential events required for stable inheritance of HGT genes are

1. The DNA or RNA is prepared for transfer by excision and circularization or it is packed into phages or it is prepared for conjugal transfer by means of a plasmid and mating-pair formation protein complex.
2. This DNA fragment is later transferred to the recipient cell by conjugation/transformation/transduction.
3. In the third step, the recipient bacteria may prohibit or reject the transferred genetic material or
4. The genetic material may undergo circularization as observed with plasmids or it can integrate site specifically into the recipient chromosome. During such events the genetic material may not be maintained in the new host because of host restriction modification system or failure to integrate into the host chromosome or because of the incompatibility with the resident plasmids.
5. After the stable transfer and maintenance into the new recipient the transferred genetic material has to replicate along with the recipient genome and has to transmit to the daughter cells in a stable fashion over successive generations by vertical gene transfer [Fig 1-2].

1.2 Role of HGT in bacterial evolution

Many horizontally transferred genes are being identified by genome sequence information and genome-by-genome content comparisons among the living organisms, and HGT is now seen with a different view. In bacteria, horizontal gene transfer (HGT) is widely recognised as the mechanism responsible for the widespread distribution of antibiotic resistance genes, gene clusters encoding bio-degradative pathways and pathogenicity determinants (SCHMIDT and HENSEL 2004; DOBRINDT *et al.* 2004; SPRINGAEL and TOP 2004; JUHAS *et al.* 2009). Among these, evolution of bio-degradative pathways is a delayed opportunistic response in which case the genes that

are required for the complete degradation of a xenobiotic compound have to be assembled. In such situation in comparison with the other genetic adaptation mechanisms HGT offers dynamic exchange of the essential genes within in a short duration of time.

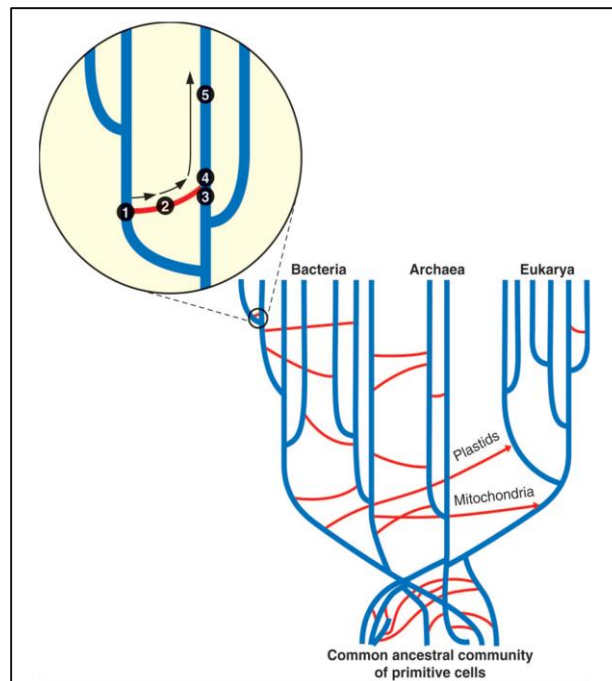


Fig 1-2 | Horizontal gene transfer and its impact on the evolution of life. The inset illustrates the series of events that lead to the stable inheritance of a transferred gene in a new host. (Tamar Barkay et al., 2005).

In comparison with the antibiotic resistant genes, degradation of xenobiotic compounds requires more complex genetic systems, usually operons of ten or more genes, or regulon of several operons and requires the development of appropriate mechanisms for controlling these regulons (WILLIAMS and SAYERS 1994; WYNDHAM *et al.* 1994; DE LA CRUZ and DAVIES 2000; COPLEY 2000) . These adaptive traits are known to be transferring to the recipients under different conditions by the traditional mechanisms of conjugation, transformation, and transduction (THOMAS and NIELSEN 2005). The main agents of gene transfer in these mechanisms are plasmids, integrons, phage, prophage-like gene transfer agents, transposons, retrotransposons, cassette-like

chromosomal elements etc altogether referred as “mobilome”. Transformation is a process in which naked or free DNA is taken up by the bacteria. Gene transfer that is mediated by certain type of bacteriophages is known as transduction. The mechanism in which effective contact between donor and recipient bacteria is established for gene exchange between bacteria is known as conjugation [Fig 1-3].

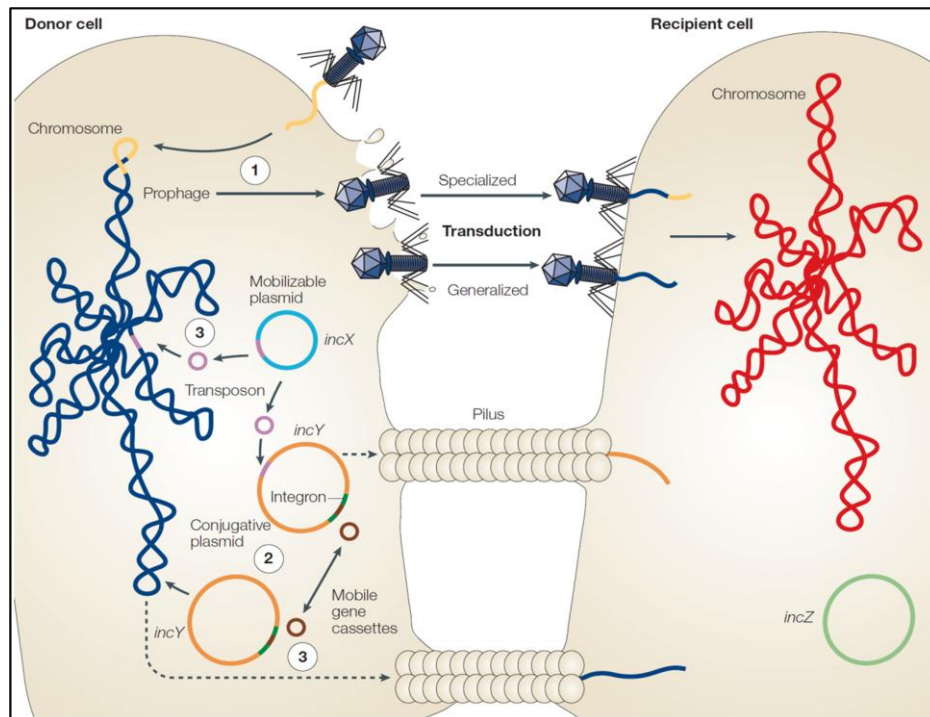


Fig 1-3 | Transfer of DNA between bacterial cells (AZAD and LAWRENCE 2012).

The genetic material that got transferred by above mechanisms can integrate into the existing replicon by illegitimate recombination, transformation or site-specific recombination or it can exist as an independent replicon. Many of these genes that got integrated but not serving any function are found to be existing as integrated prophages, transposons and DNA fragments will eventually be lost in course of evolution (HAO and GOLDING 2006). Other class of alien genes have found to be of great interest and contribute for shaping bacterial physiology. Among them Genomic islands (GIs) are large regions of chromosome, containing dozens of genes, that were introduced by

LGT. These are further scrutinized for their potential to introduce multiple traits that confer novel physiological abilities to their recipients (DOBRINDT *et al.* 2004). To identify foreign genes on the chromosome two major approaches are in use (AZAD and LAWRENCE 2012).

1.2.1 Phylogenetic Approach

In this method of identification of alien genes, the distribution of homologues of a gene of interest among genomes of nearby species is considered. In such observations, the gene that exists only in one genome of closely related organisms indicates its acquisition by HGT into this genome. A novel gene may appear in the genome in five possible ways. A gene can arise by gene duplication and its subsequent divergence from the parent gene. If the genome sequence of this organism is incomplete, identification of such paralogous genes will be difficult. Secondly a gene may be appearing by its retention only in one organism and its loss in all other closely related organisms. Thirdly, the orthologues of the gene of interest might be present in other genomes but have evolved such a way that they have not been identified as orthologues. Fourthly, the gene in question may not be a gene at all, merely an annotation fact. Lastly, the gene might have been introduced by horizontal transfer. Taking all these set of parameters into consideration, a phylogenetic tree can be constructed to identify laterally transferred genes.

1.2.2 Parametric approach

This strategy follows a statistical method to quantify the distribution of genes depending on a set of similarities in the DNA properties of the complete genome (LAWRENCE and OCHMAN 1997). Because of the common set of mutational tendencies and cumulative action of the mutational proclivities of DNA polymerase, efficacy of various mismatch correction systems, composition of dNTP pools, action of the tRNA

pools and other forces, native genes of a species are compositionally similar (AZAD and LAWRENCE 2012). But the genes transferred laterally differ from the rest of the genome in three different sorts of analyses as guanine plus cytosine (GC) content and codon usage in individual genomes, genome-by-genome content comparisons and individual gene trees (SUEOKA 1962; MUTO and OSAWA 1987; KARLIN *et al.* 1998). As a result recently transferred genes may be detected as those which do not reflect the common compositional features of the majority of genes in the genome. However because of the two demerits of the parametric methods like, after the transfer of alien genes into a new host they may ameliorate their differences and become indistinguishable for the native genes of the genome. Second, the compositional properties of native genes do vary, so the distinction between native and alien genes is often ambiguous. Irrespective to these aspects the combinatorial approaches will provide high confidence results by abolishing the merits and demerits of the parametric and/or phylogenetic approaches.

Basing on these methods many alien genes or gene clusters are identified by genome sequence analysis. In all such situations the HGT was identified to be implicated in the wide-spread transfer of the gene content. The traditional mechanisms of HGT are well known even from undergraduate text books, however the importance of the HGT in bacterial evolution gained much attention in the last 10 years due to the emergence of increased antibiotic resistance as evidenced by emergence of multidrug resistance (MDR) strains like penicillin-resistant *Streptococcus pneumoniae* (PRSP) and sudden rise in ESBL (Extended-spectrum β -lactamase) rates. Horizontal gene transfer provides single most driving force to augment the dispersal of these xenobiotic resistance genes. Consistent with the concept of the recent evolution of antibiotic resistance plasmids and multi-resistant strains, studies with collections of bacterial pathogens isolated before

the “antibiotic era” showed that plasmids were common but antibiotic resistant genes are not. In conclusion, because of anthropogenic activities the evolution of resistance genes is intensified in light of which the slow natural selection pressure can be ignored. In a similar way because of the rapid industrialization many environmental microbes that are encoding novel multigene pathways responsible for the biodegradation of xenobiotic molecules such as the polychlorinated Phenolic compounds are also found to be evolved. The existing processes of gene acquisition, transfer, modification, and expression that were in place are expanding and accelerating in the modern biosphere to effectively catabolise xenobiotic compounds.

1.3 HGT in xenobiotic compound degradation

Bacterial evolution studies carried using phylogenetic and parametric approaches have become much more feasible due to wide genome sequence data. Comparisons of genomes of different species have revealed the patch work assembly of identical genome regions among different bacteria. In recent years much more is made on host-microorganism interaction studies. The role played by HGT is mainly considered for the presence of such organizations. The importance of HGT in the field of bacterial adaptations is considered in two ways. One is the bacterial and eukaryotic host interactions in which case defense/pathogenicity and symbiosis mechanisms and the other field is interaction of microorganisms with the chemical compounds. Different studies on bacteria capable of degrading synthetic organic compounds as source of carbon or energy or both and nitrogen in few cases suggested involvement of HGT mechanisms in increasing or fostering their catabolic properties by shaping their genetic makeup. Among these mechanisms, plasmid transfer and catabolic transposons are well studied, recent years the role played by genomic islands in augmenting the catabolic properties is also being studied. The genetic machinery required for the catabolism of chlorocatechol and

aminobenzoate were initially identified as plasmid-borne in *Pseudomonas knackmaussii* B13; however the integration of this plasmid at two specific sites on the chromosome was identified (RAVATN *et al.* 1998a). Subsequently, existence of this plasmid as an integrative conjugative element (ICE) was identified and the dynamic mobilization of ICE were demonstrated to be influenced by the concentration of chlorocatechol (SENTCHILO *et al.* 2009).

Similarly differently sized mobile DNA elements or conjugative transposons involved in the metabolism of novel carbon compounds were identified and their role in distribution of novel genetic traits between different microorganisms came into light. During the evolution of metabolic pathway responsible for the mineralization of novel chemical bonds, a promiscuous enzyme that is capable of hydrolyzing a novel chemical ligature eventually evolve from an existing enzyme. The gene encoding this enzyme can subsequently be mobilized into a new bacterial species wherein there is scope for a second enzyme to evolve to achieve complete mineralization of the so called recalcitrant compound. In such a way different set of enzymes may evolve to mineralize the novel chemical compounds into simple chemical structures that are easily utilized by the bacteria. In this process, natural selection plays a major role in selectively enriching the enzymatic capabilities of a novel trait. Further these genes if located on mobile genetic elements and conjugative transposons can find a way into new hosts and can be incorporated or recombined, resulting in a new mosaic of genetic structures. When the bacteria utilizing the novel chemical compounds were investigated, mechanisms responsible for shaping the genetic structure of these organisms to metabolize novel chemical were identified. Due to these mechanisms new gene mosaics express in new organism, a metabolic pathway formed from promiscuous enzymes of different organisms, now express within one organism and help in selectively strengthening such organism. In

subsequent generation, the population of this super-bug will dominate when specific chemical compound for the metabolic pathway is present. The same situation might have taken place in the formation of pathways for the degradation of chlorobenzene, nitrobenzene, phenoxyalkanoic acids and atrazine (WERLEN *et al.* 1996; BEIL *et al.* 1999). In many degradation genes encoding bacteria, degradative traits are found on plasmid. However in recent years, the degradative traits are found on large genomic islands and conjugative transposons, collectively called as integrative conjugative elements (ICEs).

Recent findings of various mobile catabolic genes have provided some insights into the evolution of microbial degradation systems for anthropogenic chemical compounds. Basing on the genetic organizations and transposition mechanisms 3 major classes of bacterial transposons have been identified (TAN 1999; MASATAKA TSUDA 1999).

1.3.1 Class I transposon:

These are the insertion sequences (IS) carrying only the genetic determinants for the transposition. IS-encoded transposons are not stable and are suggestive of decreasing the transposition events in case of increasing the sizes of the intervening sequence in an IS-composite transposon. However, various catabolic genes have been found to be located between the two copies of IS element. Eg: Tn5542 class I transposases carrying Benzene degradation gene (*bedDC1C2BA*) (TAN and MASON 1990) with *IS1489* element in *P. putida* ML2 (TAN and FONG 1993) and Tn5280 Chlorobenzene degradation transposon (*tcbAB*) in *Pseudomonas* sp. P51 (VAN DER MEER *et al.* 1991b) (VAN DER MEER *et al.* 1991a).

1.3.2 Class II transposon

These are the composite transposons that carry two copies of insertion sequences in direct or inverted orientation and carry genetic traits unrelated to transposition. During the

transposition of class II transposons 5 bp duplication of target sequence after transposition, and carry short (<50bp) terminal repeats. The transposons carry various genes for drug and heavy metal resistance, toxins, some anabolic and catabolic pathways and DNA modification. Eg: pWVO plasmid borne Tn4651 and Tn4653 transposons coding for *xyl* genes involved in toluene degradation of *Pseudomonas putida* mt-2 (GRINSTED *et al.* 1990; KHOLODII *et al.* 1997)

1.3.3 Mobile genetic elements other than class I and II transposons

Structural similarity among the conjugative transposons and the pathogenicity and symbiosis islands suggests that they represent a class of transmissible chromosomal elements with combined genetic features of phages, plasmids and transposons. Mobile genetic elements are a class of transmissible chromosomal elements that are having the combined features of phages, plasmids, and transposons. Few examples of mobile genetic elements that are having specific regulatory elements for their mobilization are described in brief. Tn4371 is a 55 kb transposon identified in *Ralstonia eutropha* that carries 13 Kb *bph* region of strain A5 (MERLIN *et al.* 1999). And it catabolizes biphenyl and chlorobiphenyl to benzoate and chloro-benzoate respectively (SPRINGAEL *et al.* 1993). This catabolic transposon contains Int protein showing significant similarity with the members of integrase family and possesses motifs conserved in the integrase family (NUNES-DUBY *et al.* 1998). The right 2 kb end of Tn4371 also carries the genes that show similarity with the two genes of plasmid RP4 involved in the conjugation process. Biphenyl and salicylate metabolic pathways associated with the *P. putida* strain KF-715 are encoded by *bph* and *sal* gene clusters respectively on the chromosome. Conjugal transfer of this *bph-sal* element is aided without the help of co-resident plasmids. The 3-chlorobenzoate (3CBA) degradation pathway element ICE*clc* is well studied in *Pseudomonas knackmaussii* B13. Initially this element was thought to be located on a

plasmid (RAVATN *et al.* 1998b). Later *clc* element was demonstrated to be existing as a 105 Kb tandemly amplifiable genetic element (*clc* element (RAVATN *et al.* 1998a; RAVATN *et al.* 1998c) . Further the genetic machinery required for its rapid mobilization consists of Int B-13 protein showing high similarity/ homology to P4 integrase subfamily and integrated in a specific orientation, site specifically available at the 3' end of *t-RNA* (gly-tRNA and cys-tRNA) (SENTCHILO *et al.* 2003; SENTCHILO *et al.* 2009).

Burcholderia cepacia contains gene involved in the metabolism of 2, 4, 5-trichlorophenoxy acetic acid on five independent replicons. The genes encoding 2, 4, 5-T metabolism are organized as 3 different clusters *tft* AB, *tft*CD, *tft* EFGH on different plasmids. High frequency translocation of *tft* gene clusters aided by *IS931* were identified under the influence of 2, 4, 5-T. Such clusters of IS elements may serve as the targets for rearrangements of the DNA region carrying the *tft* clusters (HAUGLAND *et al.* 1990; HUBNER *et al.* 1998).

1.4 HGT of OP degradation genes

Synthetic organophosphates (OPs) are used generally as insecticides and chemical warfare agents. They contain three phospho-ester linkages and hence the enzymes that are involved in the hydrolysis of this chemical ligature are referred as phospho-triesterases (PTEs). The bacterial PTEs that are recognized till date are grouped into three major classes as detailed below.

1.4.1 Organophosphate hydrolases (OPHs)

These groups of enzymes are implicated in the hydrolysis of a wide range of organophosphate compounds such as parathion, methyl parathion and fenusulfothion and organophosphate chemical warfare agents like sarin, soman with high catalytic efficiency. They have wide range substrate specificities that contain different chemical bonds

containing P-O, P-F, P-CN and P-S bonds with different efficiency. They show maximum activity against P-O linkage. The purified form of the OPH shows more specificity towards P-O bond with a highest catalytic rate of K_{cat}/K_m $4 \times 10^7 \text{ M}^{-1} \text{ S}^{-1}$ identified for paraxon (GHANEM and RAUSHEL 2005) and shows less specificity for P-S bond with a catalytic efficiency of K_{cat}/K_m $4 \times 10^7 \text{ M}^{-1} \text{ S}^{-1}$ for VX (EFREMENKO 2001). The OPH are homodimeric metalloproteins and consists of two identical subunits containing 336 aminoacids. They are the members of the amidohydrolase superfamily and are studied to be evolved from the quorum quenching lactonases during the last 70 years (ROODVELDT and TAWFIK 2005; AFRIAT *et al.* 2006; ELIAS and TAWFIK 2012). The *opd* gene encodes for OPH and are identified from different soil microorganisms. The OPH was initially characterized from the *Flavobacterium* sp. ATCC 27551, a soil microorganism isolated from the paddy fields of Philippines (SETHUNATHAN and YOSHIDA 1973). Later the *opd* gene encoding OPH, *opd* was identified to be located on the indigenous plasmid of pPDL2. Further identical *opd* genes were identified from the *Brevundimonas diminuta* MG isolated from the agricultural soils of Texas, USA (MULBRY *et al.* 1986; MULBRY *et al.* 1987), *Flavobacterium balustinum* isolated from the agricultural soils of Ananthapur, India (SOMARA and SIDDAVATTAM 1995), *Sphingomonas* sp. JK1 isolated from Mumbai, India (Unpublished) and *Agrobacterium tumifaciens* C28 isolated from agricultural soils of Australia (HORNE *et al.* 2002). In all these cases OPH encoded by *opd* is 89%-100% identical. Presence of identical *opd* genes in taxonomically and geographically diverse soil bacteria suggests existence of HGT of genes among soil bacteria. The indigenous plasmids pPDL2 and pCMS1 isolated from *Flavobacterium* sp ATCC 27551 and *Brevundimonas diminuta* MG, a region of about 5.1 Kb containing 1.5 kb *opd* was identified to be highly conserved (MULBRY *et al.* 1987). Our lab has recently determined the complete sequence of these two indigenous plasmids. As shown in fig 1-4 various genetic modules required

for the degradation of OPs, machinery required for HGT of degradation module were identified in pPDL2.

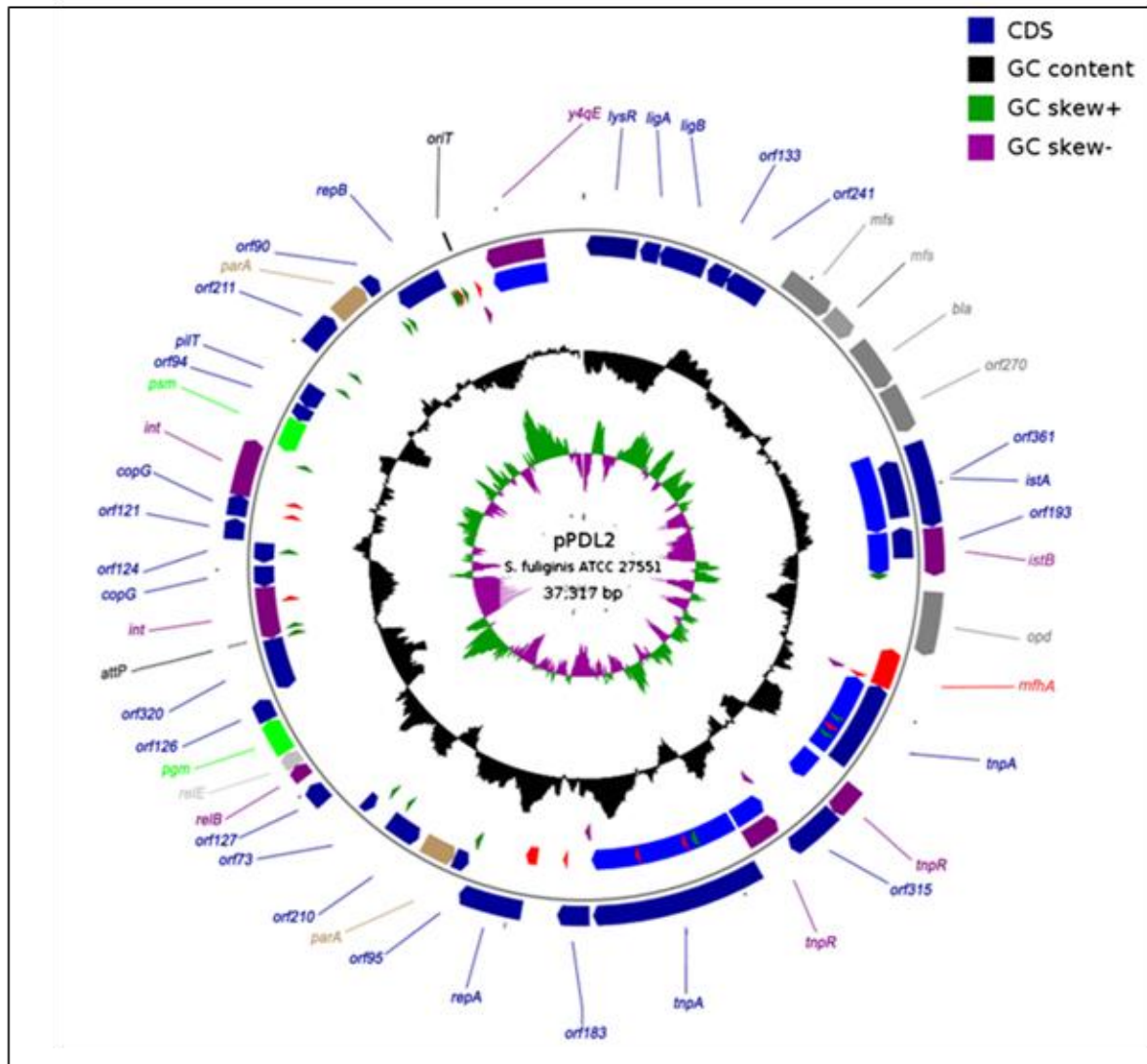


Fig 1-4| Physical map of plasmid pPDL2. Outer and inner circles represent the proteins encoded by sense and antisense strands respectively. Third circle represents the mobile elements and repeat sequences. Direct (DR) and Inverted (IR) repeats are shown with filled red and green triangles respectively. Tn3-specific repeats appear with filled purple triangles in the fourth circle. The fifth circle shows GC content across the plasmid sequence. The sixth and seventh circles represent GC-skew in sense and anti-sense strands (Pandeeti et al, 2012).

1.4.2 Methyl parathion hydrolases (MPHs)

The second group of PTEs are methyl parathion hydrolases. They were reported from *Plesiomonas* sp. M6 (ZHONGLI et al. 2001), *Pseudomonas* sp. WBC (CHEN Y et al. 2002),

and *Pseudomonas* sp., A3 (Zhongli et al., 2002) isolated from different regions of the China. Most of the MPH enzymes known to date have been purified from *Pseudomonas* strains isolated from OP-polluted Chinese agricultural soils (LIU *et al.* 2005; ZHANG *et al.* 2006; ZHONGLI *et al.* 2001). Despite having functional similarity,

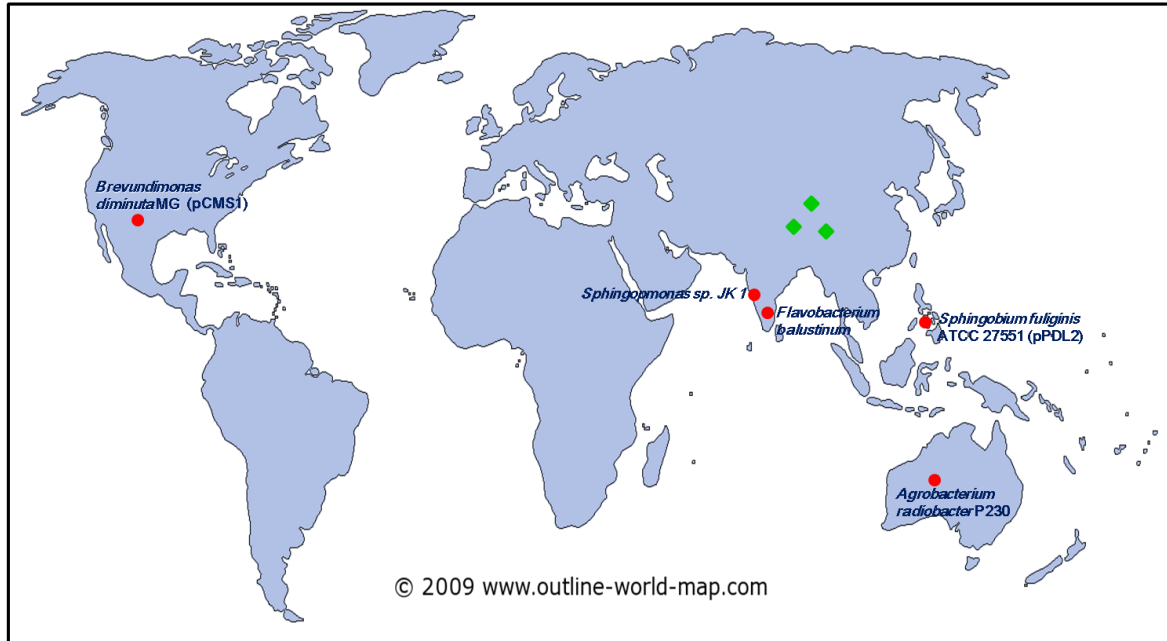


Fig 1-4 | Geographical distribution of identical *opd* or *mpd* genes among soil bacteria. Red circles represent *opd* gene and green squares represent the identical *mpd* genes.

MPH enzymes share no homology with OPH, indicating the existence of structurally independent organophosphate-degrading enzymes among soil bacteria (DONG *et al.* 2005). MPH belongs to the protein family of β -lactamases, the enzymes that confer resistance to β -lactam-derived antibiotics (TIAN *et al.* 2008). Interestingly these two structurally different enzymes have an identical active site structure (DONG *et al.* 2005). This type of functional convergence pointed to the existence of independent paths in the evolution of organophosphate-hydrolyzing enzymes [Fig 1-6]. Lateral transfer of *mpd* genes became evident with the discovery of identical *mpd* genes among bacterial strains isolated from OP-polluted Chinese soil samples (ZHANG *et al.* 2006), and the *mpd* genes were shown to be part of an active transposon (WEI *et al.* 2009) [Fig 1-6].

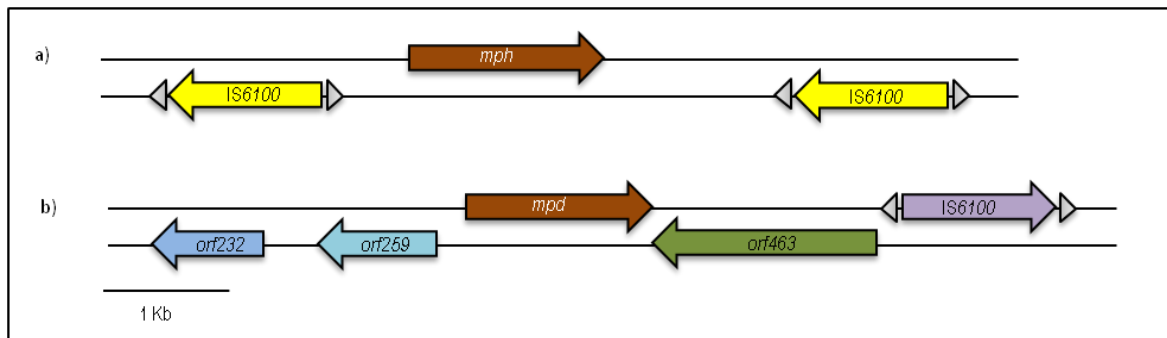


Fig 1-6 | Genetic organization of *mpd* genes found on the chromosome of *Plesiomonas* sp. strain M6, (Panel a) and on plasmid pZWLO of *Pseudomonas* sp. strain WBC-3 (Panel b).

1.4.3 Organophosphate acid anhydrase (OPAA)

These are the third group of enzymes isolated from *Alteromonas* sp. JD6.5 (DEFRANK *et al.* 1993; CHENG *et al.* 1996). It is a monomeric protein with a molecular mass of 60 kDa and possesses high activity against a range of organophosphorus compounds including the G-agents. However the catalytic efficiency of OPAA against P-O bond containing OP compounds is less when compared with the P-F bond containing OPs. They were proposed to be belonging to the di-peptidase family and catalyze the di-peptide linkage with a proline residue at the C-terminus (CHENG *et al.* 1996). They are aminopeptidases that catalyze the cleavage of amino terminal X-Pro peptide bonds. The OPAA activity on G-class nerve agents appears to be due to existence of structural similarities between dipeptide and nerve agents. The gene *opaa* coding for OPAA identified from the *Alteromonas* sp. are found on the chromosome.

The phosphotriesterases identified in eukaryotic organisms appears to have common ancestor and their evolution is orthologous. In prokaryotes the evolution of OP compound degrading enzymes appears to have evolved from different progenitors suggesting their paralogous evolution. Basing on the paralogous relationship [Fig 1-7] of PTEs and identification of identical *opd* genes on dissimilar plasmids in taxonomically distinct soil bacteria suggests for existence of HGT of *opd* gene cluster, lateral transfer of *opd* genes was predicted among soil bacteria.

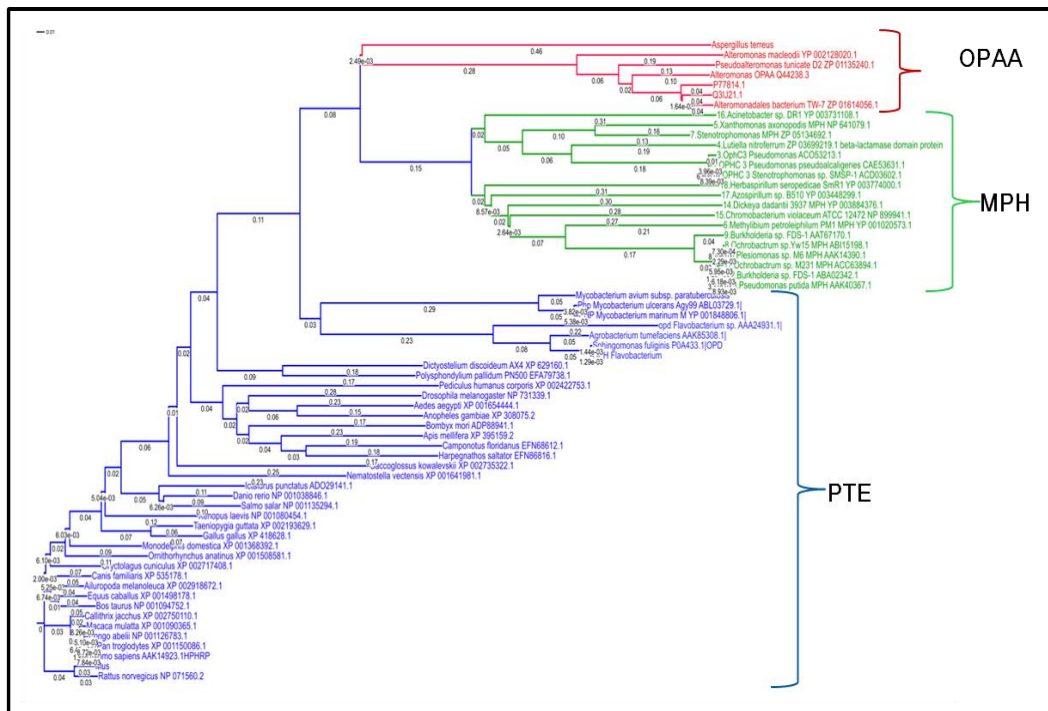


Fig 1-7 | Phylogenetic tree of bacterial phosphotriesterases. The homologues of *opd* (OPH), *mpd* (MPH) and *opaA* (OPAA) coding sequences available in NCBI database were used to construct phylogenetic tree using online tool 'interactive tree of life' (www.itol.embl.de).

In support of these predictions the lateral transfer of *mpd* and *opda* have been experimentally demonstrated. Despite of having identical *opd* genes among taxonomically diverse group of bacterial strains, experimental evidence is not obtained to demonstrate HGT of *opd* genes. The present work is therefore undertaken with the following objectives.

1.5 Objectives

1. To demonstrate Horizontal Gene Transfer of *opd* genes among soil bacteria.
2. To assess the function of novel esterase found as part of *opd* island.
3. To establish relationship between *p*-Nitrophenol degradation and the novel esterase, MfhA.

Materials and Methods

2.1 Materials

Table 2.1-1| Antibiotics

Name of the antibiotic	Name of the Supplier
Ampicillin sodium salt	HIMEDIA
Kanamycin Sulfate	HIMEDIA
Tetracycline hydrochloride	HIMEDIA
Chloramphenicol	HIMEDIA
Streptomycin	HIMEDIA
Gentamycin	HIMEDIA
PolymyxinB	HIMEDIA

Table 2.1-2| Chemicals

Name of the Chemical	Name of the Supplier
Acrylamide	SRL
Agar agar	HIMEDIA
Ammonium chloride	Qualigens
Ammonium persulfate	Sigma Aldrich
Ammonium nitrate	Qualigens
Ampholytes	GE Healthcare
Bovine serum albumin	GE Healthcare Lifesciences, USA
Bromophenol blue	GE Healthcare Lifesciences, USA
Butanol	Qualigens
Calcium chloride	Qualigens
Calcium nitrate	Qualigens
CHAPS	GE Healthcare
Chloroform	Qualigens
Coomassie Brilliant blue G-250	Merck
Coomassie Brilliant blue R-250	SRL
Cobalt chloride	SRL
3-11 NL IPG buffer	GE Healthcare Lifesciences, USA
Deoxynucleotide triphosphates	MBI Fermentas

Dipotassium hydrogen orthophosphate	Merck
N,N-Dimethylformamide	SRL
DNase	Qiagen
Ethidium bromide	SRL
Ethylene diamine tetraacetic acid (EDTA)	SRL
Ethyl acetate	SRL
Ferrous Sulphate	Qualigens
Glucose	Qualigens
Glycerol	Qualigens
Glycine	SRL
Hydrochloric acid	Qualigens
L-Arginine	SRL
Isopropanol	SRL
Isopropyl thiogalactopyranoside (IPTG)	SRL
Lysozyme	Bangalore GeneI
Magnesium chloride	SRL
Magnesium sulphate	SRL
Methanol	SRL
N,N'-Methylene bis acrylamide	SRL
β -mercaptoethanol	Sigma Aldrich
Orthophosphoric acid	Merck
4-Nitrophenol	Sigma Aldrich
2,3,5,6 Deuteriated 4-Nitrophenol	Sigma Aldrich
4-Nitrophenyl acetate	Sigma Aldrich
NP-40	Sigma Aldrich
Phenol Saturated	Bangalore GeneI
Potassium chloride	Qualigens
Potassium dihydrogen ortho phosphate	Merck
PMSF	GE Healthcare
Protease inhibitor cocktail	Sigma Aldrich
Sodium citrate	SRL
Sodium chloride	SRL
Sodium Deoxycholic acid	SRL

Sodium dodecyl sulfate	SRL
Sodium hydroxide	SRL
Sodium Sulphate	Merck
Sucrose	SRL
RNase A	Banglore GeneI
Tetra ethyl methylene diamine (TEMED)	Sigma Aldrich
Tris-base	SRL
Triton X-100	SRL
Tryptone	Himedia
Thiourea	GE Healthcare
Tween 20	USB
Urea	GE Healthcare
X-gal	Calbiochem nhyu8i M,
Yeast extract	Himedia
Zinc chloride	SRL
Trifluoroacetic acid	Sigma Aldrich

Table 2.1-3| Restriction enzymes and DNA modifying enzymes

Name of the enzyme	Name of the Supplier
<i>ApaI</i>	MBI, Fermentas
<i>ApoI</i>	MBI, Fermentas
<i>BamHI</i>	MBI, Fermentas
<i>BglII</i>	MBI, Fermentas
<i>EcoRV</i>	Bangalore GeneI
<i>EcoRI</i>	MBI, Fermentas
<i>HindIII</i>	MBI, Fermentas
<i>NdeI</i>	MBI, Fermentas
<i>NotI</i>	MBI, Fermentas
<i>PstI</i>	MBI, Fermentas
<i>SalI</i>	MBI, Fermentas
<i>SmaI</i>	MBI, Fermentas
<i>XhoI</i>	MBI, Fermentas
T ₄ DNA Ligase	MBI, Fermentas

Klenow fragment	MBI, Fermentas
<i>Pfu</i> DNA polymerase	MBI, Fermentas
<i>Taq</i> DNA polymerase	MBI, Fermentas
Plasmid safe (DNase)	Epicenter Biotechnologies, USA
DNase free RNase A	Bangalore GeneI

Table 2.1-4| Bacterial Strain

Strain	Genotype or Phenotype	Reference or Source
<i>E. coli</i> DH5a	<i>supE44 ΔlacU169 (□80 lacZ ΔM15) hsdR17 recA1 endA1 gyrA96 thi1 relA1</i>	(HANAHAH 1983)
<i>E. coli</i> BL21 DE3	<i>hsdS gal(λcIts857 ind1 sam7 nin5lac UV5 T7 gene 1</i>	(STUDIER and MOFFATT 1986)
<i>E. coli</i> JM109 DE3	<i>rec A1 endA1 gyrA96 thi hsdR17 supE44 relA1_ (lac-proAB) [F_traD36 proAB lac 1qZ_M15]</i>	(YANISCH-PERRON <i>et al.</i> 1985)
<i>E. coli</i> K-12 MG1655	F-, λ, <i>rph-1</i>	(BLATTNER <i>et al.</i> 1997)
<i>E. coli</i> K-12 BW25113	F-, Δ(<i>araD-araB</i>)567, Δ <i>lacZ</i> 4787(::rrnB-3), λ, <i>rph-1</i> , Δ(<i>rhaD-rhaB</i>)568, <i>hsdR514</i>	(HAYASHI <i>et al.</i> 2006)
<i>E. coli</i> pir-116	F- <i>mcr</i> Δ(<i>mrr-hsdRMS-mcrBC</i>) φ80 <i>dlacZ</i> Δ <i>M15</i> Δ <i>lacX74 recA1 endA1 araD139 Δ(ara, leu)</i> 7697 <i>galU galK λ- rpsL (StrR) nupG pir-116(DHFR)</i>	Epicentre Biotechnologies, USA
<i>E. coli</i> EP 1300	F ⁻ <i>e14 (McrA⁻) D(mcrC⁻ mrr) (Tet^R) hsdR514 supE44 supF58 lacY1 or D(lacIZY)6 galK2 galT22 metB1 trpR55 l⁻</i>	Epicentre biotechnologies, USA
<i>E. coli</i> S17-1	<i>thi pro hsdR hsdM recA</i> RP4 2-Tc::Mu-Kn ^r ::Tn7(Tp ^r Sp ^r Sm ^r)	(SIMON 1983)
<i>E. coli</i> HB101	F ⁻ <i>mcrB mrr hsdS20(r_B⁻ m_B⁻) recA13 leuB6 ara-14 proA2 lacY1 galK2</i>	(ROULLAND-DUSSOIX and BOYER 1969)

	<i>xyl-5 mtl-1 rpsL20(Sm^R) glnV44 λ⁻</i>	
<i>E coli pir⁺</i> BW25141	<i>lacI^q rrnB_{T14} ΔlacZ_{WJ16} ΔphoBR580 hsd514 ΔaraBAD_{AH33} ΔrhaBAD_{LD78} galU95 end-A_{BT333} uid(ΔMluI)::pir⁺ recA1)</i>	(HALDIMANN <i>et al.</i> 1998)
<i>Sphingobium fuliginis</i> (previously classified as <i>Flavobacterium</i> sp. ATCC 27551)	Wild type strain, Sm ^r , Pm ^r , OPH ⁺	(SETHUNATHAN and YOSHIDA 1973; KAWAHARA <i>et al.</i> 2010)
<i>Brevundimonas diminuta</i>	Wild type strain, Sm ^r , Pm ^r , OPH ⁺ .	(SERDAR <i>et al.</i> 1982)
<i>Pseudomonas putida</i> KT2440	<i>hdsMR</i> , Cm ^r	(FRANKLIN <i>et al.</i> 1981)

Table 2.1-5| Plasmids

Plasmid Name	Genotype or phenotype	Reference
pTZ57R/T	Ap ^r , <i>lacZ⁺</i> , Easy T cloning vector	Fermentas, USA
pGEM-T	Ap ^r , <i>lacZ⁺</i> , Easy T cloning vector	Promega
pBluescript KS(II)	Ap ^r , <i>lacZ⁺</i> , cloning vector	Fermentas, USA
pGEX-4T-1	Ap ^r , expression vector	Amersham Biosciences, UK
pRSETA	Ap ^r , expression vector	Invitrogen
pET-28a(+)	Km ^r , expression vector	Novagen
pMMB206	Cm ^r , a low copy number broad host range expression vector	(MORALES <i>et al.</i> 1991)
pCC1FOS	Cm ^r , copy control fosmid vector	Epicenter Biotechnologies, USA
pKD46	Ap ^r , red recombinase expression plasmid	(DATSENKO and WANNER 2000)
pRK2013	Km ^r , Helper plasmid carrying genes for conjugation	(FIGURSKI and HELINSKI 1979)

pMP220	Tet ^r , Promoter probe vector	(SPAINK H. P 1987)
pPDL2	OP ⁺ , 37.3Kb indigenous plasmid	(MULBRY <i>et al.</i> 1986)
pPDL2-K	Km ^r , Tn5<R6Kγori/KAN-2> inserted into indigenous plasmid, pPDL2	(PANDEETI <i>et al.</i> 2012)
pPDL2-KT	Km ^r , Tet ^r , <i>opd</i> gene of pPDL2-K disrupted by insertion of <i>tet</i> cassette	(PANDEETI <i>et al.</i> 2012)
pCMS1	OP ⁺ , 66Kb indigenous plasmid	(SERDAR <i>et al.</i> 1982)
pCMSA	Cm ^r , 35 kb pCMS1 fragment cloned in fosmid vector pCC1FOS.	(PANDEETI <i>et al.</i> 2011)
pCMSB	Cm ^r , 40 kb pCMS1 fragment cloned in fosmid vector pCC1FOS	(PANDEETI <i>et al.</i> 2011)
pSM2	Ap ^r , complete <i>opd</i> -cluster of <i>Sphingobium fuliginis</i> ATCC 27551 cloned in pUC19	(SIDDAVATTAM <i>et al.</i> 2003)
pSM3	Ap ^r , Tet ^r , pSM2 having <i>opd::tet</i> in place of <i>opd</i> gene.	(SIDDAVATTAM <i>et al.</i> 2003)
pPHLC400	Cm ^r , Native form of <i>opd</i> with C-terminal His tag cloned in pMMB206 as an <i>EcoRI</i> - <i>BamHI</i> fragment	(GORLA <i>et al.</i> 2009)
pSDP1	Tet ^r , 471bp upstream region of <i>mfhA</i> cloned in pMP220 as <i>EcoRI</i> - <i>PstI</i> fragment	This study
pSDP2	Tet ^r , 157 bp upstream region of <i>mfhA</i> cloned in pMP220 as <i>EcoRI</i> - <i>PstI</i> fragment	This study
pSDP3	Ap ^r , pRSETA with <i>mfhA</i> as <i>BamHI</i> fragment	This study
pSDP4	Ap ^r , <i>mfhA</i> cloned in pGEX-4T-1 as <i>BamHI</i> fragment. Codes for MfhA _{N-GST} fusion protein.	This study
pSDP5	Cm ^r , <i>mfhA</i> amplified from pSDP1 and cloned in pMMB206 as <i>BglIII</i> fragment. Codes for MfhA _{N-6His} fusion protein.	This study
pSDP6	Cm ^r , <i>mfhA</i> amplified from pSDP3 as <i>BglIII</i> fragment and cloned in pMMB206. It codes for MfhA _{N-GST} fusion protein.	This study
pSDP7	Ap ^r , The pTac- <i>lacZ</i> cassette of pMMB206 taken	This study

	as <i>EcoRV</i> and <i>DraI</i> and ligated to <i>oriR101</i> and <i>bla</i> fragment taken from pKD46, as <i>EcoRV</i> and <i>SmaI</i> fragment.	
pSDP8	Ap ^r , synthetic <i>attB</i> sequence of pPDL2 cloned in pSDP7 as <i>HindIII</i> fragment	This study
pSDP9	Cm ^r , GST gene cloned in pMMB206 as <i>BglIII</i> fragment	This study
pSDP10	Km ^r , <i>mfhA</i> cloned in pET-28a(+) as <i>NcoI</i> and <i>BamHI</i> fragment.	This study
pSDP11	Cm ^r , contains <i>opd</i> gene with 3' deletion as <i>EcoRI</i> and <i>SalI</i> fragment and codes for truncated OPH with deletion of 13 aminoacids from C-terminus	This study
pSDP12	Cm ^r , contains <i>opd</i> gene with 3' deletion as <i>EcoRI</i> and <i>SalI</i> fragment and codes for truncated OPH with deletion of 42 aminoacids from C-terminus	This study
pSDP13	Cm ^r , contains <i>opd</i> gene with 3' deletion as <i>EcoRI</i> and <i>SalI</i> fragment and codes for truncated OPH with deletion of 69 aminoacids from C-terminus	This study
pSDP14	Tet ^r , 190bp upstream region of <i>mhpA</i> cloned in pMP220 as <i>EcoRI-PstI</i> fragment	This study
pSDP15	Tet ^r , 190bp upstream region of <i>mhpR</i> cloned in pMP220 as <i>EcoRI-PstI</i> fragment	This study
pSDP16	Tet ^r , 560bp <i>srna46</i> coding sequence along with promoter region cloned in pMP220 as <i>EcoRI-SalI</i> fragment	This study

2.1.6 Preparation of Antibiotic or Chemical stocks

Ampicillin: Ampicillin stock solution was prepared by dissolving 1g of ampicillin in 10 mL of sterile milliQ water and filtered through 0.2µM syringe filter. This stock solution

was distributed into 1 mL aliquots and stored at -20°C . When required 10 μl of stock solution was added to 10 mL of medium to get a final concentration of 100 $\mu\text{g}/\text{mL}$ of medium.

Chloramphenicol: Chloramphenicol stock solution was prepared by dissolving 300 mg of chloramphenicol in 10 mL of 70% ethanol (V/V) and filtered through 0.2 μM syringe filter. This stock solution was distributed into 1 mL aliquots and stored at -20°C . When required 10 μl of stock solution was added to 10 mL of medium to get a final concentration of 30 $\mu\text{g}/\text{mL}$ of medium.

Tetracycline: Tetracycline stock solution was prepared by dissolving 200 mg of tetracycline in 10 mL of 70% ethanol (V/V) and filtered through 0.2 μM syringe filter. This stock solution was distributed into 1 mL aliquots and stored at -20°C . When required 10 μl of stock solution was added to 10 mL of medium to get a final concentration of 20 $\mu\text{g}/\text{mL}$ of medium.

Kanamycin: Stock solution of kanamycin was prepared by dissolving 500 mg of kanamycin sulfate in 10 mL of milliQ water and sterilized by filtration. The stock solution was stored in 1 mL aliquots at -20°C . When required 10 μl of kanamycin stock solution was added to 10 mL of medium to get a final concentration of 20 $\mu\text{g}/\text{mL}$ of medium.

Gentamycin: Stock solution of gentamycin was prepared by dissolving 200 mg of gentamycin sulfate in 10 mL of milli Q water and sterilized by filtration. The stock solution was stored in 1 mL aliquots at -20°C after filter sterilization. When required 10 μl of gentamycin stock solution was added to 10 mL of medium to get a final concentration of 20 $\mu\text{g}/\text{mL}$ of medium.

Streptomycin: Stock solution of streptomycin was prepared by dissolving 200 mg of streptomycin in 10 mL of milliQ water. The stock solution was stored in 1 mL aliquots at -

20°C after filter sterilization. When required 10 µl of streptomycin stock solution was added to 10 mL of medium to get a final concentration of 20 µg/ mL of medium.

Polymyxin-B: Stock solution of PolymyxinB was prepared by dissolving 100 mg of polymyxinB in 10 mL of milliQ water. The stock solution was stored in 1 mL aliquots at -20°C after filter sterilization. When required 10 µl of PolymyxinB stock solution was added to 10 mL of medium to get a final concentration of 10 µg/ mL of medium.

IPTG: 1M IPTG stock solution was prepared by dissolving 236.8 mg IPTG in 1 mL of autoclaved milli Q water and stored as aliquots of 100 µl at -20°C. When required the stock solution was thawed on ice bath and 100 µl of stock solution was added to get 1 mM working concentration of IPTG.

X-Gal: 4% of X-gal stock solution was prepared by dissolving 40 mg of X-gal in 1 mL of N, N'-dimethylformamide. When required 100 µl stock solution of X-gal was added to 100 mL of medium after cooling it to 45°C.

2.1.7 Substrates for growth / enzyme assays

50% glucose

Glucose stock solution was prepared by adding 50g of Dextrose in 30 mL of deionised water; the contents were dissolved by heating and finally made upto 100 mL and sterilized by autoclaving. This stock solution was added to minimal salts medium to get a final concentration of 0.05g per 100 mL.

Methyl parathion (MP) (*O,O*-dimethyl-*O*-paranitrophenyl phosphorothioate)

0.2 M stock solution of methyl parathion was prepared by dissolving 263.2 mg of methyl parathion in 5 mL methanol and was stored at -20°C until further use. While performing enzyme assay appropriate amount of methyl parathion was used to get a final concentration of 100 µM in the reaction mixture.

***p*-nitrophenol (50 mM)**

50 mM *p*-nitrophenol stock was prepared by dissolving 347.7 mg of *p*-nitrophenol in 50 mL of deionised H₂O and the solution was filter sterilized using 0.2µm syringe filter and stored at 4°C.

Catechol (50mM)

50 mM catechol stock was prepared by dissolving 110 mg of catechol in 20 mL of double deionised water and the solution was filter sterilized using 0.2µm syringe filter and stored at 4°C.

4-Nitrocatechol (50 mM)

50 mM 4-nitrocatechol stock was prepared by dissolving 155 mg of 4-Nitrocatechol in 20 mL of deionised water and the solution was filter sterilized using 0.2µm Syringe filter and stored at 4°C.

1,2,4-Benzenetriol(50 mM)

50 mM Benzenetriol stock was prepared by dissolving 126 mg of Benzenetriol in 20 mL of deionised water (pH 2.0) and the solution was filter sterilized using 0.2µm sartorius filter and stored at 4°C.

2.1.9 Growth Media

The following growth media were prepared and used for the propagation of bacteria. The media were stringently autoclaved for 20 minutes at 15 psi (1.05 kg/cm²) on liquid cycle. For preparation of solid media 2 g of agar was added to 100 mL of broth and sterilized. Whenever required appropriate concentrations of antibiotic and chemical stocks were added after cooling the medium to 50⁰-60⁰C.

Luria-Bertani (LB) medium

To prepare LB medium, 10g of tryptone or peptone, 5g of yeast extract and 10 g of Sodium chloride were dissolved in 1000 mL of deionised H₂O. The pH of the medium

was adjusted to 7.0 with 5 N NaOH (approx. 0.2 mL) and sterilized by autoclaving for 20 minutes at 15 psi (1.05 kg/cm²) on liquid cycle.

Minimal salts medium

Minimal salts medium was prepared by dissolving 6g of Na₂HPO₄, 3g of KH₂PO₄, 1g of NH₄Cl, 0.5g of NaCl to 1000 mL of deionised water. This medium was autoclaved at 15 psi (1.05 kg/cm²) on liquid cycle for 20 minutes. After sterilization the solution was allowed to cool to room temperature and sterile stock solutions of MgSO₄.7H₂O and CaCl₂ were added to obtain a final concentration of 0.12g of MgSO₄.7H₂O and 0.01g of CaCl₂ per 1000 mL of above solution to get complete minimal salts medium. Whenever required adequate quantity of sterile glucose (50% stock) or *p*-Nitrophenol (50mM stock) solution were added as growth supplements.

Wakimoto medium

Wakimoto medium or ATCC medium was used to propagate *Sphingobium fuliginis* ATCC 27551. It was prepared by dissolving 1.379g of Na₂HPO₄ 2H₂O, 5.0g of peptone and 15g of sucrose in 500 mL of deionised water. The contents were stirred and finally made up to 1liter with deionised water. The medium is then sterilized by autoclaving for 20 minutes at 15 psi (1.05 kg/cm²) on liquid cycle. After autoclaving stock solutions of Calcium nitrate and Ferrous sulphate (final concentration as 0.5g of Ca(NO₃)₂ 4H₂O and 0.5g of FeSO₄.7H₂O) are added to make the complete medium. When required, antibiotics were supplemented after cooling the medium to 50⁰C. Wakimoto agar plates were prepared by adding 1.5% agar to wakimoto broth.

2.1.8.1 Solutions for plasmid isolation

Solution I: 10 mL of 250mM glucose, 6.25 mL of 0.2M Tris pH 8.0, 1 mL 0.5M EDTA pH 8.0, were dissolved in 25 mL sterile millQ water and finally the volume was made upto

50 mL with sterile milliQ water. This solution was autoclaved for 20 minutes at 15psi on liquid cycle and stored at 4⁰C. Whenever required stock solution of DNase free RNase A was added at a final concentration of 100µg/ mL.

Solution II: Equal volumes of 0.4N NaOH and 2% SDS solutions were freshly mixed and used as Solution II.

Solution III (3M sodium acetate pH 4.8): To prepare Solution III, 24.61g of sodium acetate was dissolved in 80 mL of sterile milliQ water and its pH was adjusted to 4.8 with glacial Acetic acid. Finally the volume of the solution was made upto 100 mL and stored at 4⁰C.

Phenol chloroform solution: Phenol chloroform solution was prepared by mixing equal volumes of water saturated phenol and chloroform.

Chloroform: Isoamylalcohol solution: 96 mL of chloroform and 4 mL of Isoamyl alcohol were mixed and stored in amber colour bottle at at 4⁰C.

TE buffer: Working solution of TE buffer was prepared by adding 5 mL of 0.2M Tris-Cl, 0.2 mL of 0.5M EDTA to 80 mL of deionised water and finally upto 100 mL. This solution is autoclaved and stored at 4⁰C.

2.1.8.2 Solutions for Agarose gel electrophoresis

TAE buffer

A stock solution of 50 X TAE buffer was prepared by mixing 242 g of Tris base, 57.1 mL of glacial acetic acid and 100 mL of 0.5 M EDTA (pH 8.0) to 900 mL of deionised water, after complete dissolution of the contents the volume the solution was made upto 1000 mL with deionised water. Whenever required 1X working solution containing 40mM Tris-acetate and 1mM EDTA was prepared by diluting with deionised water. 0.4% or 0.8 % or 2.0 % of agarose in 1X TAE buffer was used to resolve 5-60 Kb or 0.5-10 Kb or 0.1-0.2 Kb of dsDNA.

6X Gel loading buffer

12.5mg of bromophenol blue, 12.5mg of xylene cyanol FF and 7.5g of Ficoll (Type 400; Pharmacia) were dissolved in 75 mL of sterile milliQ H₂O and finally made up to 50 mL and stored at room temperature.

Ethidium bromide stock solution

100 mg of Ethidium bromide was mixed with 10 mL of sterile water and kept for vortex overnight in a brown glass bottle. This solution was further diluted to get a final working stock solution of 1 mg/1mL. While preparing agarose gel 5 µL of working stock solution was added to 100mL of gel solution to get a final concentration of 0.05 µg/mL.

2.1.8.3 Solutions for Southern hybridization

5X TBE buffer: To prepare TBE stock solution 54 g of Tris-base and 27.5 g of boric acid and 20 mL of 0.5M EDTA were mixed and made up to 1000 mL to distilled water. Working stock solution was prepared by diluting 10mL of stock solution to 100mL.

Depurination Solution: 11mL of conc HCl was mixed with 989 mL of double distilled water and stored at room temperature until further use.

Denaturation solution: To prepare denaturation solution 87.66g of NaCl and 20g of NaOH were dissolved in 800mL of double distilled water and finally made upto 1000mL. This solution was stored at room temperature until further use.

Neutralisation solution: 87.66g of NaCl and 0.5g of Tris base were dissolved in 800mL of double distilled water. The pH of this solution was adjusted to 7.5 with conc HCl and finally made upto 1000mL. This solution was stored at room temperature until further use.

Nucleic acid transfer buffer (20X SSC): Dissolve 88.23g of Tri-sodium citrate and 175.32 g of NaCl in 800mL of distilled water. Check the pH is 7-8 and finally make upto 1000mL. This solution can be stored up to 3 months.

Pre-hybridization buffer: This solution was prepared by mixing 342 mL of 1M Na_2HPO_4 and 158mL of 1M NaH_2PO_4 to 200 mL of double distilled water and finally the pH of this solution was adjusted to 7.2. To this buffer 2mL of 0.5M EDTA, 70 g of SDS and 10g of BSA were added one after the other and dissolved completely. Finally this solution was made upto 1000mL and stored at room temperature until further use.

2.1.8.4 Solutions for SDS-Polyacrylamide Gel electrophoresis

Acrylamide Solution: A 30% stock solution of Acrylamide was prepared by mixing 30g of acrylamide and 0.8 g of N, N'- methylene-bis-acrylamide in 70 mL of deionised water for overnight, till the contents were dissolved completely and finally made up to 100 mL and stored at 4°C.

Resolving gel buffer: 181.71g of Tris base was dissolved in 800 mL of deionised water and pH of the solution was adjusted to 8.8 by adding 30 mL of conc HCl. Finally the volume of the buffer solution was made up to 1L using deionised water, autoclaved for 20 minutes at 15 psi (1.05 kg/cm^2) on liquid cycle and stored at room temperature. When required the stock was added to the gel components to get a final concentration of 390mM Tris-Cl, pH8.8.

Stacking gel buffer for SDS-PAGE: 121.14g of Tris base was dissolved in 800 mL of deionised water and the pH of the solution was adjusted to 6.8 by adding 42 mL of conc HCl and finally the volume of the buffer was made up to 1L with deionised water. This solution was autoclaved and stored at room temperature. When required the stock was added to the gel components to get a final concentration of 130mM Tris-Cl, pH 6.8.

Tris glycine electrophoresis buffer (pH 8.3): 10X stock solution of Tris glycine buffer was prepared by mixing 30.03g of Tris base, 144g of Glycine (electrophoresis grade) and 10g of SDS in 1L of milliQ H_2O and stored at room temperature. For running SDS

PAGE, 1X Tris glycine buffer containing 25mM Tris base, 250mM Glycine, and 0.1% SDS was used.

2X SDS gel loading buffer: 2X stock solution of SDS loading buffer was prepared by mixing 1 mL of 1M Tris-Cl pH 6.8, 2g SDS, 10mg of bromophenol blue and 10 mL of glycerol in 25 mL of milliQ water and kept at 45⁰C for 10 min for complete solubilization of SDS. To this reagent 0.699 mL of β -Mercaptoethanol was added and finally made upto 50 mL with milliQ water. 10 mL aliquots of this buffer were distributed and stored at -20⁰C. For running protein samples on SDS-PAGE, equal volume of this buffer was added to the protein sample, boiled for 5 min and loaded on to the gel.

Staining solution: 0.2 g of coomassie brilliant blue R-250 was dissolved in 50 mL of methanol. To this 7.5 mL of acetic acid was added and finally the volume was made up to 100 mL using deionised water. The contents were filtered through coarse filter paper and stored at room temperature in amber color bottle until further use.

De-staining solution: 50 mL of methanol is mixed with 7.5 mL of glacial acetic acid before making up the volume to 100 mL using deionised water. The contents were freshly made and used once to destain the PAGE gels.

Protein Markers: Low molecular weight protein markers supplied by MBI Fermentas were used. Size of the protein markers include, 116.0, 66.2, 45.0, 35.0, 25.0, 18.4 and 14.4 kDa.

2.1.8.5 Solutions for protein estimation

Standard BSA

A 10mg/mL stock solution of Bovine serum albumin (BSA) was prepared by dissolving 10mg of BSA in 0.17M NaCl. This solution was store at -20⁰C. When required 1mg/mL BSA working solution was prepared and used for the construction of standard graph.

Bradford's reagent

To prepare Bradford's reagent 10mg of coomassie brilliant blue G-250 was dissolved in 50 mL of 95% ethanol, to this 10 mL of 85% (W/V) *ortho*-phosphoric acid was added. After complete solubilization of the dye the solution was made upto 100 mL with deionised water. Finally the reagent was filtered through whatman#1 paper in dark, and stored in amber colour bottle at 4⁰C for 3 months.

2.1.8.6 Buffers and solutions for TwoD-electrophoresis

Sample buffer

2D sample buffer was prepared by dissolving 420mg of urea, 152mg of thiourea, 20mg of CHAPS, 20µl of NP-40 and 50 µl of 1% bromophenol blue solution, and the final volume was made up to 1 mL with miliQ water. Protein sample to be analysed was directly resuspended in this buffer. Before applying the protein sample to the IEF strip 20µl of 3-11NL IPG buffer and 5.6mg of DTT was added per 1 mL of the sample.

SDS equilibration buffer solution

72.1 g of urea, 10 mL of Tris-Cl 1.5M (pH 8.8), 69 mL of glycerol, 4 g of SDS and 4 mL of 1% bromophenol blue stock solution were added and the final volume was made upto 200 mL with milliQ water. Equilibration solution-I was made by adding 100 mg of DTT to 10 mL of the stock solution. Similarly, equilibration solution II was made by adding 250 mg of iodoacetamide to 10 mL of stock solution.

Colloidal coomassie Staining solutions:

Fixative: To fix the gel 40 mL of ethanol, 10 mL of acetic acid and 50 of deionised water were mixed and used immediately.

Dye stock solution: 18.81 mL of *ortho*-phosphoric acid and 100g of ammonium sulphate were completely dissolved in 800 mL of water, to this 1 g of Coomassie Brilliant Blue G-250 was added while stirring and made upto 1L and kept for stirring for 24h.

Dye working solution: To 4 parts of stock solution 1 part of methanol was added while stirring and used immediately.

Destainer: 1%(V/V) acetic acid was used for destaining 2D gels.

2.1.8.7 Solutions for western blotting

Towbin buffer (protein transfer buffer)

3.03 g of Tris-base and 14.4 g of glycine was dissolved in 650 mL of distilled water. To this 200 mL of methanol was added and final volume was made up to 1000 mL with distilled water. The buffer was stored at 4⁰C until further use.

TBS-T Buffer

20 mL of 1M Tris-Cl (pH 7.6), 8 g of sodium chloride and 1 mL of Tween-20 were dissolved in 800 mL of millQ water and finally made upto 1L.

Blocking Reagent

10% solution of skimmed milk powder prepared in TBS-T was used for blocking PVDF membrane.

Membrane stripping solution

6.25 mL of 1M Tris-Cl (pH 6.8), 2 g of SDS were completely dissolved in 80 mL of deionised water, to this solution 0.699 mL of β -Mercaptoethanol was added and finally made upto 100 mL. This solution was stored in screw capped amber coloured bottle and stored at 4⁰C until further use.

Primary antibody solution

2 μ l of Anti-His mouse antibody or Anti-GST HRP conjugate antibody (Amersham Biosciences) or Anti-OPH antibody raised in mice was added to 10 mL of blocking reagent to get a titre of 1:5000 and used for probing the proteins transferred onto PVDF membranes.

Secondary antibody solution

2 μ l of Anti-mouse goat antibody conjugated with HRP was added to 10 mL of blocking reagent to get a titre of 1:5000 and used as secondary antibody solution.

Ponceau S reagent

100mg of Ponceau salt was dissolved in 100mL of 5% acetic acid.

2.1.8.8 Solutions for Protein purification and protein interaction studies

Phosphate buffered saline (pH 7.3)

To prepare 10X stock solution of PBS 8.18g of NaCl, 0.2012g of KCl, 1.4196g of Na₂HPO₄, and 0.2449g of KH₂PO₄ were dissolved in 800 mL of deionised water. The pH of this solution was adjusted the pH of the medium to 7.3 with 1N HCL or 1N NaOH and finally made upto 1L. This solution was sterilized by autoclaving at 15psi on liquid cycle for 20 minutes and stored at room temperature. 1X working solution containing 140mM NaCl, 2.7mM KCl, 10mM Na₂HPO₄, and 1.8mM KH₂PO₄ was prepared by diluting 100mL of 10X stock solution to 1L with deionised water, filter sterilized and used for GST fused protein purification as equilibration or washing buffer.

Elution buffer

Glutathione elution buffer was prepared by dissolving 0.6057g of Tris base and 0.3073g of reduced glutathione in 80 mL of deionised water. The pH of this solution was adjusted to 8.0 with 1N HCL and stored in amber coloured bottle at 4^oC.

2.1.8.9 Solutions for LC-MS/MS chromatography

Mobile phase for HPLC: To prepare mobile phase 500 mL of LC MS grade Methanol, 500 mL of ultra-pure milliQ water and 2 mL of HPLC grade glacial acetic acid were mixed and filtered through 0.45 μ M filter and stored at room temperature.

2.1.8.10 Reagents for β -galactosidase activity

Z buffer

16.1 g of $\text{Na}_2\text{HPO}_4 \cdot 7\text{H}_2\text{O}$, 5.5 g of $\text{NaH}_2\text{PO}_4 \cdot \text{H}_2\text{O}$, 0.75 g of KCl and 0.246 g of $\text{MgSO}_4 \cdot 7\text{H}_2\text{O}$ and 2.7 mL of β -mercaptoethanol were dissolved in 950mL of deionized water and its pH was adjusted to 7.0 with either NaOH or HCl. Finally the volume was made up to 1 L with water.

ONPG (*ortho*-Nitrophenyl galactoside) solution

1.61 g of $\text{Na}_2\text{HPO}_4 \cdot 7\text{H}_2\text{O}$ and 0.55 g of $\text{NaH}_2\text{PO}_4 \cdot \text{H}_2\text{O}$ were dissolved in 90mL water and adjusted to pH to 7.0 with either NaOH or HCl. 400mg of ONPG was added to this solution. Stirred to dissolve and brought the volume up to 100 mL with water. This solution was stored at 4°C away from light.

1M Sodium carbonate

Dissolve 12.4g of sodium carbonate in 100mL of deionized water. This solution was stored at room temperature.

2.2 Methodology

2.2.1 Isolation of cloning vectors by Alkaline Lysis method

Mini preparations of plasmid DNA was carried out by the following procedures of Birnboim and Doly (1979), and Ish-Horowicz and Buker (1981) with slight modifications. A single bacterial colony carrying plasmid to be isolated was inoculated into 3 mL of LB broth containing appropriate antibiotic and was incubated overnight at 37°C with vigorous shaking. Overnight culture of 1mL was centrifuged at 13400 rpm for 1 minute and supernatant was discarded. Bacterial cell pellet was resuspended in 100 μL of ice-cold solution I (50mM glucose, 25mM Tris-Cl pH 8.0, and 10mM EDTA, pH 8.0) containing 10mg/mL of DNase free RNase by vigorous vortexing. The above bacterial suspension was resuspended in 200 μL of freshly prepared solution II and the contents were mixed by inverting the tube 5-6 times. Then 150 μL of ice-cold solution III was added to the above bacterial lysate and mixed by inverting the tube 4-5 times. Then tube was kept on ice for

3-5 minutes. Precipitate formed in the above mixture was centrifuged by spinning the contents at 13400 rpm for 10 minutes. Then the supernatant was transferred into a fresh tube and equal volumes of phenol: chloroform mixture was added. The contents were briefly mixed by vortexing and subjected to centrifugation at 13000 rpm for 5 minutes. Aqueous phase was transferred to a fresh tube and 1/10th volume of solution III and 2 volumes of ethanol was added and tubes were kept at -20°C for 30 minutes. Then the tubes were centrifuged at 13400 rpm for 20 minutes at 4°C in a micro-centrifuge. The DNA pellet was further washed with 70% ethanol to remove traces of salts associated with plasmid. Subsequently the plasmid DNA was dried before redissolving it in 50 μl of TE buffer and stored at -20°C until further use.

2.2.2 Purification of plasmids using QIAgen Mini preparation kit method

Plasmids were purified using QIAgen mini preparation kit especially when used for cloning and sequencing reactions. A single bacterial colony carrying plasmid was inoculated into 3 ml of LB broth containing appropriate antibiotic and was incubated overnight at 37°C with vigorous shaking (~ 150 rpm). The overnight culture was centrifuged at 13000 rpm for 1 min and supernatant was discarded. The bacterial cell pellet was resuspended in 250 μl of P1 buffer and was lysed by adding 250 μl of P2 buffer prior to mixing of the tubes by inverting 4-6 times. After lysis of the cells the contents were neutralized by adding 350 μl of buffer N3 prior to mixing of the contents by inverting immediately for 4-6 times. Then tubes were centrifuged at 13000 rpm for 10 minutes. After centrifugation the supernatant was directly transferred to a QIAprep column placed in a collection tube. The entire assembly was placed in a microfuge and centrifuged at 13000 rpm for 1 minute. The column was then washed with 500 μl of PB buffer followed by 750 μl of buffer PE. To remove the residual wash buffer PE, column was placed in the collection tube and centrifuged at 13000 rpm for 1 minute. Finally,

plasmid DNA was eluted by adding 50 μ l buffer EB or H₂O to the centre of QIA preparation column followed by brief centrifugation at 13000 rpm. The plasmid DNA was stored at -20°C until further use.

2.2.3 Isolation of Large indigenous plasmids

Large scale preparation of indigenous plasmids either from *Brevundimonas diminuta* or *Sphingobium fuliginis* was carried out by following the Lysis method of Currier Nester, with modification suggested by Prof. Gonzaliz lab, Texas A & M University, USA (CURRIER and NESTER 1976). Native bacterial strains were grown at 30°C on appropriate agar media plate for 2 days. The cell mass was scrapped from the fresh plates using sterile 1 ml micropipette tips and a suspension of bacterial cells was made in 5 mL of 10mM Tris pH 8.0 to a cell density at $A_{425nm} = 0.75-0.8$. This suspension was centrifuged at 10000rpm for 10 min at 4°C and the supernatant was discarded. Bacterial pellet was resuspended in 5.4 mL of TE buffer. To this cell suspension 0.21 mL of lysozyme in TE buffer (10mg/ mL) was added before incubating at 37°C water bath for 15 min. After incubation 0.3 mL of 20% SDS (in TE buffer) was added and gently mixed by inversion. Subsequently, the whole mixture was vortexed at a maximum speed for 2 min to shear chromosomal DNA. To this sheared DNA 0.2 mL of 3N NaOH was added, and mixed well by inversion. Further the contents were incubated at room temperature for 15 min with occasional shaking. The contents were then neutralized by addition of 1 mL of 2M Tris pH 7.0 followed by incubating at room temperature for 5 min. Subsequently 1.5 mL of 5M NaCl was added and extracted with equal volume of salt saturated phenol. The contents were mixed by inversion and centrifuged at 5000 rpm for 10 min to get clear aqueous phase. The plasmid DNA from the aqueous phase was precipitated by addition of 2 volumes of ice cold ethanol and incubated at -80°C for 30 min. Then the tubes were centrifuged at 8000 rpm for 10 min at 10°C to pellet down the plasmid DNA. The DNA

pellet was further washed with 70% ethanol to remove traces of salts associated with plasmid. Subsequently the plasmid DNA was dried before redissolving it in 50 µl of TE (pH 8.0) and stored at -20°C until further use.

2.2.4 DNA manipulations

Plasmid DNA isolation, purification of PCR amplicons, Gel extraction of DNA fragments was done using QIAGEN kits following manufacturer's protocols. PCR amplification, ligation, and other DNA manipulation techniques were performed basically following standard procedures (SAMBROOK).

2.2.5 Agarose gel electrophoresis

A slab of 0.8% agarose was prepared by adding 0.8 g of agarose in 100mL of 1XTAE and boiling for 3 minutes. This molten agarose was allowed to cool to approximately 45°C, and 0.5µg/ml of ethidium bromide was added. This whole sample was poured into the casting unit along with 1mm thickness comb, and allowed to solidify. Samples were applied by keeping the wells towards anode, and DNA sample was resolved by applying constant voltage of 100V.

2.2.6 Southern hybridization

2.2.6.1 Preparation of probe: Probe for southern hybridisation was prepared using Random hexamer Labelling kit, (M/S Bangalore Genei, Bangalore) according to the manufacturer's instructions. Approximately 200ng of *Pst*I digested fragments of pPDL2-K or pSDP8 in 5 µl volume was taken in a sterile eppendorf tube and 5 µl of autoclaved milli-Q water was added and the whole boiled for 5 min in a hot water bath. Immediately the sample was kept in ice bath for 5min. This sample was briefly spinned and 25ul of 10X labelling buffer, 1ul of 100ng/ul random primers, 2.5 µl of 20mM DTT, 2µl each of dATP, dGTP, dTTP (10mM), 3µl of αP³²CTP (20uCi) 3µl of autoclaved milli-Q water and 2 µl of 3U/µl of klenow fragment was added. The whole reaction mixture was mixed

gently and incubated at room temperature for 4 h. This sample was directly used in pre-hybridization buffer.

2.2.6.2 Hybridization: DNA sample to be analysed was resolved on a 0.8% agarose gel. And DNA bands in the gel were visualised using UV gel documentation and the gel image was preserved for later analysis. This gel was pretreated by immersing in 0.125N HCl for approximately 10 min with shaking till the colour of the bromophenol blue changes to brown. This the gel was submerged in sufficient quantity of denaturation buffer for 30 min with gentle agitation till the colour of the bromophenol blue comes back to original. This is followed by submerging the gel in neutralization buffer for 30 min while shaking. Finally the gel was washed with 0.5X TBE for 2 times each for 2 minutes. Meanwhile Whatmann No.3 filter papers and Hybond N⁺ Nitrocellulose membrane were cut exactly into the same size and soaked into 0.5X TAE along with pre-treated gel for 10 min. Soaked Whatmann paper, nitrocellulose membrane, gel and Whatmann paper were placed one after the other in order without trapping the air bubbles on anode plate. Cathode plate was placed on the top of the whole set up and DNA was blotted on to the nitrocellulose membrane by passing 750 mA of current at 4V for 2h. After blotting, transfer apparatus was dismantled carefully and the membrane was placed on a paper towel wetted with 0.4N NaOH for exactly 5 min. This blot was further washed with 2X SSC buffer for 2 times 5 min each. Nucleic acid blotted onto the membrane was fixed by baking at 85°C for 2 h. These blots were used immediately or stored after thoroughly drying at room temperature under vacuum in sealed cover. For hybridization to continue blot was rinsed briefly with 2X SSC buffer and immersed in pre-hybridization buffer for 2h at 65°C and 40rpm. At the end of incubation time radio-labelled probe was made ready by keeping the probe for 5 min and immediately keeping on ice water bath for 2 min. This probe sample was added to freshly prepared pre-hybridisation solution and kept at 65°C for 16 h. The blot was

washed twice with 2X SSC buffer containing 0.1% SDS for 30 min each at 65°C. Finally the blot was packed in saran wrap and exposed to X-ray film in a hypercassette. Depending upon the radioactive count autoradiogram was developed within 2-4 days.

2.2.7 Gene Transfer Methods

2.2.7.1 Transformation

Preparation of Ultra-competent cells: A single colony of *E coli* DH5 α was taken from 16-20h old plate, inoculated into 25mL of LB broth and incubated at 37°C with vigorous shaking. Around 5mL of this culture was inoculated into 250mL of LB broth and incubated at 18-22°C for 20h with moderate shaking. The culture was allowed to grow till the culture density reaches to 0.55 when measured at 600nm. Cells from these cultures was harvested by centrifuging at 2500g for 10 min at 4°C and washed with 80mL of sterile ice cold Inoue transformation buffer (55mM MnCl₂·4H₂O, 15mM CaCl₂·2H₂O, 250mM KCl, 10mM PIPES, pH 6.7). Finally the cell pellet was resuspended in 20mL of ice cold Inoue transformation buffer along with 1.5mL of DMSO and kept on ice for 10 minutes. Working quickly, the cell suspension was distributed into 100 μ l aliquots in chilled sterile micro-centrifuge tubes and immediately snap-frozen in a bath of liquid nitrogen and stored at -70°C until further use.

Transformation: The frozen competent cells were thawed by placing them on ice bath. The ligation mixture/plasmid of interest was added and incubated on ice for 30 minutes. After 30 minutes, the cells were subjected to heat shock at 42 °C for exactly 90 sec and immediately chilled on ice for 2 min. Further, 800 μ l of LB broth was added and incubated at 37 °C for 45 min. The cells were collected by centrifugation and resuspended in 70 μ l of LB broth and plated on required selective LB media. When needed 2% X-gal and 1mM IPTG was added along with required antibiotic. The plates were then incubated at 37°C for more than 12 hr for colonies to appear.

2.2.7.2 Transduction

Phage P1 lysate preparation: In order to create mutant strains of *E coli* K-12 MG1655, 0.3mL of overnight culture of donor *E coli* strain was mixed with 8 μ l of P1 phage (10^7 Pfu) prepared on *E coli* K12 BW1153 mutant. Adsorption of P1 phage particles was allowed to occur for 15 min by incubating at 37 $^{\circ}$ C without shaking. This infection mixture was added to 10mL of LB broth along with 5mM CaCl₂ incubated with shaking at 37 $^{\circ}$ C for 3-6h till the lysis occurs. To the phage lysate 200 μ L of chloroform was added and shaken well. This preparation was centrifuged at 5000rpm for 10 min to remove the cell debris. Phage lysate prepared in this way was used for infecting the *E coli* K-12 MG1655.

Phage infection: To 2mL of overnight culture of *E coli* K-12 MG1655, and 100 μ l of phage preparation and 5mM CaCl₂ was added and phage adsorption was allowed to occur for about 15 min at 37 $^{\circ}$ C. Unabsorbed phage particles were removed by centrifuging for 10 min. Further 5mL of LB broth containing 5mM sodium citrate was added and allowed to incubate for 45 min at 37 $^{\circ}$ C. Finally the cells were pellet down and resuspended in 0.3 mL of fresh LB broth and plated on LB containing 5mM sodium citrate and 30 μ g/mL of kanamycin. Finally the mutation in respective gene was confirmed by performing PCR amplification with gene loci specific primers.

2.2.7.3 Conjugation

The mobilization of broad host range expression plasmids was carried out by using *E.coli* S17-1 and *Sphingobium fuliginis* as donor and recipient using the protocol described by Cornelis et al, 1975 with the following modifications as shown in the Fig 2-1. Donor and recipient cells were grown on LB medium along with appropriate antibiotics till the culture density reaches to $A_{600nm}=0.6$. The recipient cells were harvested and thoroughly washed with citrate saline buffer (pH.7.2) and finally resuspended in 50 μ l of citrate saline

buffer. These cells were then incubated at 45⁰C for 3 minutes, to inactivate the host restriction modification system. About 0.5ml of donor strain was added to the 50µl of recipient cells and spotted on 0.45 µm sterile filter membrane placed on a non selective wakimoto plates and incubated at 30⁰C for 4 hours. This mating mixture was scrapped with sterile tooth pick, serially diluted and plated on wakimoto plates containing polymyxin B and chloromphenicol. The donor and recipient cells were also plated on same antibiotic plates to check the contamination.

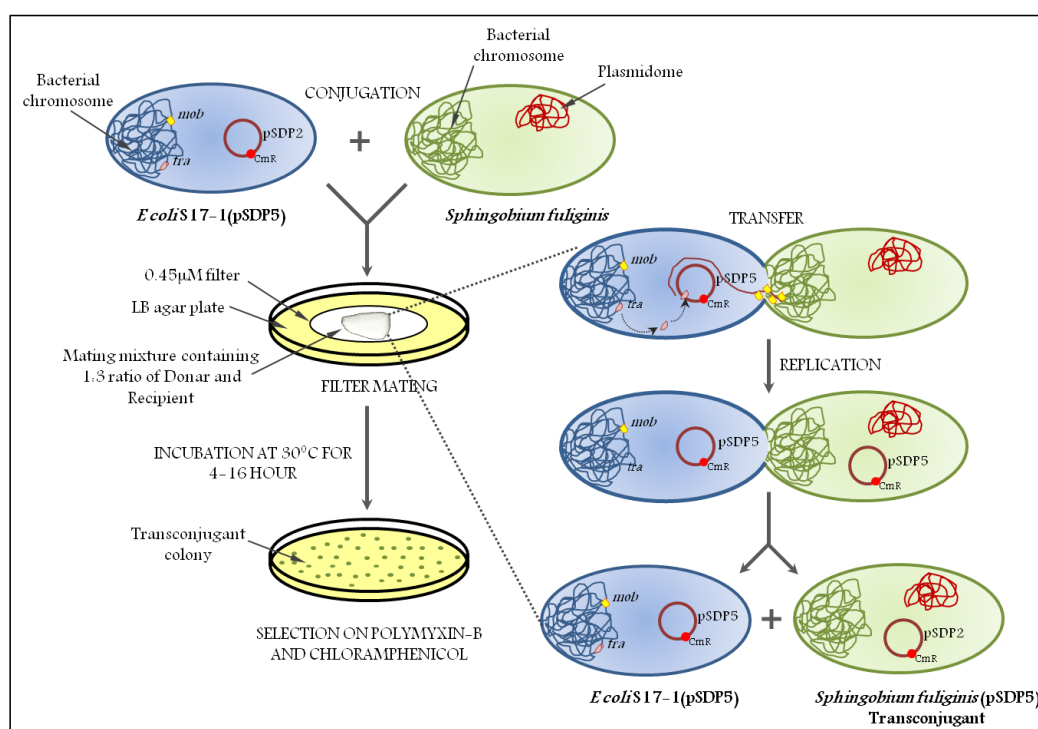


Fig 2-1| Pictorial representation of mobilization of pSDP5 into *Sphingobium fuliginis* ATCC 27551

2.2.8 Expression of MfhA

MfhA was expressed as a GST fusion protein (MfhA_{N-GST}) either in *E. coli* BL21 DE3 or in JM109DE3. *E. coli* BL21 DE3(pSDP4) was inoculated into 1000mL of LB broth containing appropriate antibiotic and incubated at 37°C till the culture density measured at 600nm, reached 0.5. Subsequently the culture was induced by adding IPTG to the medium to a final concentration of 0.9mM. The culture flask was immediately shifted to an

incubator maintained at 16°C. The induction process was continued for 20 hr. The cells were harvested from the induced culture by centrifuging at 8000rpm for 10 minutes. The cell pellet obtained was washed with phosphate buffered saline (PBS, pH. 7.3) and stored at -70°C until further use.

2.2.9 Purification of MfhA_N-GST protein

2.2.9.1 Affinity chromatography

The cell pellet obtained from the induced culture was resuspended by adding 7 mL of PBS saline per gram of cell pellet and the cells were lysed by sonication (Amplitude 30%, Temperature 4°C, and pulse on: 30 sec and pulse off: 30 sec for each cycle). The cell lysate was then centrifuged at 15000 rpm for 30 minutes and care was taken to keep the cell lysate at 4°C. The clear lysate obtained was applied to the Glutathione Sepharose-4B column pre-equilibrated with PBS saline. After passing the soluble cell lysate fraction through the column matrix, the column was washed with 20 column volumes of PBS saline (pH: 7.3). At each stage 50 µL of sample was collected to check the binding of fusion protein to the matrix. Finally the fusion protein was eluted using the buffer containing 50mM Tris-HCl (pH 8.0) and 10mM reduced glutathione. The eluted protein was analyzed on the SDS-PAGE to check the purity of the fusion protein.

2.2.9.2 Gel exclusion chromatography

As there were some impurities, mainly free GST in the affinity purified protein, it was again purified by passing through Sephacryl HR-200 column (1.5 x 30cm). Gel exclusion matrix was pre-equilibrated with PBS saline and the affinity purified protein sample was applied to the column connected to the FPLC system (AKTA Basic, GE healthcare, USA). The protein peaks monitored through the FPLC system were collected and analyzed on 12.5% SDS-PAGE to assess the extent of purity.

2.2.9.3 Thrombin cleavage

The concentration of fusion protein was estimated by standard Bradford's protein assay (Bradford 1976) and the GST tag was cleaved by incubating 100µg of fusion protein with 1U of thrombin at 20°C for 6-8 hr. Further the cleavage of GST tag was confirmed by running the sample before cleavage and after cleavage on SDS PAGE. The cleaved GST tag was further removed by Sephacryl HR-200 gel exclusion chromatography.

2.2.10 Purification of MfhA from inclusion bodies

Attempts to express *mfhA* with N-terminal GST tag has resulted in generation of number of truncated versions of MfhA_{N-GST}. The situation has created problem to purify full length MfhA_{N-GST}. To resolve this issue MfhA was expressed without any affinity tag. However, expression of native protein resulted in the formation of inclusion bodies. Therefore an attempt was made to refold the inclusion bodies of MfhA expressed from 150 mL culture of *E.coli* BL21 (pSDP6) which were induced by 1 mM IPTG at 37°C for 4 h in LB broth. The whole culture was then centrifuged at 10000 rpm for 10 min. One gram of this cell pellet was resuspended in 20mL of lysis buffer containing 50 mM Tris-HCl, pH 8.0, 10mM EDTA, 5% (v/v) Glycerol, 1mM DTT, 50mM NaCl, 1mM PMSF, 0.2% (w/v) Sodium deoxycholate (NaDOC) and 200 µg/mL lysozyme, and incubated on ice for 30 minutes. The cell suspension was then sonicated on ice for 3X30 sec bursts and then centrifuged at 15000 rpm. Supernatant was discarded and the pellet was washed with 20 mL wash buffer containing 50 mM Tris-HCl, pH 8.0, 0.1mM EDTA, 5% (v/v) Glycerol, 0.1mM DTT, 50mM NaCl, and 2% (w/v) Sodium deoxycholate (NaDOC) for 1 h by stirring at 4°C on a magnetic stirrer at 500 rpm. This suspension was then sonicated as above and centrifuged at 15000rpm for 20 min at 4°C. The pellet obtained was washed again for another 2 times and used for solubilization of the protein.

To solubilize the protein pellet, the pellet was resuspended in solubilization buffer containing 5M Guanidinium chloride, 50 mM Tris-HCl pH 8.5 and 400mM L-Arginine for 1 h. This was then centrifuged at 15000 rpm for 30 min at 4°C to remove unsolubilized protein. The solubilized protein was then added slowly to a refolding buffer (50mM Tris-HCl, pH: 8.0, 200mM L-Arginine) to get a final concentration of 50-250 µg per mL of the buffer. MfhA in this refolding buffer was kept at 4°C for 24 h to allow proper refolding of the protein. Later, the protein solution was centrifuged at 15000 rpm at 4°C for 30 min. to remove protein aggregates. The clear protein solution was then concentrated by using Amicon ultra filter (Millipore).

2.2.11 Protein interaction studies

2.2.11.1 GST pull down assay

In order to examine if MfhA interacts with the OPH (Organophosphate hydrolase) Magne GST Pull down system (Promega Biosciences, Inc. USA) was used as per manufacturer's protocol with slight modifications. Before performing GST Pull down assay, *E coli* JM109DE3 cells were transformed with expression plasmid pSDP4 coding MfhA_{N-GST}. This *E coli* strain containing pSDP4 was then used as host to transform second expression plasmid like pPHLC400 that codes for precursor organophosphate hydrolase (OPH) with C-terminal His tag (OPH_{C-6His}). Control cultures having only vectors and either of the expression plasmids were induced as mentioned in earlier section. About 50 mg of the cell pellet was taken from each of these cultures and lysed using 200 µL of MagneGST cell lysis reagent. The lysate was then incubated with 2 µL of RQ1 RNase free DNase for 1 hr at room temperature on a rotating platform. About 20µL of pre equilibrated MagneGST-Glutathione particles were added to cell suspension and the contents were incubated for 1hr at room temperature on a rotating platform. Later the MagneGST-Glutathione particles were captured by placing on the magnetic stand. These particles were

washed 3-4 times with Magne GST washing buffer. Finally 5 μ L of MagneGST-Glutathione particles obtained from each of the culture were mixed with 20 μ L of 1X SDS loading buffer and analyzed on SDS PAGE following the standard procedure.

2.2.11.2 Western Blotting

Protein interactions between MfhA_{N-6His} or MfhA_{N-GST} and OPH were monitored by performing western blots. The expression plasmid coding for MfhA has N-terminal GST-tag, similarly the OPH coded by plasmid pHLNS400 contain C-terminal His-tag. The protein extracts prepared from cultures having appropriate expression plasmids and control vectors were analyzed on 12.5% SDS-PAGE and transferred on to PVDF membrane (Amersham Pharmacia Biotech Ltd, UK). Western blots were performed using anti-GST antibody to detect MfhA_{N-GST}. After detecting the MfhA_{N-GST} the membrane was completely stripped out from the antibodies by immersing in stripping buffer followed by incubating at 50⁰C for 30 minutes with occasional agitation. The membrane was then washed with large volumes of TBS-T buffer before blocking using 10% skimmed milk powder in TBS-T. The blocked membrane was then reused to perform western blot using anti-OPH antibody . The second western indicates presence of OPH. The specific protein bands on the western blot were detected by using ECL plus western blot detection kit (GE Health Care, USA) by following the manufacturer's protocol.

2.2.11.3 Sub-cellular localization of MfhA in *Sphingobium fuliginis*

MfhA_{N-6His} was expressed in *Sphingobium fuliginis*. 250mL of LB broth was inoculated with 2.5mL overnight culture of *Sphingobium fuliginis* (pSDP5) and grown at 30⁰C at vigorous shaking till the culture density reaches to A_{600nm}=0.5. To this culture 1M IPTG was added to attain a final concentration of 5mM. The culture was allowed to induce for 16h at 30⁰C with shaking of 200rpm. Cells were harvested from the culture medium and washed once in 40mM Tris-Cl pH 8.0. Finally the cells were resuspended as 1 gm in

7mL SET buffer (10mM Tris pH 8.0, 1mM EDTA, 50mM sucrose) and lysed by sonication. Cell debris and unbroken cells from the lysate were removed by spinning at 15000rpm for 30 min. The clear supernatant obtained was then subjected to ultracentrifugation for 45000rpm for 60 min. Membrane fraction obtained in the pellet fraction was separated and resuspended in the same volume of SET buffer. Finally the presence of MfhA_{N-6His} in the cell lysate, cytosolic and membrane fractions was detected by performing western blotting with anti-His antibodies.

2.2.12 Construction of pCMS1 fosmid library

Fosmid DNA library for indigenous plasmid, pCMS1 was generated by using CopyControl™ Fosmid Library Production Kit, Epicentre Biotechnologies, USA following the manufacturer's protocols. Plasmid pCMS1 was isolated from *B. diminuta* and mechanically sheared by vortexing at 500 rpm for 2 minutes. The plasmid DNA fragments thus obtained were end repaired using end-repair enzyme mix and subsequently ligated into Cloning-Ready CopyControl pCC1FOS vector. This ligation mixture was packaged into MaxPlax Lambda Packaging Extracts, and infected to EPI300-T1^R plating strain. Further the clones were grown overnight on chloramphenicol plates to obtain chloramphenicol resistant colonies having recombinant fosmid.

2.2.13 TwoD Electrophoresis

In order to gain information on MfhA mediated changes in the proteome profile of *E. coli* TwoD electrophoresis was performed. *E. coli* MG 1655 harboring either pSDP2 or pMMB206 was grown in minimal medium (1 gm NH₄Cl, 3 gm K₂HPO₄, 6 gm Na₂HPO₄, 0.5 gm glucose, 0.01 gm CaCl₂ and 0.12 gm MgSO₄) until the culture density reaches 0.5. The cultures were then induced with 0.5mM IPTG to a final concentration and were allowed to grow at 30°C until the culture density reaches 0.8-0.9. At this stage the cultures

were harvested and washed with 40mM Tris-Cl pH 8.0 and stored at -80°C until further use.

2.2.13.1 Preparation of protein sample for TwoD Electrophoresis

E. coli cell pellet obtained was lysed in 5ml of 40mM Tris-Cl, pH 8.0 by sonication with 30 seconds pulse on and 30 seconds pulse off for 5 cycles. The cell lysates were then centrifuged at 15000 rpm for 20 min to remove the unbroken cell debris. The supernatant obtained was further centrifuged at 45000 rpm for 60 min at 4°C to remove lipid and nucleic acid contamination. Proteins present in the supernatant fraction were precipitated by methanol: chloroform precipitation. Around 100µl of protein sample was taken in a 1.5mL eppendorf tube, to this 400 µl of methanol was added and vortexed. To this suspension 100 µl of chloroform was added and mixed thoroughly by vortexing. This is followed by the addition of 300 µl of sterile milliQ water. The whole contents were mixed by vortexing for 2 min and centrifuged at 13000rpm for 2 min, aqueous phase formed on the top of the protein layer was carefully separated and discarded. The protein content in the preparation was finally precipitated by the addition of 400 µl of methanol followed by thorough vortexing and centrifugation at 13000 rpm for 2 min. Finally the supernatant was discarded and the pellet was air dried and used immediately (BARNIDGE *et al.* 1999). The precipitated protein pellet was air dried and resuspended completely in TwoD sample preparation buffer containing 7M Urea, 2M thiourea, 2% NP-40, 2% 3-11, NL Ampholytes, 40mM DTT and 0.002% Bromophenol blue for 4 hr at 20°C. Undissolved protein in the sample was eliminated by centrifuging at 15000 rpm for 20 minutes.

2.2.13.2 Iso-electric focusing (IEF): Protein (200 µg) dissolved in 320 µl of TwoD sample preparation buffer (7M Urea, 2M thiourea, 2%CHAPS, 2%NP-40, 40mM DTT, 0.0025% bromophenol blue dye, 2% 3-11NL pharmalytes) was loaded on 18 cm 3-10 NL

IPG strip (Amersham Biosciences, USA) for 1 hr. Further the strip is actively rehydrated for 12 hrs at 20 V and isoelectrofocussing was performed on EttanIPG phor 3 system using a four step programme [500 V for 30 min (gradient), 500 V for 30 min (step), 10000 V for 3 hr (gradient) and continued till 60000 V hr]. Finally the strips were equilibrated in equilibration buffer [75mM Tris, 6M Urea, 2% SDS, 20% glycerol] containing 2% DTT for 30 minutes followed by 30 minutes equilibration in equilibration buffer containing 2% Iodoacetamide. The 2nd dimension electrophoresis was performed in 12.5% SDS-PAGE in a Ettan DALTsix system (GE Healthcare) at a constant voltage of 200 V. The gels were stained by colloidal coomassie staining protocol (27) and image analysis of the gel is performed using Image Master TwoD platinum software (GE Healthcare). Protein spots whose volume ratios are more than 1 when compared to the same in protein spot of control culture were considered as overexpressed and are picked up for MALDI analysis.

2.2.13.3 In-gel digestion

The protein spots identified by the image analysis were excised manually from the gel and the gel pieces were destained with a solution of LC-MS grade Acetonitrile (ACN) and 25 mmol/l NH_4HCO_3 in 1 : 1 (v/v), dried with ACN and reduced with dithiothreitol (DTT) in 25 mmol/l NH_4HCO_3 for 1 h at 50°C, alkylated using a 55 mmol/l iodoacetamide in 25 mmol/l NH_4HCO_3 for 45 min at room temperature. The gel pieces were dehydrated with ACN, rehydrated with a minimum volume of 50 mmol/l of NH_4HCO_3 containing Trypsin (10 ng/ μl), and digested at 37°C for 16 hours. The peptides were extracted twice with 50% (v/v) ACN containing 1% (v/v) trifluoroacetic acid (TFA). The peptide mixture was concentrated under vacuum in a Concentrator (Eppendorf) for 10 h at room temperature.

2.2.13.4 MALDI-TOF/TOF

The tryptic peptides were dissolved in 2 μl solution of 50% (v/v) ACN containing 1% (v/v) TFA and mixed with 2 μl of 1% cyano-4-hydroxycinnamic acid (HCCA) dissolved in

50% ACN and 1% TFA and 1 μ l of it was applied on the MALDI target plate. Peptides were analysed using MALDI TOF/TOF Autoflex (Bruker Daltonics) in reflectron mode. MS/MS of selected peptides were performed by LIFT. The spectra were calibrated by Pepmix (Bruker Daltonics). The spectral data were analysed using Biotoools software and searches were performed for protein identification using MASCOT search engine (<http://www.matrixscience.com>) against NCBI nr (<http://www.ncbi.nlm.nih.gov/>). The following search parameters were used: trypsin is the enzyme and one missed cleavage was allowed, the peptide tolerance was set at ± 0.4 -1.8 Da, carbamidomethyl and oxidized methionine were set as fixed and variable modifications respectively. MS/MS data was analysed using Biotoools software and mass tolerance of ± 0.2 -1.2 Da was used.

2.2.14 Esterase assay of MfhA

Esterase activity of MfhA was assayed by the method of Higgins and Lapides (HUGGINS 1947) and Krish (KRISCH 1966). Enzyme assay was done in 1 mL reaction volume containing 50 μ g of MfhA in 75mM potassium phosphate [pH 7.0] containing 10mM MgSO₄. The substrate 4-nitrophenyl acetate (PNP-Ac) was added at different concentrations ranging from 15 to 75 μ M from stock solution prepared by dissolving the compound in 100% ethanol. The reaction mixture was kept at 30°C for 2 hr and release of PNP was measured at 405 nm in Shimadzu UV-1800 spectrophotometer with the automatic zero, reference control. The enzyme activity was expressed in nanomoles of PNP released per min per mg of protein (the extinction coefficient of PNP at 405nm is 9940 liters / mole / cm).

2.2.15 *p*-Nitrophenol (PNP) supported growth in *E. coli* K-12 MG1655 (pSDP5)

One mL overnight culture of *E. coli* K-12 MG1655 harboring either pMMB206 or pSDP5 was washed for 2 times with minimal medium containing 0.5% glucose and grown at 37°C with shaking until the culture density reaches to 0.45-0.5 (A_{600nm}). The cells were

then harvested and washed twice with minimal salts medium. Finally the cell pellet was resuspended in minimal volume of minimal salts medium and inoculated to the PNP supplemented (100 μ M) minimal medium to a final cell density of 0.1-0.2. After this the cells were allowed to grow at 30 $^{\circ}$ C and depletion of PNP concentration was observed regularly by monitoring absorbance at 410nm. When the supplemented PNP was depleted 100 μ M PNP was freshly added and the change in cell density was observed by taking OD value at 600nm. The experiment was done in triplicates and growth curve was constructed.

2.2.16 Oxygraph studies

During the degradation of PNP, in *E. coli* (pSDP5) culture medium, rate of oxygen consumption was measured polarographically in a Clark-type oxygen electrode (Hansatech Oxytherm Electrode Unit) equipped with high sensitivity membrane. Approximately 1 ml of cell suspension ($A_{600nm}=1.2$) in 100mM Potassium phosphate buffer (pH 7.2), was transferred to oxygraph chamber sealed with a hollow-core glass stopper. The suspension was mixed vigorously using a micro-stir bar and stir plate and micro volume (10 μ l) injections were made through the centre of glass stopper from 50-100 μ M PNP solution. 10-20 min of oxygen uptake data was recorded using oxygraph software.

2.2.17 Nitrite estimation in the culture medium

The amount of nitrite released into the culture medium was estimated by following the procedure described by Barnes and Folkford, 1951 (BARNES H AND FOLKFARD A.R. 1951). Cells were harvested from the induced *E. coli* K-12 MG1655 (pSDP5) cultures and resuspended them in minimal medium to get a cell density of 1 O.D. The culture was then supplemented with PNP (100 μ M) and incubated at 37 $^{\circ}$ C. At every 30 min of time interval 2mL of this culture was withdrawn and cells were harvested from the medium by centrifugation. This spent medium (1mL) was taken into a new test tube and 25 μ l of 0.8%

sulphanilic acid in 5N v/v acetic acid was added and incubated for 2 minutes at room temperature. After incubation 25 μ l of 0.6% 1-Naphthylamine in 5N acetic acid was added. The contents were thoroughly mixed, before measuring absorbance at 543nm. The resulting 1 mL of spent medium was used to measure the amount of PNP present in the culture medium by taking absorbance at 410nm.

2.2.18 Isolation and characterization of PNP degradation products

2.2.18.1 Resting cell assay

E coli K-12 MG1655 (pSDP5) grown in minimal medium supplemented with glucose as carbon source was induced with 1mM IPTG. This culture is harvested and inoculated in minimal medium supplemented with PNP as sole source of carbon. *E coli* (pMMB206) obtained under same conditions was taken as control. All the cultures were taken at a cell density of $A_{600} = 1.2$ and incubated for 3 hr after adding 0.5M PNP. About 200 μ L sample was taken for every one hour and the cell free spent medium (10 μ L) obtained after centrifugation was injected into C18 column (4.6 x 250 mm) using a binary pump HPLC. An isocratic buffer system of 50% (v/v) methanol having 0.02% (v/v) acetic acid was used at a flow rate of 0.75 ml/min. The spectrum was recorded for 20min at UV range (254 nm). When necessary, similar experiments were done by using stable isotope of PNP, 4-Nitrophenol-2,3,5,6-d₄ (D⁴-PNP) in place of normal PNP.

2.2.18.2 HPLC-MS/MS analysis of PNP metabolites

While performing the LC MS/MS analysis of PNP metabolites, 100 μ l of reaction mixture was mixed with excess of methanol (1 mL) and centrifuged at 12000 rpm for 5 min. The clear supernatant was further evaporated and reconstituted in 50% methanol containing 0.1% formic acid. In-line MS/MS was performed using a Agilent mass spectrometer with a Z-Spray electrospray interface in the negative mode, specifically with a capillary voltage of -3.10 kV and cone voltage of -60 V. Nitrogen was used for both the cone gas (160 l/h)

and the desolvation gas (600 l/h), with the source and desolvation temperatures being held at 80°C and 350°C, respectively. During daughter ion analysis (DIA), argon was used as the collision gas and was present in the collision chamber at 1.6×10^{-3} mbar with a collision energy of 25 V. All DIA results reported here used specific parent ion(s) selected in MS1 and were further fragmented in MS2 before display as total ion current (TIC) or as full mass spectra (m/z 50–350).

2.2.19 β -Galactosidase assay

The β -galactosidase activity was made by essentially following the protocol described by Miller, 1972 (MILLER 1972). Cells harvested from the 2mL of the *E coli* or *Sphingobium fuliginis* were taken and centrifuged at 6000rpm for 10 min. After discarding the supernatant cells were resuspended in same volume of chilled Z-buffer. The cell density of this suspension was measured at 600nm. The cells were further diluted as 1:1 or 1:10 with Z-buffer in 1mL and permeabilized by adding 100 μ L of chloroform and 50 μ L of 0.1% SDS. Mix the cells by vortex and kept at 28°C for 5 min. In order to initiate the reaction 0.2mL of 4mg/mL ONPG was added to the cell suspension. The samples were incubated at 28°C until the faint yellow color is developed. The reaction was stopped by adding 0.5mL of 1M sodium carbonate. The time length of incubation was recorded. The reaction mixture was then centrifuged at maximum rpm for 5 min and 1mL of clear supernatant was taken to check the absorbance at 420nm and 550nm. Control culture containing only pMP220 plasmid was processed under the same experimental conditions and used as blank. The β -Galactosidase activity was expressed in Miller Units.

$$\text{Miller Unit} = \frac{1000 \times [A_{420\text{nm}} - 1.75 \times A_{550\text{nm}}]}{T \times V \times A_{600\text{nm}}}$$

Where T is the length of incubation time and V is the volume of the cells in mL.

2.2.20 Isolation of RNA

In order to isolate RNA from *E coli* cultures having either expression plasmid pSDP5 or vector pMMB206, the cells were induced to express MfhA collected at cultures at a regular time interval (0h, 1.5h, 3.0h) and RNA was isolated using qiagen RNeasy Minikit following manufacturer's protocol with minor modifications. A cell pellet containing approximately 7.5×10^8 Cfu was obtained from the culture medium and resuspended in 200 μ l of TE buffer (10mM Tris-Cl and 1mM EDTA, pH8.0) containing 1mg/mL of lysozyme. The cells were resuspended for 10 Sec with vigorous vortexing and incubated at room temperature for another 5 min with intermittent vortexing for every 2 min. After addition of RLT buffer (700 μ l) the cell suspension, was vortexed and centrifuged briefly to remove particulate matter. Further 500 μ l of absolute alcohol was added to the lysate and mixed thoroughly. This mixture was then applied to the RNeasy Mini spin column placed in a 2 mL collection tube and centrifuged at 11000xg for 1 min. About 95 μ L of DNase reaction mixture was added to the center of the column and incubated at room temperature for 15 min. This is followed by inactivation of DNase by adding 200 μ L of RA2 buffer to the column and centrifuged for 1 min at 11000xg. Further the flow through was discarded and RNeasy mini spin column was taken into a fresh collection tube and washed with 500 μ l of RPE buffer for two times by centrifuging at 8000xg for 2 min. Finally mini spin column was taken into a new collection tube and 30-50 μ l of RNase free water was added to the center of the spin column to elute the bound RNA. To perform microarray analysis RNA preparations were analyzed using the Agilent 2100 Bioanalyzer (Agilent Technologies) to verify sample quality and integrity. Each sample that met the criteria $A_{260}/A_{280} \geq 2.0$ and $A_{260}/A_{230} \geq 1.9$ were taken for quantitative measurement of specific gene. Concentrations of total RNA and cDNA samples were determined using a NanoDrop ND-1000 spectrophotometer (Thermo Scientific).

2.2.21 Microarray

2.2.21.1 cDNA synthesis, labeling and microarray hybridization

cDNA was synthesized for total RNA isolated from different samples as mentioned above, using the Superscript Double-Stranded cDNA Synthesis system (Invitrogen) according to the manufacturer's instructions. The cDNA was then labelled and hybridized by Agilent's Quick-Amp labelling kit (p/n:5190-0442) and Agilent's *In situ* Hybridization kit 5188-5242 respectively according to their standard protocols. Briefly, cDNA was labeled with Cy3 using the Random hexamer method of labelling followed by T7 promoter based-linear amplification to generate labelled complementary RNA (One color Microarray-Based Gene Expression Analysis). Following hybridization, microarrays were washed and scanned using a GenePix 4000B Scanner (Agilent). Data were extracted and analyzed using the GeneSpring GX 11.5 Software, which normalizes expression data using Percentile shift normalization and Microsoft excel.

2.2.21.2 *E. coli* K12 MG1655 gene-specific microarray and data normalization

The *E. coli* K-12 MG1655 microarray (Agilent control grid: IS-15744-8-V1_8x15K_Gx_EQC_V20060608) contains 14 to 60-mer perfect match probes 3 for each of 4294 coding regions available, 1 probe for each of the 172 structural RNA sequences and 2 probes for each 2240 non-coding regions available, altogether these probes represent 15208 probes designed from the annotated *E. coli* K-12 MG1655 genome http://www.ncbi.nlm.nih.gov/entrez/viewer.fcgi?db=nucleotide&val=NC_000913 as shown fig 1 and commercially analysed at Genotypic pvt. Ltd, Bengaluru. Gene expression heat maps were generated using TreeView 1.60.

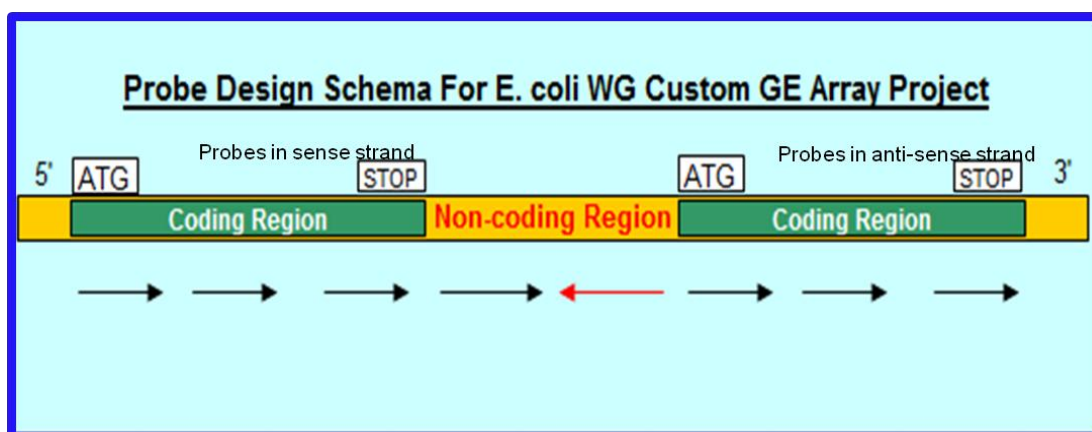


Fig 2-2| Pictorial representation of probes designed for microarray

2.2.22 Quantitative Real Time PCR

In continuation to microarray analysis transcript levels of different genes were quantified using the RNA and cDNA as described above. Reactions were conducted in a Eppendorf qPCR machine operating with Realplex 2.2 software using 30 ng cDNA template, 0.25 μ M primers, and Brilliant SYBR Green reagents (Biorad). Data were normalized to *16sRNA* and analyzed by absolute quantification by comparing the CT value of the test sample to a standard curve.

2.2.22.1 Primer design and selection of target sequence for qPCR

When multiple gene expression analysis was performed 16S rRNA gene was taken as internal control for the expression calibration of other genes. DNA sequences of target genes of *E. coli* were retrieved from GeneBank. Primer 3 program available online was used for the primer design (<http://www.ncbi.nlm.nih.gov/tools/primer-blast/primertool.cgi>). For each target gene, a primer pair capable of amplifying a DNA fragment of about 150-250bp were chosen and commercially synthesized at Sigma-Aldrich pvt. Ltd, Bengaluru.

2.2.22.2 Absolute quantification of target genes

In order to quantify the expression levels of target gene the amplicons of each of the target gene was cloned into pTZ57T/T easy T-vector. Using these constructs as template, a 10-

fold dilution series was made resulting in a set of standards containing 10^2 - 10^7 copies of the target gene. The standards and test samples were assayed in the same run. A standard curve was constructed, with the logarithm of the initial copy number of the standards plotted along the x-axis and their respective C_T values plotted along the y-axis. Finally the copy number of the target gene in the test sample was obtained by interpolating its C_T value against the standard curve.

Results and Discussion|Chapter 1

3.0 Background

Organophosphate (OP) pesticides are the most recently introduced xenobiotic compounds (about 65 years ago) as an alternatives to the most persistent organochlorine pesticides (DAVIES 1985). They are also being used as plasticizers, petroleum additives and warfare agents etc (DRAGUN 1984; DUMAS *et al.* 1989; BENNING *et al.* 2000; RAUSHEL 2002). Due to their potent inhibitory nature to acetylcholine esterase (AChE), many neuro-pathological disorders and serious illnesses have been reported either by direct intake or as a continuous exposure to a low doses to these compounds (SINGH and SHARMA 2000; RITTER *et al.* 2002; SINGH and KHURANA 2009). In many developed countries usage of these pesticides was banned. However, their usage is still continued in many underdeveloped and developing countries due to lack of alternative technologies to control agricultural pesticides. Despite of having toxic effects on humans and other higher animals, a wide range of soil bacteria have shown ability either to transform or mineralize several OPs used as insecticides (SETHUNATHAN and YOSHIDA 1973; DEFRANK and CHENG 1991; SOMARA and SIDDAVATTAM 1995; FU *et al.* 2004; ZHANG *et al.* 2006; PAKALA *et al.* 2007; GHANEM *et al.* 2007). Such remarkable property of soil bacteria is attributed to the presence of novel esterases known as phosphotriesterases (PTEs) (BIGLEY and RAUSHEL 2012). They hydrolyse triester linkage found in structurally diverse group of organophosphates and make them less toxic to mammals. The known PTEs reported till date are grouped into three distinct classes viz., organophosphate hydrolase (OPH), Methylparathion hydrolase (MPH) and Organophosphate acid anhydrases (OPAA) (DUMAS *et al.* 1989; BENNING *et al.* 2000; RAUSHEL 2002; SINGH and WALKER 2006). The OPHs found in geographically and taxonomically distinct soil bacteria are highly conserved (SERDAR *et al.* 1982; SOMARA and SIDDAVATTAM 1995; SIDDAVATTAM *et al.* 2003). They belong to the amidohydrolase superfamily and have a TIM (β/α)-barrel fold

and an active site with two transition metal ions such as cobalt, manganese, or zinc (VANHOOKE *et al.* 1996). The OPHs show highest catalytic activity towards organophosphates (OPs), the catalytic rates approach close to the diffusion limit ($K_{cat}/K_M > 4 \times 10^7$) where paraxon is used as substrate (RAUSHEL and HOLDEN 2000). Though OPH acts on a wide range of OP compounds, the precise physiological substrate is still unknown. It is coded by a 1.5 kb *organophosphate degrading (opd)* gene and is associated with the transposable elements (SIDDAVATTAM *et al.* 2003; HORNE *et al.* 2003). High catalytic efficiency on OP compounds like paraxon and their genetic location adjacent to the transposable elements suggests that the OPHs have recently been evolved to withstand stress conditions generated due to continuous addition of OPs to agricultural soils. Existence of weak lactonase activity and striking structural similarities of OPH with quorum quenching lactonases suggests evolutionary link between OPH and lactonases (AFRIAT *et al.* 2006; ELIAS *et al.* 2008; ELIAS and TAWFIK 2012).

Second group of PTEs are methyl parathion hydrolases (MPHs). They are purified from bacterial strains isolated from methyl parathion polluted soil samples. The MPHs hydrolyse methyl parathion more efficiently than parathion. Therefore, they are designated as methyl parathion hydrolases (CHU *et al.* 2003). The gene encoding MPH (*mph*) is also shown to be a part of complex transposon (ZHONGLI *et al.* 2001; LIU *et al.* 2005). The *mpd* genes isolated from different genera collected from different geographical locations of China were found to be identical (ZHANG *et al.* 2006). Infact Wei et al, have demonstrated transposition of *mph* element in *Pseudomonas putida* PaW340 and *Ralstonia* sp. U2 (WEI *et al.* 2009). If organization of *mph* as mobile genetic element is seen together with high level sequence similarities of *mph* genes collected from taxonomically diverse bacterial strains, horizontal gene transfer (HGT) of *mpd* genes among soil bacteria is apparent.

Phylogenetic analysis and structural studies have pointed towards having β -lactamases as progenitors for MPH enzyme (DONG *et al.* 2005; TIAN *et al.* 2008).

Third group of PTEs are organophosphate acid anhydrolases (OPAAs) isolated from *Alteromonas sp.* and *Agrobacterium radiobacter* P230 (DEFRANK and CHENG 1991; CHENG *et al.* 1993; DEFRANK *et al.* 1993; HORNE *et al.* 2002). They hydrolyze broad range of G-type chemical warfare (CW) nerve agents. The OPAAs are later shown to be prolidases, the dipeptidases that act on the peptide bond contributed by Xaa-Pro (CHENG *et al.* 1996; CHENG *et al.* 1997). Their activity on nerve agents was found to be due to structural similarities between di-peptides and nerve agents. Therefore, among these three known PTEs, the physiological substrate is only known for OPAA. The physiological substrates for other two classes of PTEs, viz OPH and MPH are still unidentified. They appear to have evolved from quorum-quenching lactonases and β -lactamases by divergent evolution, probably due to presence of increased concentration of OP compounds in soil samples (ELIAS and TAWFIK 2012).

Lateral transfer (LT) of genes containing drug resistance, pathogenicity and catabolism of recalcitrant compounds is quite evident among microbial communities (JUHAS *et al.* 2009). In general LT of genetic elements is achieved either by direct uptake of DNA or by establishing physical contact between donor and recipient bacteria. Conjugation is one of the oldest and well studied mechanisms of LT (TATUM 1946). In conjugation the Type IV secretory system is involved in LT of self transmissible plasmids (DING *et al.* 2003; SILVIA RUSSI 2008). Recent studies have shown involvement of Type IV secretory system in LT of genomic islands (GIs). The GIs have been shown to have type IV secretory system along with site specific integrase, relaxase and other components that confer resistance to drugs, pathogenicity or catabolism of aromatic compounds. The LT of *mph* elements is experimentally proved (WEI *et al.* 2009). Existence of *mph*

elements on plasmids and presence of identical *mph* genes among soil bacteria strengthens the proposition of LT of *mph* genes among soil bacteria.

Identical *opd* genes are found either on plasmid or on chromosome (HARPER *et al.* 1988). Such wide spread distribution of identical *opd* genes among taxonomically distinct bacteria, that to isolated form a diverse geographical regions, suggests existence of horizontal gene transfer (HGT) in spreading the *opd* genes among bacterial communities. However till date there exists no experimental evidence pertaining to the HGT of *opd* genes. The present study is therefore undertaken to unravel mechanisms involved in HGT of *opd* genes. *Flavobacterium* sp. ATCC27551, reclassified as *Sphingobium fuliginis* ATCC 27551, is the first OP compound degrading bacterium isolated from the diazinon contaminated agricultural soils of Philippines (SETHUNATHAN and YOSHIDA 1973). Subsequently, parathion degrading *Brevundimonas diminuta* MG was isolated from the agricultural soils of Texas, USA (SERDAR *et al.* 1982). In both the cases the *opd* gene was found on large dissimilar plasmids (MULBRY *et al.* 1986; MULBRY *et al.* 1987). However a 7.1 kb region found around the *opd* gene was identical between these two dissimilar plasmids. Beyond this 7.1 Kb, no homology is seen between these two indigenous plasmids. In pPDL2, this 7.1Kb conserved region containing *opd* gene was found as part of a complex transposon (SIDDAVATTAM *et al.* 2003). While gaining further evidence on HGT of *opd* genes our laboratory has generated complete sequence for the 40 kb plasmid, pPDL2 isolated from *Sphingobium fuliginis* ATCC 27551. We have also generated sequence to the *opd* containing region of plasmid pCMS1 isolated from *B. diminuta*. The work presented in this chapter describes well designed genetic experiments to show HGT of *opd* genes among soil bacteria.

3.1 Physical comparison of *opd* regions between pCMS1 and pPDL2

Our lab has generated complete sequence information for plasmid pPDL2 isolated from *S. fuliginis* ATCC 27551 (PANDEETI *et al.* 2012). Generating sequence of pCMS1, especially for the conserved *opd* region is expected to provide information pertaining to the acquisition of *opd* cluster. If it is through transposition, inverted repeat (IR) and direct repeat (DR) sequences will be seen at the flanking regions of *opd* cluster. Therefore in this study, sequencing was done to the *opd* cluster found on plasmid pCMS1. Initially, a fosmid library was constructed to isolate *opd* cluster and to generate its physical map.

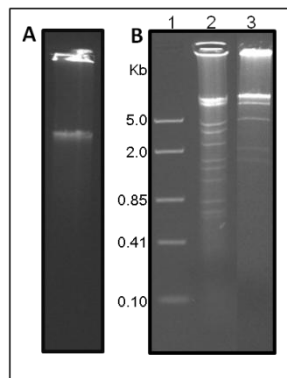


Fig 3-1a| Plasmid pCMS1 isolated from *B. diminuta* (Panel A) The *SalI* (Lane 2) and *BamHI* (Lane 3) restriction profile is shown in Panel B

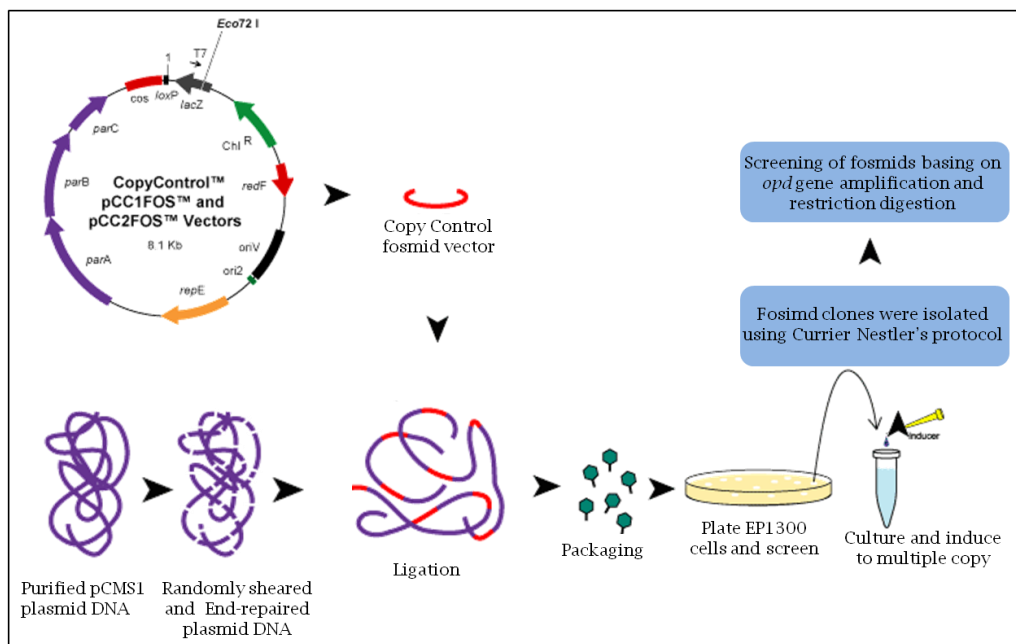


Fig 3-1b| Construction of fosmid library of pCMS1 isolated from *B. diminuta*

3.1.1 Construction and screening of fosmid library

pCMS1 plasmid was isolated from *B. diminuta* by Currier Nester's protocol as mentioned in materials and methodology section (CURRIER and NESTER 1976). After observing the similarities between the restriction pattern of isolated pCMS1 plasmid with that of the published restriction profile (MULBRY *et al.* 1987) it was used to construct fosmid library [Fig 3-1]. Fosmid DNA library for 66 Kb pCMS1 was generated by using CopyControl™ Fosmid Library Production Kit, Epicentre Biotechnologies, USA following the manufacturer's protocols. The pCMS1 plasmid was isolated and mechanically sheared by vortexing at 500 rpm for 2 minutes. The plasmid DNA fragments thus obtained were end repaired using end-repair enzyme mix and subsequently ligated into Cloning-Ready CopyControl pCC1FOS vector. This ligation mixture was packaged into MaxPlax Lambda Packaging Extracts, infected to EPI300-T1^R plating strain. The infected EPI300-T1^R was then plated on chloramphenicol plates and grown for overnight. About 19 fosmid colonies were obtained; clones from all of them have shown unique restriction profile indicating cloning of fragments from different regions of pCMS1. These recombinant fosmid containing *E. coli* cells were screened initially by colony PCR using *opd* specific primers PDS3 (5'- GGG TGC GCG AGC GTG CAT ATG TCG ATC GGC ACA GGC-3') and PDS4 (5'-GGA TCC AGA TGC TCG AGT GAC GCC CGC AAG G-3'). One of these fosmid clones, fosmid 15 gave *opd* specific amplification. The recombinant fosmid containing *opd* region of pCMS1 was isolated and its restriction profile was generated. The restriction profile of this recombinant fosmid was then compared with the restriction profile of plasmid, pCMS1 [Fig 3-2]. The recombinant fosmid clone pCMS-A showed existence of considerable lengths of upstream and downstream region of conserved *opd* cluster. In fact, the insert found in pCMS-A measured nearly half of the 66 Kb pCMS1 plasmid and hence it was taken for obtaining

the sequence of flanking regions of the *opd* cluster. Further, based on the restriction profile, the recombinant fosmid, that contained complete pCMS1 DNA in an overlapping manner were selected and used for further studies. As shown in fig 3-2A the recombinant fosmids pCMS-B and pCMS-C were found to have complete pCMS1 DNA in an overlapping manner. The restriction profile of plasmid pCMS1 and the extent of pCMS1 DNA found in the recombinant fosmids were shown in Fig 3-2.

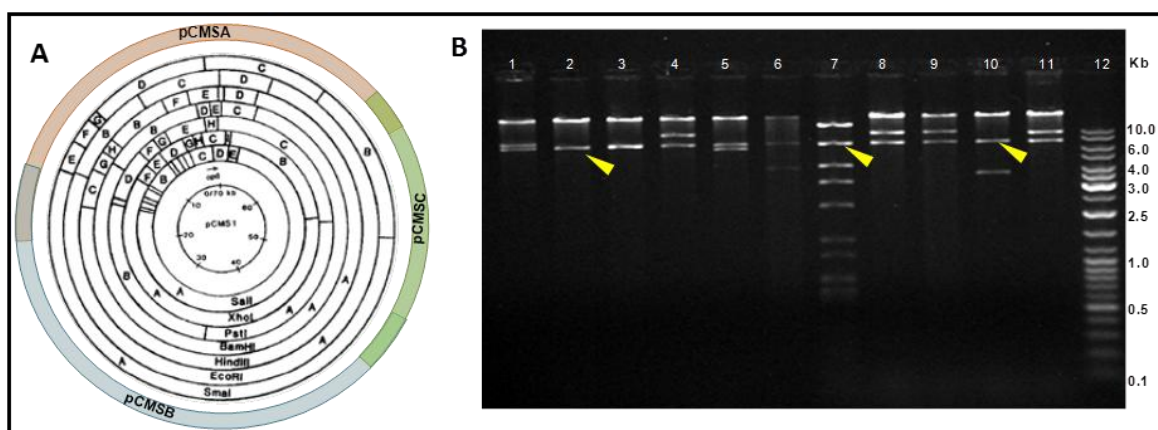


Fig 3-2| The restriction pattern of pCMS1 is taken to show the extent of pCMS1 DNA cloned in recombinant fosmids (Panel A). The *SalI* restriction pattern of pCMSA (Lane 7), pCMSB (Lane 2), and pCMSC (Lane 10) are shown in Panel B. The overlapping regions are indicated with arrow marks.

3.1.2 Cloning of flanking region of *opd* cluster

As stated before plasmids pCMS1 and pPDL2 contain identical *opd* genes. As shown in fig 3-3, the *opd* gene has unique *XhoI* and *SalI* sites. Fosmid pCMS-A was digested with *XhoI* and the resulting 1.141 Kb fragment was subcloned in pBluescript KS II(-). As shown in fig 3-3 it will have considerable upstream region to the conserved *opd* gene. Simultaneously, the 2.262 Kb *SalI* fragment provides DNA region found downstream of conserved *opd* cluster of pCMS1. These constructs were then sent for sequencing and the sequence generated was analysed using ORF finder software (www.ncbi.nlm.nih.gov/projects/gorf/). Polypeptides coded by predicted to be encoded by

each of these predicted ORFs, were analysed using NCBI-BLAST. The sequence strategy of pCMSA is shown in Fig 3-3.

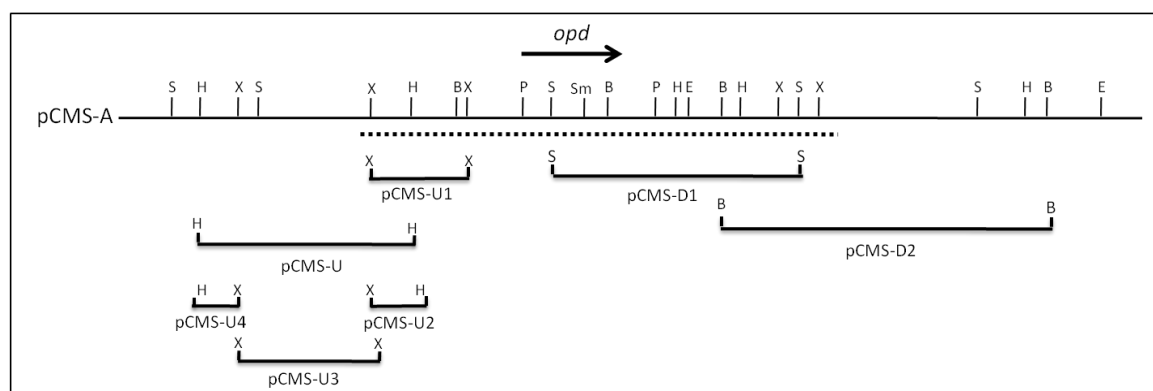


Fig 3-3| Schematic representation showing sub-cloning of *opd* flanking regions of pCMS1 in pBluescript KS II (-). Restriction sites shown are B, *Bam*HI; H, *Hind*III; S, *Sal*I; and *Xho*I. Dotted line represent the conserved region in pCMS1 and pPDL2.

About 8.91 Kb DNA sequence generated from these sub-clones was analyzed using online bio-informatic tools. Sequence analysis of this region exhibited six ORFs in addition to the *opd* gene. Comparison of this sequence with the pPDL2-borne *opd* gene cluster isolated from *S. fuliginis* ATCC 27551 has shown no difference in the sequence found upstream to the *opd* gene. However significant differences were observed in the downstream region. In pPDL2-borne *opd* cluster *mfhA* gene was found immediately downstream to *opd* gene in opposite transcriptional orientation. In fact the sequence similarity is only seen between these two plasmid-borne *opd* clusters till the 3' end of *mfhA*. Immediate downstream of *mfhA*, in the sequence of pPDL2, a transposable element Tn3 was identified. It contains truncated transposase (*tnpA*) and resolvase (*tnpR*) (Fig 3-4). In case of pCMS1, instead of *mfhA* a larger ORF, coding for a protein of 345 amino acids was found downstream to *opd* gene. In fact, the 3' region of *mfhA* was identical to the 3' region of *orf345*. Therefore, the 243 amino acids at the C-terminal sequence of the Orf345 was identical to MfhA [Fig 3-4]. This clearly suggests that, the transposon, Tn3 is inserted in the coding sequence of *orf345*. Though none of the pCMS1 fosmids with Tn3 transposon were identified, a

possibility of acquiring a transposon from the soil microbial community during the event of HGT cannot be ruled out. Actually insertion of Tn3 element into the coding region of *orf345* generates transposon-like organization for *opd* cluster as there already exists an IS element, IS21 upstream of *opd* gene. In fact such genetic structure can be seen in the pPDL2-borne *opd* cluster. As illustrated in fig 3-4, insertion of *opd* cluster into a new locus along with a part of *orf345* generates *mfhA* through a possible transposition event. In the sequence of pCMS1 further downstream to the *orf345*, another ORF coding for a protein of 159 amino acids was identified. It shows homology to a allophanate hydrolase the product of *ami* gene. Bio-informatic predictions made to identify promoter elements upstream to *orf345* were unsuccessful. However, a promoter element having consensus σ_{70} dependent promoter motif was found upstream to *orf159*. Absence of transcriptional terminator downstream to *orf159*, and presence of transcriptional terminator element downstream to the *orf345* suggests possible operon-like organization between *orf345* and *orf159*. There is no *orf159* in plasmid pPDL2. Similarly the sequence found downstream of *orf159* showed no sequence similarity with plasmid pPDL2 sequence. If the characterization of pCMS1-borne *opd* gene cluster is taken into consideration, it showed no features of a catabolic transposon.

Sequence analysis of pCMS1 outside the 8.9 Kb *opd* flanking region has shown existence of *tra* sequences known to be involved in the horizontal mobility of plasmids. Sequences of *traE*, *traM* and *klcA* that share considerable similarity (66-75%) with *tra* genes of *Acromobacter denitrificans* and *Comamonas* sp. CNB-1 were identified in the sequence of pCMS1. Further conventional conjugation experiments carried out in our laboratory to gain evidence on the HGT of pCMS1, clearly demonstrated the self-transmissible nature of a pCMS1 from *B. diminuta* to *Pseudomonas putida* KT2440 (PANDEETI *et al.* 2011). Considering the self-transmissible nature of pCMS1 among soil

bacteria, we tempt to speculate existence of pCMS1 variant having *opd* element with structural resemblance to the pPDL2-borne *opd* element due to acquisition of Tn3 element. Such pCMS1 variant contributes for the HGT of *opd* cluster among soil bacteria. Existence of identical *opd* genes in taxonomically diverse soil bacteria adds strength to this proposition (MULBRY *et al.* 1987).

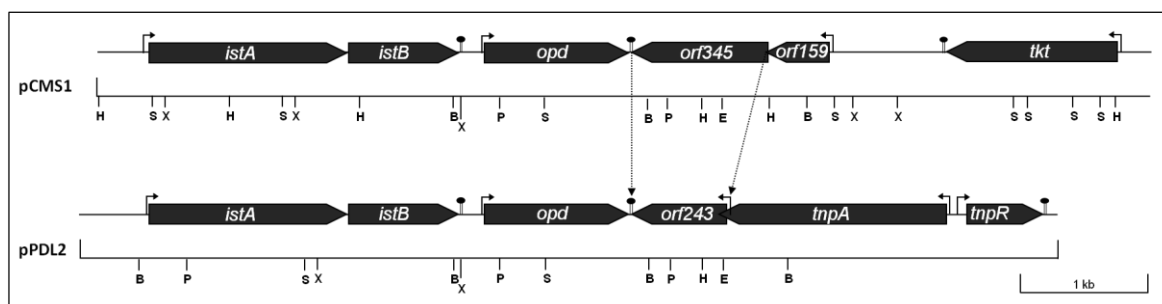


Fig 3-4| Comparison of physical map and organization of *opd* clusters of pCMS1 and pPDL2. Generation of *orf243* (*mfhA*) from *orf345* is highlighted with dotted arrows.

3.2 Lateral transfer of the *opd* island from plasmid pPDL2 of *S. fuliginis* ATCC 27551

Our previous studies have shown transposon-like organization for the pPDL2 plasmid pPDL2-borne *opd* cluster (SIDDAVATTAM *et al.* 2003). However we could not gain experimental evidence to demonstrate the event of transposition. One of the reasons for such failure was incomplete sequence information. At that point of time the sequence information was only available for *opd* cluster. Therefore, we have undertaken further studies for gaining the complete sequence information of pPDL2. The sequence of pPDL2, when analysed has shown the presence of various functional modules like replication and partition module, mobilization module, integration module, degradation module and mobile genetic elements (PANDEETI *et al.* 2012). Interesting feature observed in pPDL2 sequence was presence of integration module, a unique feature typically found in Genomic Islands (GIs). Our lab has demonstrated mobilizable nature of plasmid pPDL2 and demonstrated HGT of pPDL2 into *Acinetobacter baumannii* in presence of a helper strain (PANDEETI *et al.* 2012). However, no experimental evidence is gained to demonstrate

either transposition or chromosomal integration of *opd* island. The work described in the chapter describes experimental evidence gained to demonstrate both transposition and chromosomal integration of plasmid pPDL2-borne *opd* cluster of *S. fuliginis* ATCC 27551.

3.2.1 Integration module

Before going to describe experimental design, a brief description is presented on integration module of pPDL2, to provide more clarity to the examiner. As shown in fig 3-5a, the integration module of pPDL2 contains two units of integrase, CopG, phosphoglycerate mutase (PGM). Integrase encoded by *int* gene has highest similarity to tyrosine recombinases. The *copG* is a transcriptional regulator, it is shown to regulate the expression of *int* gene (DEL SOLAR and ESPINOSA 1992; DEL SOLAR *et al.* 1997; GOMIS-RUTH *et al.* 1998). The organization of *int*, *copG* and *pgm* is highly conserved among *Sphingobiaceae* members [Fig 3-5b]. Site specific integration mediated by integrase is possible between chromosomally located attachment sites *attB* and an identical sequence found on plasmid, designated as *attP*. The *attB* site is always found at 3' end tRNA genes. If site specific integration is to be demonstrated it requires to identify *attP* site in pPDL2 sequence.

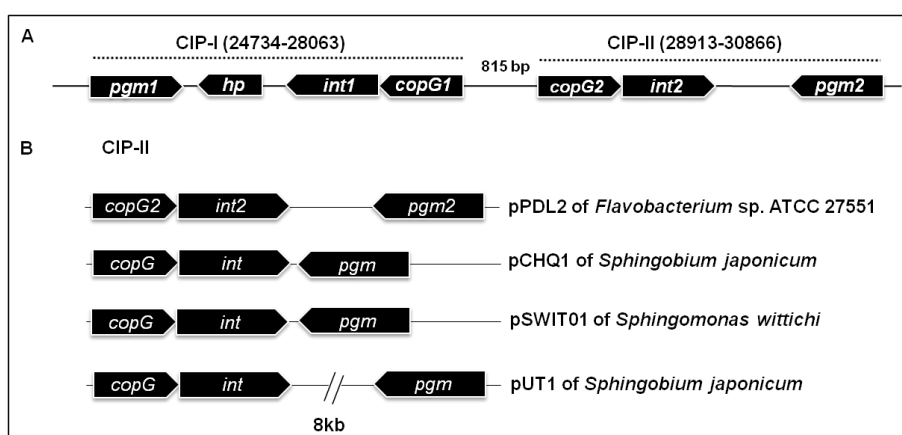


Fig 3-5| Organization of integration modules of plasmid pPDL2 (Panel A). Integration modules found among *Sphingobiaceae* members are shown in Panel B.

3.2.1.1 Prediction of *attP* sites:

The genomic island (GIs) essentially consists of cargo genes, a functional integrase gene, a regulatory module involved in regulation of expression of integrase and genes required for conjugal transfer. GI gets excised from the genome as a large discrete DNA fragment, gets circularised, before mobilizing into the recipient bacteria (JUHAS *et al.* 2009). Once mobilized into recipient, it site-specifically integrates into its genome. In due course, it may undergo gene rearrangements by acquiring new genes by patch work assembly, or may lose some genes, and again mobilizes into another bacteria aided with excisionase and integrase enzymes (WOZNAK and WALDOR 2010). This process of site specific integration of GI happens only at specific sites in the recipient genome abbreviated as *attB*, and the site from which a GI excises is called as *attP*. Site-specific recombination between *attP* and *attB* results in the integration of a GI into the chromosome. Available literature indicate presence of *attB* sites with overlapping the tRNA genes or at their 3' termini (WILLIAMS 2002; BOYD *et al.* 2009). Considering this background information an attempt was made to predict potential *attP* sites on the pPDL2 sequence.

Table 3-1| Positions of *attP* predicted on the pPDL2 sequence

S. No	Position on pPDL2	Sequence (5'→3')
<i>attP1</i>	26708-26718	CCCGCTCCACC
<i>attP2</i>	19633-19647	CCTTTGGCGTCAACG
<i>attP3</i>	32003-32011	CGCCTGGA
<i>attP4</i>	32730-32739	AGGCGCTCGC

While achieving this objective two independent approaches were followed. In the first approach, the tRNA sequences of *Sphingobium* sp. available in the database were taken and aligned with the pPDL2 sequences to identify 15-20 bp regions identical with tRNA genes or with the sequences found at their 3' end. In the second approach, the genome

sequences of bacteria having plasmids with integrase genes were collected from NCBI database. These sequences were then used to predict genomic islands (GI) using Islandviewer software (<http://www.pathogenomics.sfu.ca/islandviewer/query.php>). The predicted GI sequences were then used to make pairwise alignments with sequences of tRNA genes of *Sphingomonas wittichii* and *Sphingobium japonicum*. Short sequence repeats that exactly matched the 3' end of tRNA sequences were taken as putative *att* sites. The predicted *att* sites with a low E-value were considered as potential *attP* and *attB* sites. The *att* sites predicted in this manner were then used to align with plasmid pPDL2 sequence using BlastN to identify *attP* homologs. Alternatively, tRNA gene sequences taken from *S.wittichii* and *S. japonicum* were directly used to align with the pPDL2 sequence using BlastN to find short sequences that perfectly matched the 3' end of tRNA genes. Based on these two approaches we have identified four putative *attP* sites (Table 2) on the pPDL2 sequence. The corresponding homologous region of the *attP* region in the seryl tRNA sequence, shown encircled in Fig 3-6, is considered as *attB*.

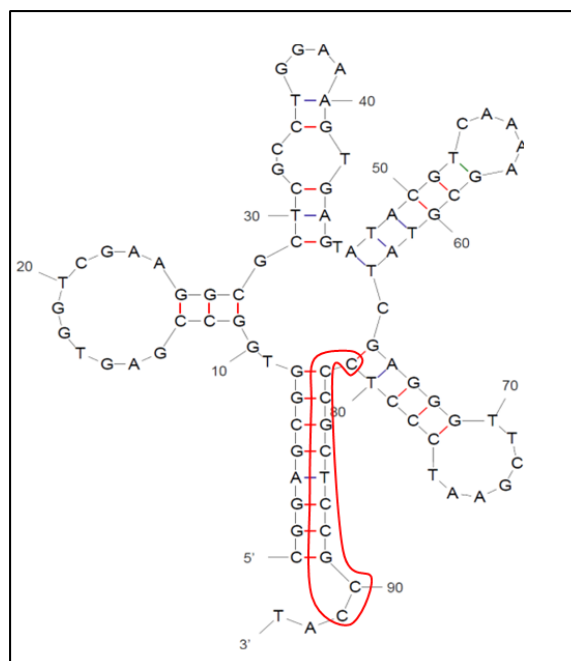


Fig 3-6| Serine tRNA sequence. The predicted *attB* sequence is encircled

3.2.1.2 Construction of temperature sensitive plasmid with *attB* sequence

In order to demonstrate site specific recombination between plasmid pPDL2, and *attB* site, a temperature sensitive plasmid, pSDP7 was constructed and used to clone *attB* sequence [Fig 3-7]. A 2.3 Kb DNA fragment containing temperature sensitive *oriR101*, *repA* and *bla* genes was amplified from pKD46 (DATSENKO and WANNER 2000) using primer set DSF0005 (TCT TGA GAT ATC ACT GAT AGA TAC AAG AGC) and DSF0006 (CAA TAA CCC GGG TAA ATG CTT CAA TA) which are appended with *EcoRV* and *SmaI* restriction sites respectively. Similarly P_{tac} promoter, MCS and *lacZ* were taken as *EcoRV* and *DraI* fragment from pMMB206 (MORALES *et al.* 1991) and ligated to the 2.3 Kb temperature sensitive replicon amplified from plasmid pKD46. The resulting plasmid construct was named as pSDP7. A synthetic seryl tRNA gene with *attB* site was then cloned in pSDP7 as *HindIII* fragment and the resulting plasmid pSDP8 was used as source of *attB* while performing site specific integration assay. Construction of temperature sensitive vector pSDP7 and cloning of seryl tRNA gene is shown in fig 3-7.

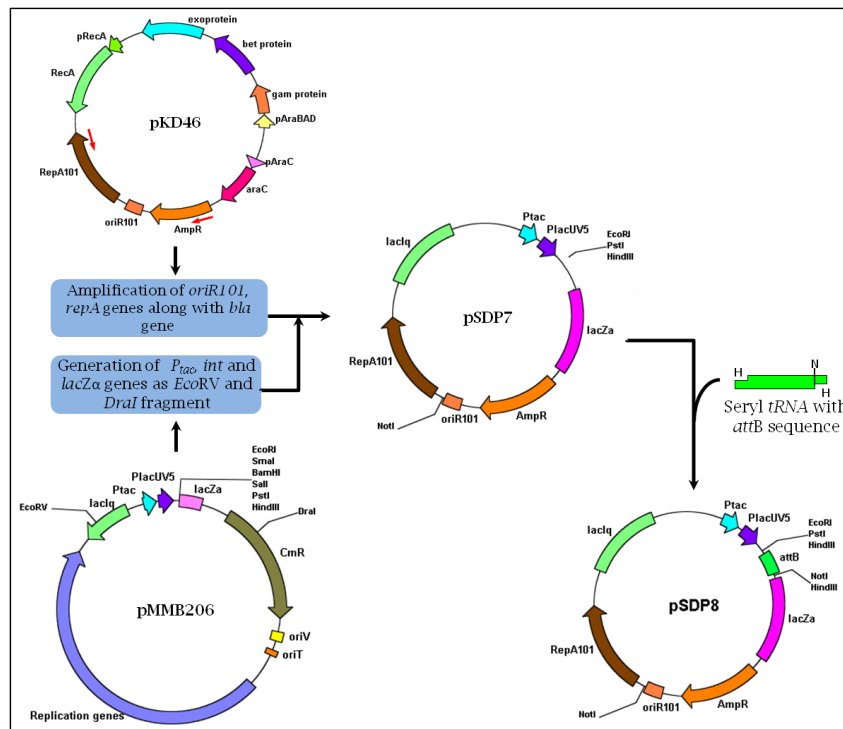


Fig 3-7| Diagrammatic representation of pSDP7 and pSDP8 construction.

3.2.1.3 *in vivo* Integration assay

While demonstrating integration event between pPDL2 and temperature sensitive plasmid pSDP8, a derivative of plasmid pPDL2, pPDL2-K were constructed by inserting a minitransposon Tn5<R6K γ ori/KAN-2> using the transposon insertion kit (Epicentre Biotechnologies, USA). The pPDL2-K, due to the presence of R6K γ ori replicative origin replicates only in *E. coli* pir 116 cells. The pSDP8 is a conditionally replicative ampicillin resistant plasmid and replicates only under permissive temperature (30°C). *E. coli* pir 116 (pSDP8, pPDL2-K) is resistant to both kanamycin and ampicillin only when the cultures are grown at permissive temperature. However when the culture is grown at restricted temperature (37°C), the plasmid pSDP8 will be lost and the cells become sensitive to ampicillin. However in the event of site specific recombination between pSDP8 and pPDL2-K, a co-integrate will be formed due to the fusion of these two plasmids and hence only in such cells which contain co-integrate show resistance to both kanamycin and ampicillin despite of culturing at restrictive temperature (37°C). While testing this hypothesis, overnight cultures of the *E. coli* pir116 (pSDP8, pPDL2-K) cells grown at 30°C, were inoculated independently and grown at 30°C and 37°C respectively. The culture grown at 30°C, when plated on Ampicillin and Kanamycin LB plates grown into a lawn indicating survival of all cells. However, the culture grown at 37°C, when plated on selective plates (ampicillin and kanamycin) gave very less number of colonies, suggesting that these cells retain ampicillin resistance due to formation of co-integrate. Plasmids isolated from these colonies were subjected to restriction digestion and differences in restriction pattern were identified by comparing with the restriction profile of pPDL2-K.

As shown in figure 3-9, site specific recombination between pPDL2-K and pSDP8 resulted in the increase of size of pPDL2-K by 6.7Kb. The same is evident in the

restriction profile. When the pPDL2-K/pSDP8 co-integrate was digested with *EcoRI*, the 11.05 Kb *EcoRI* fragment of pPDL2-K has gone up in size to 17.25 Kb (Fig 3-8). It has also generated two fragments, 15.347 and 2.2 Kb due to presence of an additional *EcoRI* site in pSDP8. Integration of pSDP8 at *attP* site was also evident when digested with *NotI* and *PstI* [Fig 3-9A].

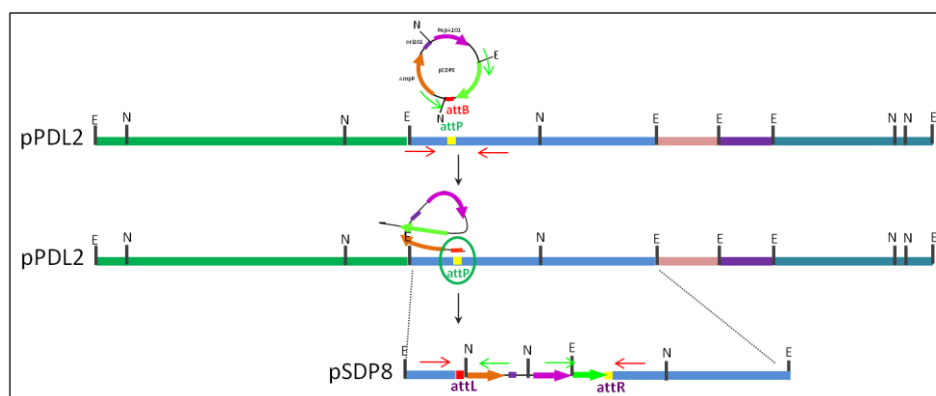


Fig 3-8| Schematic representation of site-specific recombination between *attP* site of pPDL2 and artificial *attB* of pSDP8. N and E represent the restriction sites *NotI* and *EcoRI* respectively. The positions of the M13 universal primers and pPDL2 specific primers designed to amplify junction sites are shown with green and red arrows respectively.

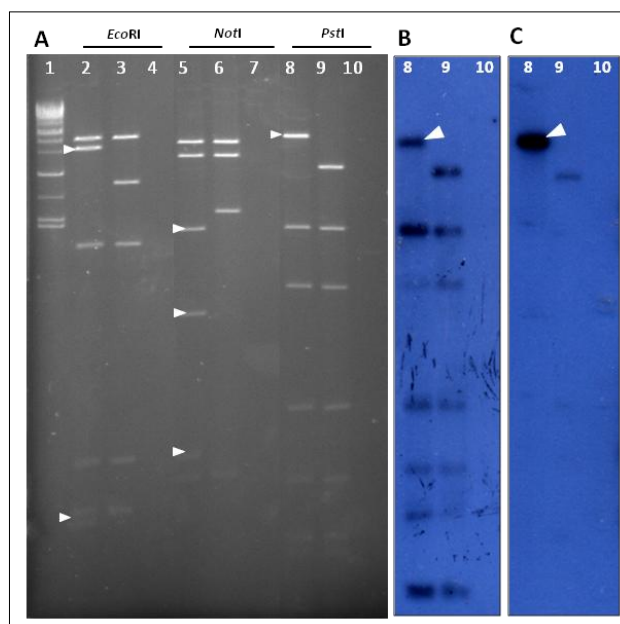


Fig 3-9| Confirmation of co-integrate formation between pPDL2-K and pSDP8. Panel A. Restriction pattern for co-integrate when digested with *EcoRI* (lane 2)/*NotI* (lane 5)/*PstI* (lane 8). Panel B and C represent autoradiograms developed using pPDL2-K (Panel B) or pSDP8 (Panel C) as probe. Lane 1. λ mix; Lanes 2, 5, 8, represent pPDL2-K/pSDP8 co-integrate; Lanes 3, 6, 9, represent pPDL2-K; Lane 4, 7, 10 represent pSDP8. The increased size of pPDL2-K specific DNA fragments due to integration of pSDP8 is shown with white arrow heads.

The differences in the sizes of the restriction fragments exactly matched with the size of the pSDP8 backbone. Integration of pSDP8 at *attP* site of pPDL2-K was further confirmed by performing southern hybridization, using either pPDL2-K or pSDP8 specific probes [Fig 3-9B,C].

In order to confirm the exact site of integration on pPDL2 plasmid we have amplified and sequenced the junction sites from pPDL2-K/pSDP8 co-integrate. Primers DSF0007 and DSF0008 were designed taking flanking regions of intact *attP* site of pPDL2 (sequence 26708-26718). Since *attB* is cloned in the multiple cloning site of pSDP8, which is a derivative of pMMB206, M13 universal primers were used to amplify intact *attB* site from pSDP8. If there is an integration event at the predicted *attP* and artificial *attB* sites, no PCR amplicon should be generated with DSF0007/DSF0008 or M13 universal forward/reverse primers. However, in the event of integration, it results in the amplification of 1.7 Kb right junction site only with M13 universal forward/DSF0008 primers. Similarly, the 2.2 Kb left junction site will be amplified with M13 universal reverse/DSF0007 primers. As shown in fig 3-10, amplification of 1.7 Kb right and 2.2Kb left junction sites were obtained when pPDL2-K/pSDP8 co-integrate was used as template. Undoubtedly, formation of such co-integrate supports existence of *opd* island on pPDL2, which is shown to be a mobilizable plasmid (PANDEETI *et al.* 2012).

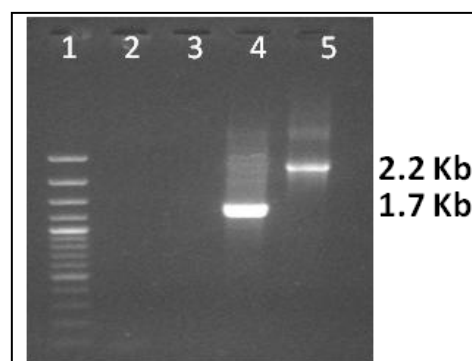


Fig 3-10| Amplification of junction sites. Lane 1. 100bp DNA ladder; Lane 2 and 3 are loaded with PCR reaction mixture used either with M13 universal primers or primer set DSF0007/ DSF0008 respectively.

PCR amplicons generated using M13F / DSF0008 (Lane 4) and M13R / DSF0007 (Lane 5) are shown in Lane 4 and 5 respectively.

3.2.2 Degradation module

Close examination of pPDL2 physical map shows existence of mobile genetic elements within and flanking the degradative module [Fig 3-11]. Presence of these transposable elements and the existence of identical *opd* clusters in pCMS1 and pPDL2 plasmids isolated from soil bacteria belonging to diverse taxonomic groups, that collected from a variety of geographical regions, suggest HGT of pPDL2-borne *opd* cluster by transposition. However transposition assay performed during our previous studies, using 7.1 Kb *opd* flanking region of pPDL2 was unsuccessful and based on these studies we have suggested that the pPDL2-borne *opd* cluster is a defective transposon. The truncated *tnpA* gene of Tn3, identified at the right side end of the *opd* cluster was one of the reasons for arriving such conclusion. However, analysis of complete pPDL2 sequence has shown presence of a second copy of the Tn3 element immediately downstream of the defective Tn3. Interestingly, while analyzing the pPDL2 sequence we have also identified another mobile genetic element, *y4qE* immediately upstream of degradation module. Surprisingly, we have even observed presence of Tn3 specific terminal repeats upstream to *y4qE* element. If Tn3 specific repeats found upstream to the *y4qE* and downstream to the Tn3 element are taken into consideration, it clearly indicates transposition event in HGT of pPDL2-borne *opd*-cluster. The genetic map of the DNA region between *y4qE* and Tn3 includes the previously reported *opd* gene cluster, transposons Tn3 and *y4qE*, and the *ligBA* operon coding for the protocatechuate-4, 5-dioxygenase alpha and beta subunits, along with a gene (*orf1*) coding for a LysR-type transcription regulator [Fig 3-11]. The *ligBA* operon codes for protocatechuate-4, 5-dioxygenase alpha and beta subunits having 83% sequence identity to the similar proteins of *Xanthomonas campestris* pv.

campestris str. ATCC 33913 (NCBI reference no. [NP_636196.1](#)). In addition to *lig* operon, *lysR*, the degradation module also contains two more ORFs showing homology to transporter proteins belonging to the major facilitator super family [Fig 3-11]. Transporters belonging to the major facilitator super family of proteins are known to be involved in the transport of aromatic compounds (PAO *et al.* 1998). If the sequence found between the Tn3-specific terminal repeats is examined, it appears that the degradation module has all necessary information for mineralization of OP insecticides like parathion and methyl parathion and to contribute for its transposition. In the present study, experiments were designed to show that the pPDL2-borne *opd* cluster is an active transposon.

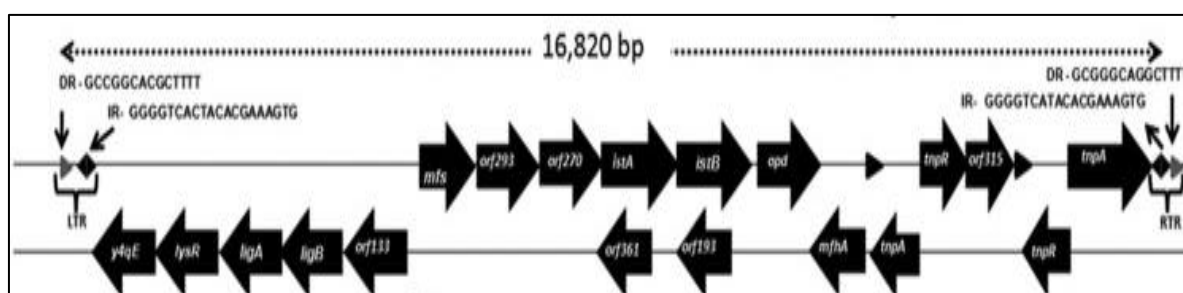


Fig 3-11| Physical map of organophosphate degradation module identified on the pPDL2 plasmid. The Tn3-specific terminal repeats found upstream and downstream of transposable element Tn3 and mobile element *y4qE* are shown with arrow heads.

3.2.2.1 Construction of pPDL2KT

The *opd* cluster of pPDL2 does not have any selectable marker. While performing transposition assay, it is desirable to have a selectable marker to facilitate monitoring transposition event of *opd*-cluster. Therefore a derivative of pPDL2K (EMMANUEL VIJAY PAUL 2012) was constructed by replacing the *opd* gene with *opd::tet* through homologous recombination (DATSENKO and WANNER 2000). Initially the pKD46 plasmid, coding red recombinase, from *P_{araB}* promoter was transformed into *E.coli pir-116* (pPDL2K) to obtain *E.coli pir-116* (pPDL2K, pKD46). These cells were then induced with 1mM arabinose before making them electro-competent. The *opd::tet* cassette was amplified

from plasmid pSM3 (SIDDAVATTAM *et al.* 2003) using primer set pDS3/pDS4 and electroporated into electro-competent *E.coli pir-116* (pPDL2K, pKD46) cells. The electroporated cells were then plated onto LB agar containing tetracycline and Kanamycin and incubated at 37°C. The resulting colonies were then streaked on to LB plate containing ampicillin to check for the selective elimination of pKD46 plasmid coding for red recombinase. Ampicillin sensitive and Tetracycline/Kanamycin resistant positive colonies were then used to confirm replacement of *opd* gene with *opd::tet* either by restriction digestion or by performing PCR amplification using *opd* specific primers. The plasmid pPDL2-K derivative where *opd* is replaced with *opd::tet* was designated as pPDL2KT [Fig 3-12] and used to perform transposition assay.

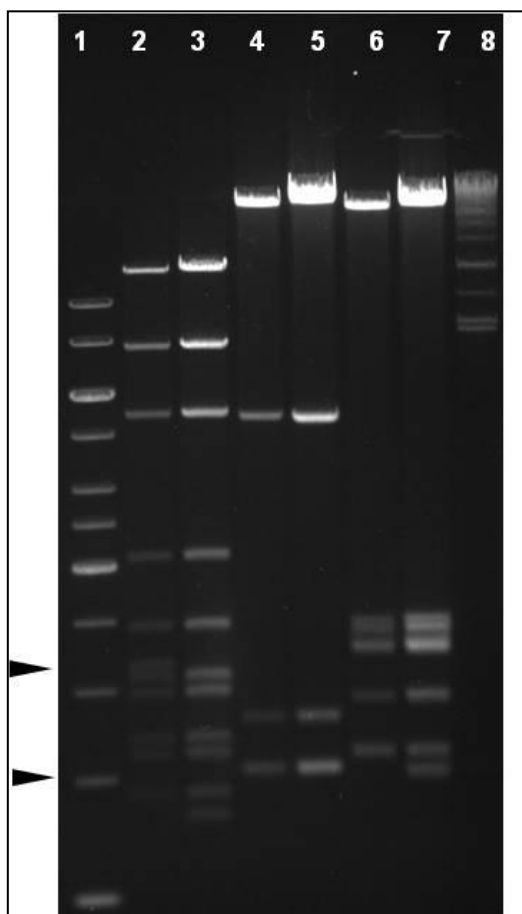


Fig 3-12| Construction of pPDL2-KT. Lane 1 1Kb DNA ladder; Lanes 2, 4, and 6 are *Hind*III, *Not*I and *Pst*I digests of pPDL2-KT. Lanes 3,5, and 7 are *Hind*III, *Not*I and *Pst*I digests of pPDL2-K. Lane 8 λ mix. The increase in size of *opd* gene due to presence of tetracycline gene is shown with arrow.

3.2.2.2 Transposition assay

Transposition assay was performed using pPDL2-KT as source plasmid and *sacB* containing, pJQ210 (QUANDT and HYNES 1993) as a reporter plasmid. The pPDL2-KT, replicates only in *E. coli pir116* cells. The other *E. coli* strains, like *E. coli* DH5 α are non permissive host for pPDL2-KT. The plasmid pJQ210, a narrow host range plasmid replicates in *E. coli* DH5 α . Due to presence of *sacB*, sucrose supplementation to the culture medium is lethal to gram negative hosts like *E. coli*. However, the *E. coli* cells can grow in presence of sucrose, if a *sacB* gene is disrupted, due to transposition of *opd* cluster from plasmid pPDL2-KT. Such event can be identified by plating the *E. coli* (pJQ210, pPDL2-KT) cells in sucrose containing LB medium, in presence of tetracycline. As *E. coli* DH5 α is non-permissive host for pPDL2-KT, presence of tetracycline colonies in sucrose containing LB medium is a clear indication for disruption of *sacB* gene due to transposition of *opd* gene cluster. The transposition assay performed in this study resulted in generation of several sucrose/tetracycline positive cells. These colonies were then screened by performing PCR.

Table 3-2| Primers used for the amplification transposition junction sites

Primer Name	Sequence (5'→3')
DSF0017	CTGACAATCGAGGAGCACTACAC
DSF0018	CTTAGTTGCAGAAATAGGCGACCTT
sacB-F	CTGGCAGGAGGCGCAACTCA
sacB-R	CAAGGATGCTGTCTTTGACAACAGATG

PCR primers DSF0017 and DSF0018 were designed by taking sequences found 758bp downstream to *y4QE* and 758bp upstream to the Tn3 element. These two primers were then used in combination of *sacB* specific primers to amplify junction sites (Table 3-2).

Primer sets sacB-F/DSF0017 and sacB-R/DSF0018 were used to amplify the left and right junction sites respectively. Amplification of 0.95 Kb left junction site and 2.45 Kb right junction site (fig 3-13) is rather a clear evidence for the event of transposition. The sequence found between the Tn3-specific terminal repeats is existing as an active transposon encoding all necessary information required for the mineralization of OP insecticides like parathion and methyl parathion [Fig 3-11].

As mentioned in earlier parts of this section, horizontal gene transfer (HGT) between unrelated species is one of the leading forces of evolution. It provides genetic variations from neighbouring species and increases the ecological fitness of the species under certain environmental conditions. Principle mechanisms like conjugation, transformation and transduction exchange genetic elements like plasmids, transposons, phages, integrons, conjugative elements, transposons, IS elements, mobile genetic elements etc between non-parent species are well known HGT mechanisms.

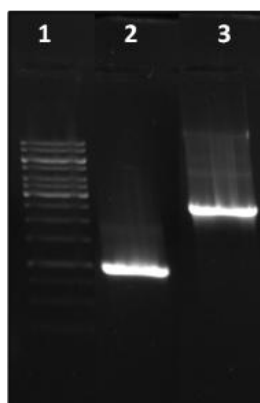


Fig 3-13| Amplification of junction sites. Lane 1. 1Kb DNA ladder; Lane 2 indicates PCR amplification of right junction sites using SacB-F and DSF0017 primers; Lane 3 PCR amplification of left junction site using DSF0018 and SacB-R primers.

These foreign genetic elements differ from the rest of the host genome content in certain characteristics of their genome like GC skew and percent of GC content etc. Clusters of genes that are mobilized as a unit into a new species are defined as Genomic islands (GIs). The genomic islands are given different names like metabolic islands, degradation islands,

resistance islands, and pathogenicity islands depending on the function of the genes. Existence of plasmid-borne catabolic transposons and plasmids is a well known phenomenon in bacteria (TAN 1999). The catabolic transposons involved in degradation of xylene (TSUDA and IINO 1987), chlorocatechol (RAVATN *et al.* 1998), benzene (FONG *et al.* 2000) are identified in bacteria isolated from polluted environments. Recently, existence of chlorocatechol and aminobenzoate degradation genes on integrative conjugative element (ICE) surprised microbiologists. The chlorobenzoate catabolic ICE, ICE*clc*, is found downstream to glycyl tRNA, and contained *int* gene coding for a site-specific integrase and attachment sites *attL* and *attR*. There is lot of structural resemblance between ICE*clc* and resistance islands. It appears that these novel mobile genetic elements have been evolved in response to the constant stress generated due to the presence of the recalcitrant compounds.

Bacterial *opd* genes implicated in the degradation of toxic OP chemicals are isolated from diverse geographical regions. Structural comparison of OPH with the existing protein structures revealed strong similarities between OPH and quorum quenching lactonases (ELIAS and TAWFIK 2012). In all possibilities the OPH appears to have evolved from lactonases due to certain critical mechanisms that contributed for addition/deletion of critical amino acid residues (AFRIAT *et al.* 2006). Since OPs are extensively used after world-war II as insecticides, their residues might have served as better substrates for these novel enzymes. The degradation products generated served carbon/nitrogen requirements of the organisms, the evolution of the new enzymes naturally contribute for their fitness. Such an event retains the new gene and if it exists on a plasmid contributes for its horizontal transfer. If the available information on *opd* genes are carefully examined majority of them are found on plasmids (SOMARA *et al.* 2002;

PANDEETI *et al.* 2011; PANDEETI *et al.* 2012). These organizations as active transposon is demonstrated in *A. radiobacter* (HORNE *et al.* 2003) and *Pseudomonas sp.* WBC-3 (WEI *et al.* 2009). The present study proves existence of *opd* cluster on a mobilizable plasmid, pPDL2. The most interesting aspect is that, pPDL2-borne *opd* cluster is having dual features. It is an active transposon and also organized on integrative mobilizable element (IME). The pPDL2 has a well defined replicative origin that supports the replication of pPDL2. If it is mobilized into new host it can replicate like a plasmid. If the new environment does not support its replication the *opd*-island can get integrated into the genome either due to transposition or through site-specific integration. It appears that plasmid pPDL2 has necessary genetic information to retain OP degradation module and to spread horizontally among soil microflora.

Results and Discussion | Chapter 2

4.0 Background

The genetic evidence gained in the first chapter proved organization of plasmid pPDL2-borne *opd*-cluster as integrative mobilizable element (IME). Organizational differences between *opd*-cluster found on dissimilar plasmids pPDL2 and pCMS1 are also explained in detail. Considering the unique location of *orf243*, our laboratory has conducted experiments to assess its role in degradation of OP compounds. Especially to assess its involvement in degradation of *p*-Nitrophenol (PNP), the stable degradation product generated due to OPH mediated hydrolysis of OP compounds like parathion and methyl parathion. The pure Orf243 hydrolyses *meta*-fission products generated during aromatic compound degradation. Therefore, we have renamed Orf243 as *meta*-fission product hydrolase MfhA (KHAJAMOHIDDIN *et al.* 2006). While performing heterologous expression and purification of Orf243, our laboratory has also assessed its role in PNP degradation due to its similarity to aromatic compound hydrolases like TodF and CumD (RIDDLE *et al.* 2003). Interestingly the PNP added to the culture medium expressing MfhA disappeared quickly indicating the involvement of MfhA in degradation of PNP (SIDDAVATTAM *et al.* 2003). However, the molecular basis for such unusual observation is not properly explained. In this study a detailed investigation is performed to assess the role of MfhA in PNP degradation.

4.1 The *mfhA* is an independent transcriptional unit

As shown in Fig 4-2, *mfhA* is located in the downstream region of *opd* gene coding OPH, the triesterase which initiating degradation of OP compounds to generate PNP [Fig 4-1].

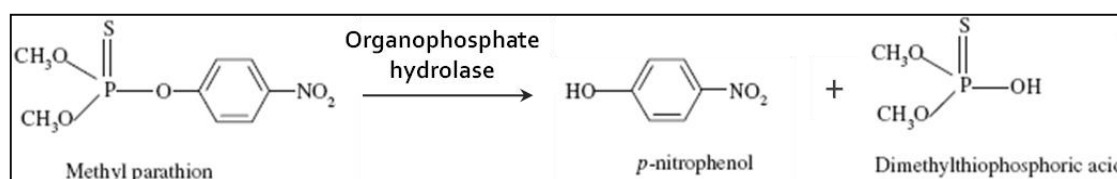


Fig 4-1| Enzymatic hydrolysis of OP compound by OPH (PAKALA *et al.* 2007).

In the upstream region of *mfhA*, the *tnpA* gene coding for a truncated transposase is identified. Both *tnpA* and *mfhA* have same transcriptional orientation. Considering the transcriptional orientation and absence of Rho-independent transcriptional terminator between *mfhA* and *tnpA*, it is initially assumed that these two genes are co-transcriptional. In order to gain a clear assessment on transcriptional organization of *mfhA* and *tnpA*, reverse transcriptase PCR (RT-PCR) was performed using total RNA isolated from *S. fuliginis* ATCC 27551. The primer set (SDP01/SDP04) having *tnpA* specific forward primer and *mfhA* specific reverse primer gave no amplification. If these two genes are co-transcriptional an mRNA molecule equivalent to the size of these two genes would have been made in *S. fuliginis* ATCC 27551. Such mRNA would have served as template to these primers and RT-PCR experiment would have generated an amplicon equivalent to the size of *mfhA* and *tnpA*.

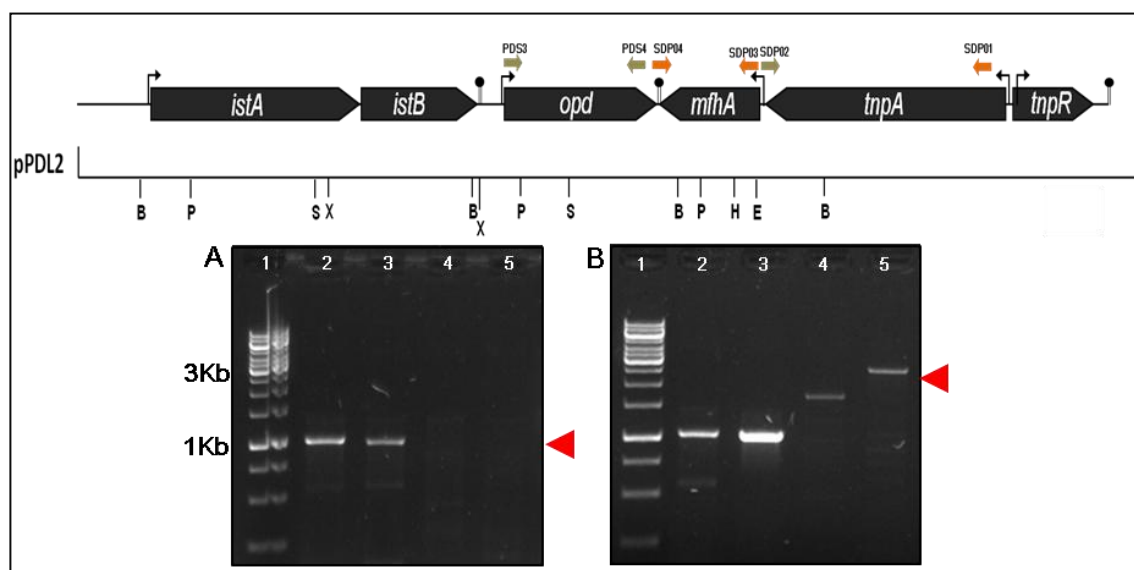


Fig 4-2| Transcriptional organization of *mfhA* in pPDL2. Panel A Represents RT-PCR experiment done using total RNA isolated from *S. fuliginis* ATCC 27551. Lane 2 and 3 indicate *opd* and *mfhA* specific amplification using primer sets PDS3/PDS4 and SDP04 /SDP03 respectively. Similar RT-PCR experiment done using either *tnpA* specific primer set SDP01/SDP02 or *tnpA* specific forward primer (SDP01) and *mfhA* specific reverse primer (SDP04) gave no amplification, Lane 4 and 5. Panel B Amplification of *opd*, *mfhA*, *tnpA* and *tnpA-mfhA* by conventional PCR using plasmid pPDL2 as template.

However, as shown in fig 4-2A no such amplicon is seen. A very specific amplification was seen in RT-PCR experiment performed using *mfhA* (SDP03/SDP04) specific forward and reverse primer. It clearly suggests that the *mfhA* and *tnpA* are organized as independent transcriptional units [Fig 4-2A, Lane 3]. While gaining further evidence on the transcriptional status on *mfhA*, promoter assay experiments were performed. The upstream region of *mfhA* sequence when examined using bio-informatic tools showed existence of promoter like motif [Fig 4-3B]. The predicted putative promoter sequence was then amplified and cloned in promoter test vector. In order to validate the transcriptional status of the predicted promoter motif, it was fused to a promoter-less *lacZ* gene using promoter probe vector, pMP220 (SPAINK H. P 1987).

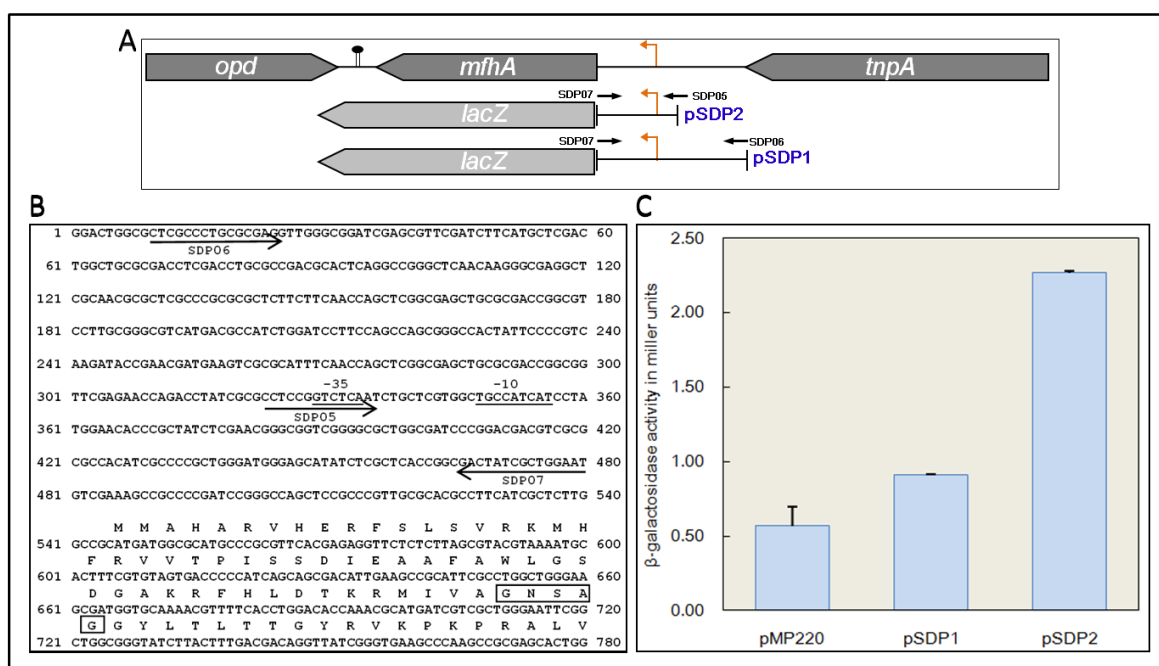


Fig 4-3| Detection of *mfhA* promoter motif: Panel A Transcriptional organization of MfhA. Predicted promoter region of MfhA is shown with bent arrow and transcriptional terminator is shown with hair pin loop. Upstream regions of MfhA cloned in pMP220 were shown to be transcriptionally fused to pMP220 vector based *lacZ* gene. Panel B Sequence of *mfhA* upstream region and deduced amino acid sequence of MfhA. The coding sequence of *mfhA* starts with ATG at 546 nucleotide position. The boxed amino acid sequence represents the typical signature sequence of esterases. Arrows indicate the primers used to amplify predicted promoter motif. The predicted promoter motif is underlined. Panel C represents β -galactosidase activity of *S. fuliginis* ATCC 27551 having vector (pMP220) and upstream regions of *mfhA*.

The upstream region of *mfhA* from start codon was amplified from pSM2 (SIDDAVATTAM *et al.* 2003), using primer sets SDP06/SDP07 and SDP05/SDP07 respectively [Fig 4-3]. These amplicons containing *mfhA* promoter were double digested with *EcoRI* and *PstI* and cloned into pMP220 digested with the same enzymes. The resulting promoter *lacZ* fusions were designated as pSDP1 and pSDP2. These two promoter fusions were then independently mobilized into *S. fuliginis* ATCC 27551 as detailed in methodology section. The promoter activity was measured by estimating the β -galactosidase activity. The two *lacZ* fusion having upstream region of *mfhA* showed promoter activity. However one of the *mfhA-lacZ* fusions, pSDP1 having 471bp upstream region of predicted promoter motif showed less promoter activity than the one having 157 bp basal promoter motif, pSDP2. However, no detailed studies were conducted to find sequence motifs that contribute for its repression. The *mfhA-lacZ* fusion studies clearly support RT-PCR data where only *mfhA* specific amplicon was seen when total RNA was used as a template and provide clear evidence on the functional status of the predicted amplicon. The presence of *mfhA* as an independent transcriptional unit and its unique location downstream of a truncated *tnpA* prompts us to perform further studies to gain its role in degradation of organophosphates. The *opd*, as shown in Fig 4-2 codes for OPH, which hydrolyses the triester linkage found in structurally diverse OP compounds and often contributes for the release of PNP, especially when acted on insecticides like methyl parathion and parathion. The studies conducted in our lab showed disappearance of PNP added to the culture medium expressing MfhA (SIDDAVATTAM *et al.* 2003). There was no explanation for such an observation. The present study therefore is aimed to gain better insights on the role of MfhA on degradation of PNP. The subsequent chapter of the dissertation explains the detailed role of MfhA in degradation of PNP.

4.2 Heterologous expression of MfhA

The work presented in this chapter describes the influence of MfhA on degradation of *p*-Nitrophenol. Before proceeding to establish its role on PNP degradation, expression plasmids were generated to express MfhA with affinity tags. Further, expression plasmids were also constructed using broad host range, mobilizable vector pMMB206. The expression systems were then used either to purify MfhA for conducting *in vitro* studies or to mobilize them into an appropriate host for conducting *in vivo* experiment.

4.2.1 Expression of MfhA with N-terminal affinity tag

To express *mfhA* with an N-terminal affinity tag, the structural gene was amplified from pSM2 (SIDDAVATTAM *et al.* 2003) using a forward primer SDP03 with a *Bam*HI site and a reverse primer SDP04. As there exists a natural *Bam*HI site at the 3' end of *mfhA*, the PCR product can be cloned into pRSETA (Invitrogen) as *Bam*HI fragment. The *Bam*HI digested PCR fragment cloned in pRSETA gave expression plasmid pSDP3.

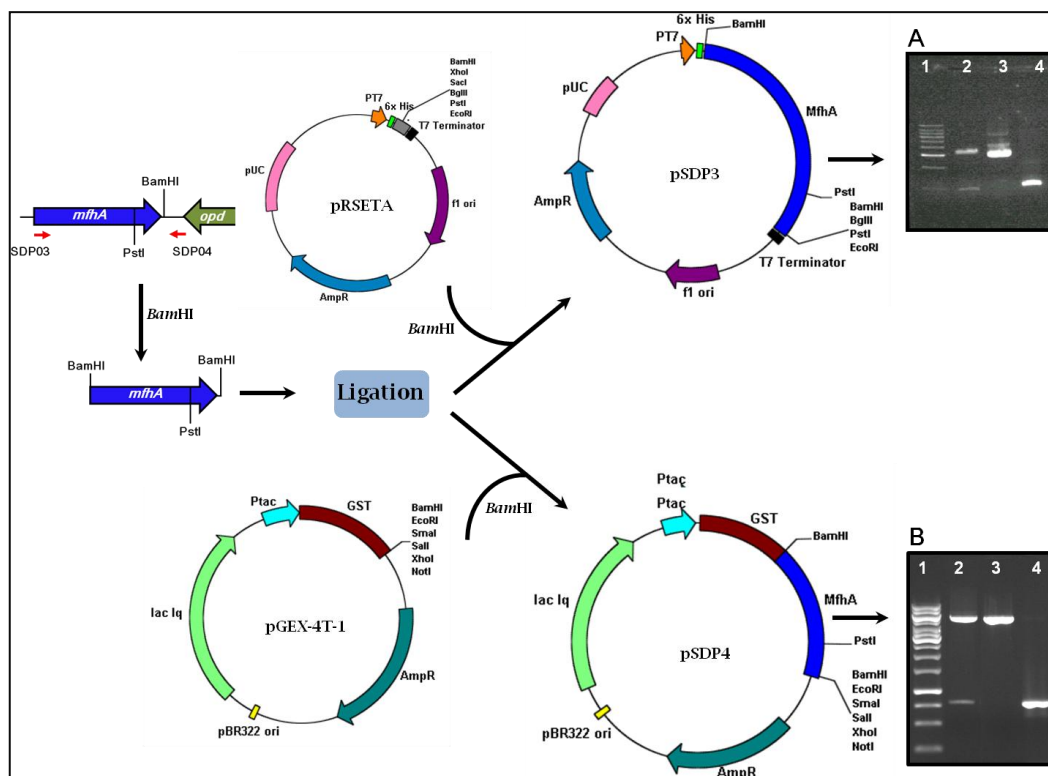


Fig 4-4| Construction of *mfhA* expression plasmids either with N-terminal affinity his-tag or with N-terminal GST-tag. Panel A and B indicate agarose gels showing release of insert from respective vector (lane 2).

Control samples such as digested vector (lane 3) and insert (lane 4) are shown in lane 2, 3 and 4 respectively.

In pSDP3 *mfhA* is translationally fused to vector specific (His)₆ tag coding sequence. The same PCR product was also cloned into pGEX-4T-1 (Amersham Biosciences) as *Bam*HI fragment to give pSDP4. In pSDP4, the MfhA is placed in frame to the GST coding sequence. The orientation of the cloned *mfhA* was confirmed by digesting with *Pst*I, as an unique *Pst*I site is located near the 3' end of the *mfhA*. Hence, digestion of pSDP3 with *Pst*I releases 0.146 Kb fragment due to existence of second *Pst*I site in the MCS of the vector [Fig 4-4].

4.2.2 Construction of pSDP5, pSDP6, pSDP7

The aforementioned expression plasmids will be useful to express MfhA in *E.coli*. The *in vivo* experiments designed in this study demanded expression of MfhA in native host, *S. fuliginis* ATCC 27551. Therefore, the *mfhA* cloned in the expression plasmids pSDP3 and pSDP4 were amplified using vector specific primers appending *Bgl*III sites and cloned into pMMB206 (MORALES *et al.* 1991), to generate broad host range mobilizable expression plasmids coding MfhA with affinity tags. Using pSDP3 or pSDP4 as templates, primer set SDP08 and SDP09 used to amplify *mfhA*_{N-6His}; similarly, SDP10 and SDP11 primer set was used for amplifying *mfhA*_{N-GST}. As all these primers have *Bgl*III site, they were independently cloned into pMMB206 digested with *Bam*HI. The constructs thus obtained were designated as pSDP5 and pSDP6 respectively [Fig 4-5]. Similarly *gst* gene sequence amplified from vector pGEX-4T-1 using SDP10 and SDP11 primers was also cloned in pMMB206 to have control expression plasmid coding only GST. The orientation of the inserts was confirmed by restriction digestion.

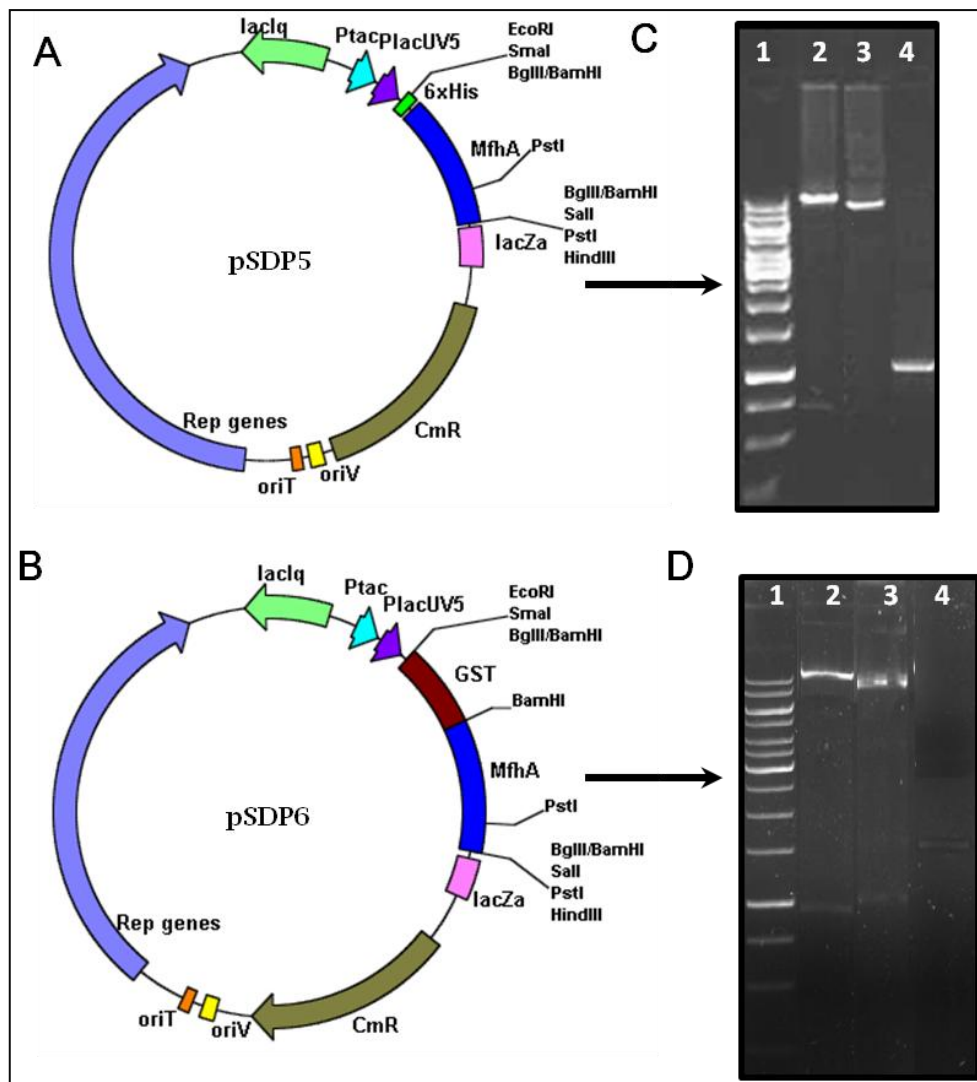


Fig 4-5| Construction of broad host range mobilizable expression plasmid coding MfhA with N-terminal affinity tag. Panel A indicates physical map of pSDP5 coding MfhA_{N-6His} and Panel B represent pSDP6 map coding MfhA_{N-GST}. Panel C and D depict agarose gels showing the presence of *mfhA* (lane 2), Control samples such as digested vector (lane 3) and insert (lane 4) are shown in lane 2, 3 and 4 respectively.

4.2.3 Construction of pSDP9

All the aforementioned expression plasmids code MfhA with affinity tags. The influence of the tag on the activity of MfhA is therefore difficult to assess. The construct pSDP6 is made to code MfhA without any tag. In order to express MfhA without affinity tag in *E. coli*, *mfhA* was amplified from pSM2 using forward primer SDP12 appending *NcoI* restriction site and reverse primer SDP04. The PCR product was digested with *NcoI* and *BamHI* restriction enzymes and directionally cloned into pET-28a (+) expression vector digested with similar restriction enzymes. The recombinant plasmid obtained was

designated as pSDP6 and used to transform in to *E. coli* BL21 (DE3). The plasmid pSDP9 codes for MfhA without any affinity tag, when induced with 1mM IPTG [Fig 4-6].

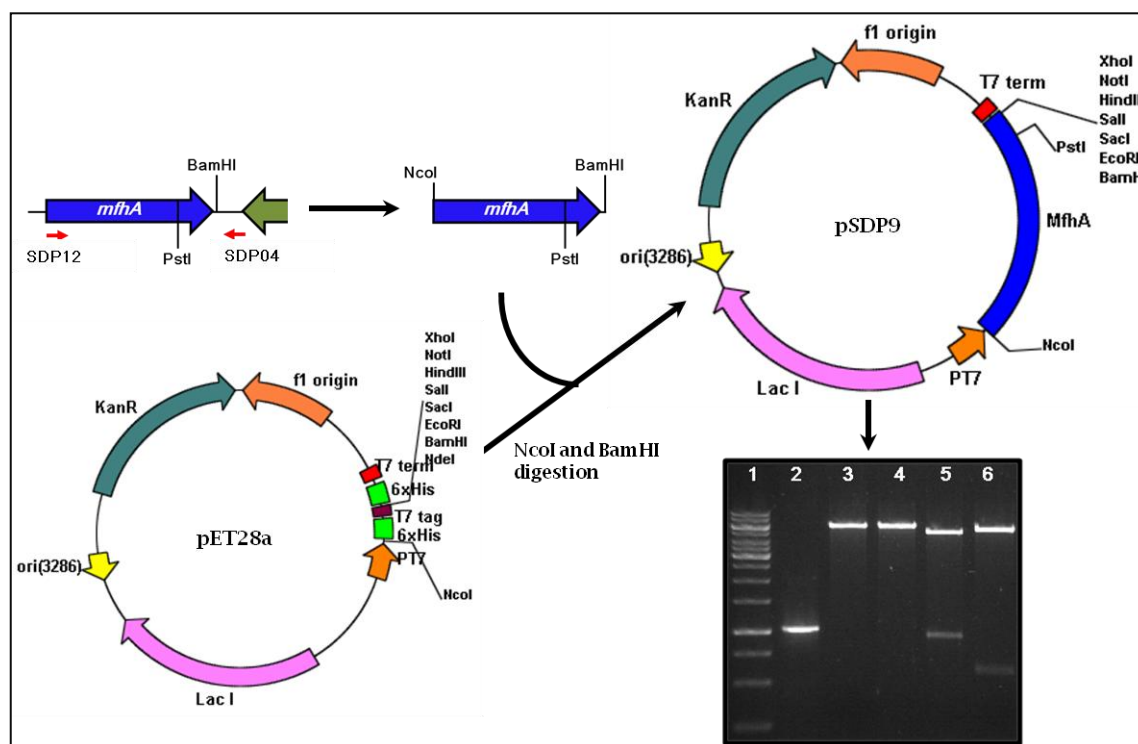


Fig 4-6| Diagrammatic representation of cloning strategy of *mfhA* expression plasmid coding MfhA without any tag. The inserted agarose gel shows the construction of pSDP9. Lane 1 Molecular weight marker, Lane 2 PCR amplicon of *mfhA*, Lane 3 and 4 *NcoI* and *BamHI* digests of pSDP9 respectively, Lane 5 *NcoI/BamHI* digest of pSDP6, Lane 6, *EcoRI* digest of pSDP9.

4.3 Expression and purification of MfhA

PNP degradation in MfhA induced cultures is an interesting observation (SIDDAVATTAM *et al.* 2003) and hence in the present study a detailed investigation was undertaken to gain clues on the role of MfhA assisted PNP metabolism in *E. coli*. Initially *in vitro* studies were performed by incubating pure MfhA with PNP. The expression plasmids constructed gave high level expression of MfhA. Plasmids pSDP3 and pSDP4 code MfhA with N-terminal His tag and N-terminal GST tag respectively. After expressing MfhA with N-terminal His tag, MfhA_{N-6His} was purified using Ni-NTA sepharose column. However over expression of MfhA_{N-6His} resulted in the formation of inclusion bodies. Change of expression conditions failed to produce MfhA_{N-6His} in soluble form. While solving this problem, the MfhA was expressed with N-terminal GST tag.

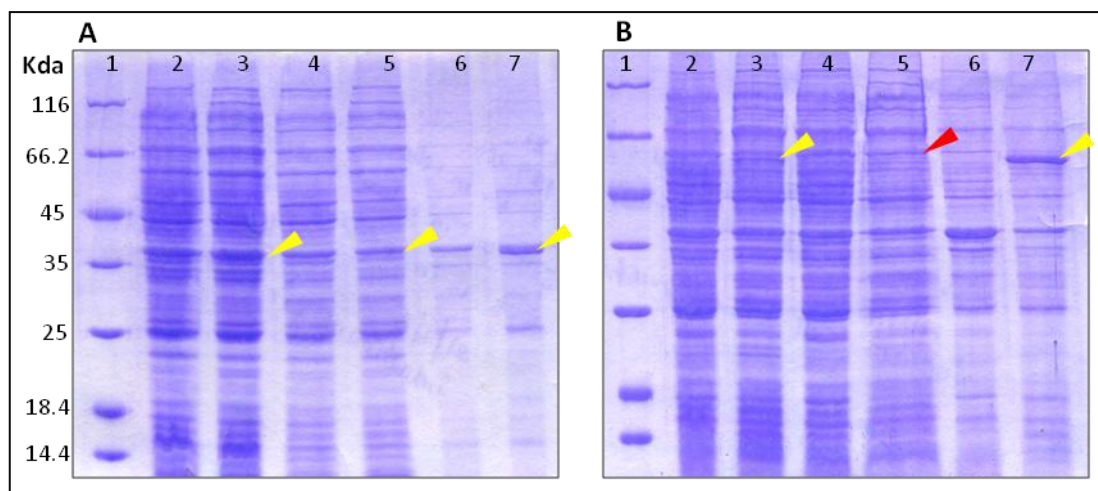


Fig 4-7| Expression of MfhA_{N-GHS} in *E. coli* BL21 DE3 [Panel A], and MfhA_{N-GST} in *E. coli* BL21 DE3 [Panel B]. Lane 1, Molecular weight marker in KDa; Lane 2, 3, represent protein extracts from uninduced and induced cells of BL21DE3 (pSDP3 or pSDP4); Lane 4, 5, Soluble fractions of uninduced and induced cells of *E. coli* BL21 DE3. Particulate fractions of uninduced and induced cells of BL21 DE3 are shown in lanes 6 and 7. Expression MfhA and MfhA_{N-GST} in soluble form is indicated with red arrow.

As shown in fig 4-7, expression of MfhA with N-terminal GST tag gave more MfhA in soluble form. The soluble portion of MfhA_{N-GST} got significantly increased when induction was carried out at low temperature (18°C) with reduced concentration of IPTG (0.5mM). As mentioned in methodology, MfhA_{N-GST} was purified using Glutathione-sepharose affinity column. However, there was considerable amount of free GST along with MfhA_{N-GST} [Fig. 4-8A Lane 2]. In order to remove free GST, gel exclusion chromatography was performed. The gel filtration separated free GST from MfhA_{N-GST} [Fig 4-8A Lane 4, 5]. The MfhA_{N-GST} was used for further studies. Furthermore the inclusion bodies of MfhA expressed without any affinity tag were solubilised and refolded (BURGESS 1996) to obtain MfhA without any affinity tags [Fig. 4-8B].

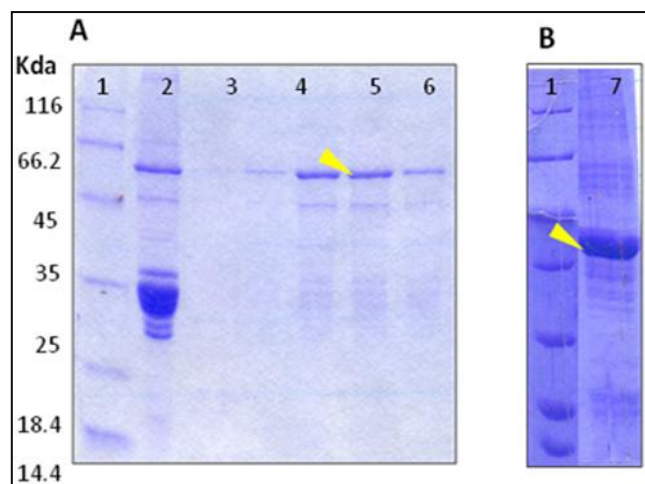


Fig 4-8| Panel A) Purification of MfhA_{N-GST} from the induced culture of *E. coli* BL21 DE3 (pSDP4). Panel B) Refolded MfhA from the inclusion bodies is shown in Panel B. Lane 1, Molecular weight marker in kDa; Lane 2, Purified protein fraction from Glutathione sepharose matrix. Lane 3-6 indicate various fractions eluted from Gel exclusion chromatography. Lane 7, Refolded MfhA protein. Arrow mark indicates MfhA_{N-GST} and MfhA.

After obtaining pure MfhA, either the purified MfhA_{N-GST} or MfhA was used to incubate, with different concentrations of PNP to assess if MfhA has any direct effect on PNP. Interestingly, added PNP was not degraded even after incubating the contents for more than 12 hr. Since the results gave clear indication to show no direct involvement of MfhA on PNP degradation, the PNP supported growth of *E. coli* K-12 MG1655 (pSDP5) is assumed due to its influence on induction of enzymes involved in catabolism of PNP. Existence of genetic information in *E. coli* for degradation of a number of aromatic compounds added strength for such a proposition (DIAZ *et al.* 2001). While perusing literature, to gain clarity on this unusual phenomenon, the author spotted two reports, where the proteins having esterase motif with a signature sequence **GXSAG** involving in metabolic diversion. These esterases hydrolyze general esterase substrate *p*-Nitrophenyl acetate (PNP-Ac) [Fig 4-9A]. Their involvement in diversion of metabolic machinery towards utilization of alternative carbon compounds as source of carbon and energy was clearly shown (PEIST *et al.* 1997; DEB *et al.* 2006). In the light of such reports, we have

initially used purified MfhA to know if it can hydrolyze *p*-Nitrophenyl ester [Fig 4-9B]. As expected PNP-Ac was hydrolysed by both MfhA_{N-GST} and refolded MfhA [Fig 4-9].

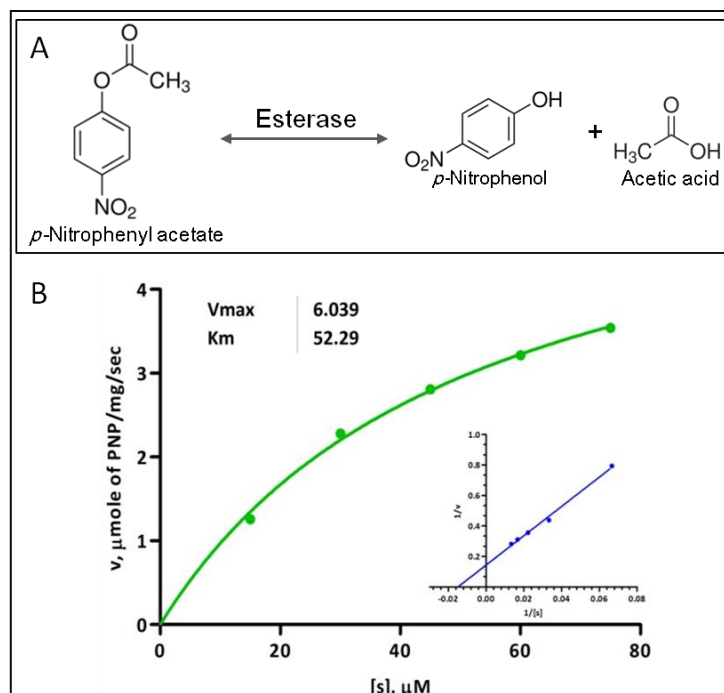


Fig 4-9| Kinetic studies using purified MfhA and using the substrate PNP-Ac (S) [Panel A]. Panel B indicated esterase activities of MfhA_{N-GST} at various substrate concentrations. Line-weaver Burk plot is shown as an insert.

When MfhA was incubated with different concentrations of PNP-Ac, complete depletion of PNP-Ac was observed in a time dependent manner, with a concomitant increase of PNP concentration. The kinetic properties of MfhA are shown in Fig 4-9. This experiment clearly demonstrated existence of esterase activity for MfhA. This observation coincided with the findings of PEIST *et al.* 1997 and DEB *et al.* 2006, where Aes of *E. coli* and Lip Y of *Mycobacterium tuberculosis*, are shown to promote by usage of alternate carbon sources. Both, Aes and LipY have typical esterase domain as seen in MfhA with a signature sequence of GXSAG and act on PNP-Ac to indicate esterase activity. Aes, identified in *Escherichia coli* codes for 35KDa acetyl esterase and it was shown to interfere in maltose metabolism by altering the maltose sensitivity in *malQ* mutant *E. coli*. The LipY is a hormone-sensitive lipase (HSL) identified in pathogenic *Mycobacterium*

tuberculosis. It was first time shown to be involved in the hydrolysis of Triglycerids (TG) with long chain fatty acids, especially when the pathogen is in dormancy stage. Both Aes and LipY are shown to promote usage of alternate carbon sources in their respective hosts. Is MfhA doing similar thing in *E. coli* K-12 MG1655? In order to gain answer to such questions further experiments were conducted.

4.4 *In vivo* studies

While performing *in vivo* studies, low copy expression plasmid pSDP5 was transformed into *Escherichia coli* K-12 MG1655 to express MfhA with N-terminal His tag. The *Escherichia coli* K-12 MG1655 (pMMB206) cells were used as control culture. The *E. coli* K-12 MG1655 (pSDP5) culture, grown in minimal medium (MM) were used to express MfhA_{N-6His}. Simultaneously, the culture was supplemented with 50 μ M PNP. As concentrations exceeding 50 μ M were toxic to *E.coli* cells, PNP was periodically added to the culture medium soon after the depletion of added PNP. The amount of PNP present in the culture medium was estimated spectrophotometrically by monitoring the absorbance at 410nm with a molar extinction coefficient of 16500M⁻¹ Cm⁻¹. As shown in fig 4-10, PNP concentration gradually decreased in *E. coli* K-12 MG1655 (pSDP5), however no such depletion of PNP was observed in the control cultures.

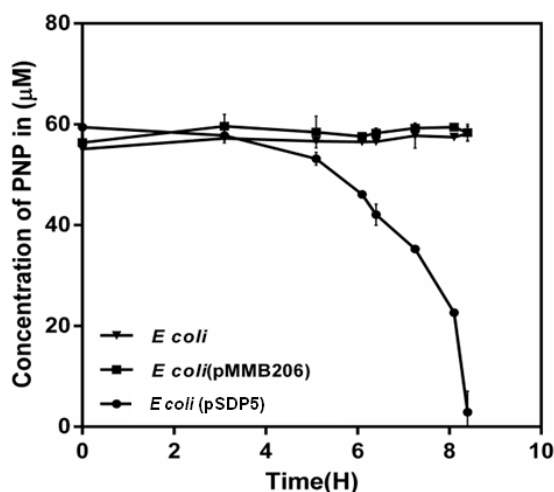


Fig 4-10| Quantification of PNP in the culture medium supporting the growth of various *E. coli* cultures.

This is rather an unusual observation which our laboratory has observed almost a decade ago (SIDDAVATTAM *et al.* 2003). In order to gain better insights into these unusual observations further experiments were conducted. Initially experiments were done to assess the fate of PNP added to the *E. coli* cultures expressing MfhA. Subsequently, experiments were also planned to see if added PNP is being utilized as carbon source. When *E. coli* K-12 MG1655 (pSDP5) cells were grown in MM using PNP as sole source of carbon there was growth [Fig 4-11] with considerably long lag period.

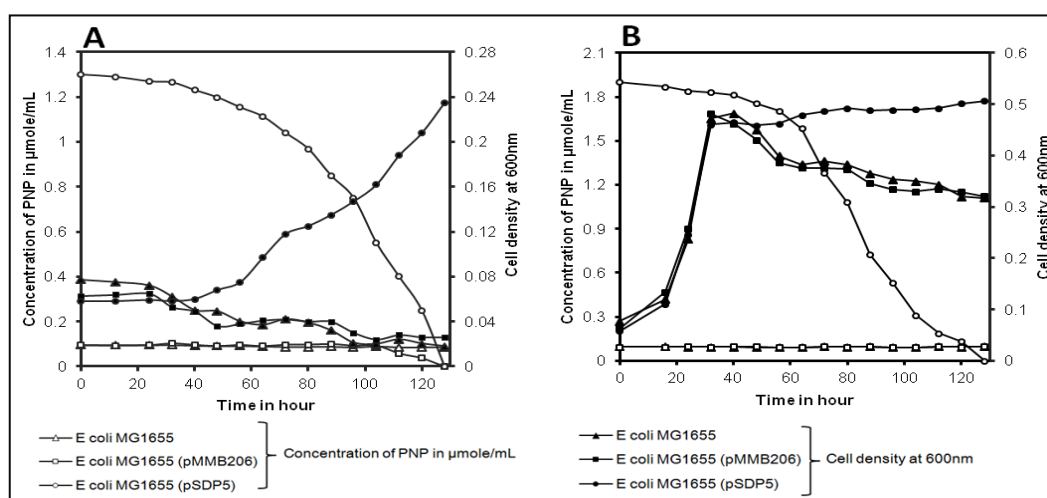


Fig 4-11| Growth studies of *E. coli* K-12 MG1655 (pSDP5) expressing MfhA_{N-6His}. Panel A Growth studies carried out using PNP as sole carbon source. Panel B Growth studies carried out using PNP and glucose as carbon source.

There was no growth for the initial 24hrs. After the initial lag the cells started growing, added PNP got completely disappeared from the medium. As more than 50µM of PNP was toxic to the cells, the PNP was added only after depletion of added PNP. That way the PNP concentration in culture medium was kept below 50 µM. As shown in fig 4-10, there was inverse relationship between depletion of PNP and growth of *E. coli* K-12 MG1655 (pSDP5) culture. Carbon catabolite repression is the known and well established phenomenon (MONAD 1942). Cells in the presence of mixed carbon source, use preferred carbon compound. Only when preferred carbon compound is exhausted, then the second carbon compound is used. This results in generation of diauxic growth curve (MONAD

1942; GORKE and STULKE 2008). However, such diauxie was not found in the growth curve of *E. coli* (pSDP5). The *E. coli* K-12 MG 1655 (pSDP5) cells grown in presence of glucose and PNP used both the compounds simultaneously. There was no expected diauxie in *E. coli* K-12 MG1655 (pSDP5) [Fig 4-11b] grown in PNP and glucose.

4.4.1 PNP metabolism in *E. coli* K-12 MG1655

Before proceeding to gain molecular basis for MfhA dependent PNP catabolism in *E. coli*, the PNP degradation pathway was initially established in *E. coli* K-12 MG1655 (pSDP5) cells. A number of studies are available on degradation of nitroaromatic compounds (SPAIN 1995; JU and PARALES 2010). Degradation of nitroaromatic compounds essentially proceeds either via reduction of $-\text{NO}_2$ group resulting hydroxylamino- or amino-derivatives or oxidation of aromatic ring ready to release of nitrite group (JU and PARALES 2010). After this initial conversion, the final oxygenolytic cleavage of aromatic ring takes place to channel the degradation products to TCA cycle. All these steps involves the stoichiometric consumption of molecular oxygen due to involvement of oxygenases in degradation process (Diaz *et al.* 2001). In most of the bacteria, aerobic degradation of *p*-Nitrophenol proceeds by two alternative pathways (Kadiyala and Spain 1998; Pakala *et al.* 2007; Zhang *et al.* 2012). Both of these pathways convert PNP finally into β -keto adipate and then to TCA cycle intermediates. Insights into existence of such pathways can be obtained by performing oxygen uptake studies and nitrite estimation studies. Further, metabolites formed during the process of oxidative degradation of PNP were detected by performing mass spectrometric analysis.

4.4.1.1 Oxygraph studies

Disappearance of PNP can be viewed in two different ways. It can be transformed due to the activity of MfhA into a non-toxic form. Such transformation may cause for disappearance of PNP. As there was PNP supported growth, it indicates an active catabolic

process leading to assimilation of PNP as carbon backbone of *E. coli* K12 MG1655 (pSDP5) culture. Bacterial PNP catabolism is a known process. Aerobic degradation of PNP in bacteria occurs in two different pathways before entering into TCA cycle. In the first pathway called *meta*-pathway, PNP is attacked by mono-oxygenases at *para* position of the aromatic ring and releases hydroquinone and nitrite group. Hydroquinone is further attacked by a ring-cleaving di-oxygenase to yield hydroxy-muconic semialdehyde which is enzymatically converted to β -keto adipic acid (WELLS and RAGAUSKAS 2012). In the second pathway, also known as *ortho*-pathway, a mono-oxygenase attacks at *ortho* or *meta* position of the aromatic ring resulting in the formation of 4-nitrocatechol which undergoes second monooxygenation at the *para* position and simultaneous release of nitrite group by the same enzyme. This results in generation of oxidised form of PNP, 1,2,4-trihydroxybenzene (BT). The BT undergoes second oxygenation step by ring-cleavage di-oxygenase to yield maleyl acetate and finally converted to β -keto adipic acid (ORNSTON 1966; HARWOOD and PARALES 1996). As stated before, in the first pathway there are two oxygenation steps and requires net consumption of 2 moles of molecular oxygen for each mole of PNP catabolism. In the second pathway, there are three oxygenation steps and hence there will be consumption of 3 moles of molecular oxygen. If in *E. coli* K-12 MG1655 (pSDP5), PNP is catabolised due to the involvement of oxygenases, addition of PNP should contribute for oxygen consumption in a MfhA dependent manner. As envisioned, the oxygen uptake was observed only in *E. coli* K-12 MG1655 (pSDP5) not in *E. coli* K-12 MG1655 (pMMB206) control culture. In the resting cells ($A_{600nm}=1.0$ approximately 10^9 cells) harvested and resuspended in sodium phosphate buffer, the shift in rate of oxygen consumption was noticed after addition of PNP only in the culture expressing MfhA [Fig 4-12]. No such consumption was seen in control cultures. When O_2 to PNP consumption was calculated it resulted in 33 nmoles of O_2

consumption for every 10 nmoles PNP. It suggests a stoichiometry between O_2 consumption and PNP degradation. Approximately 3 moles of O_2 is consumed for one mole of PNP in *E. coli* K-12 MG1655 (pSDP5) cells. It indicates involvement of two mono-oxygenation steps and a ring cleavage di-oxygenation process in degradation of PNP in *E. coli* K-12 MG1655 (pSDP5) cells expressing MfhAN-_{6His}.

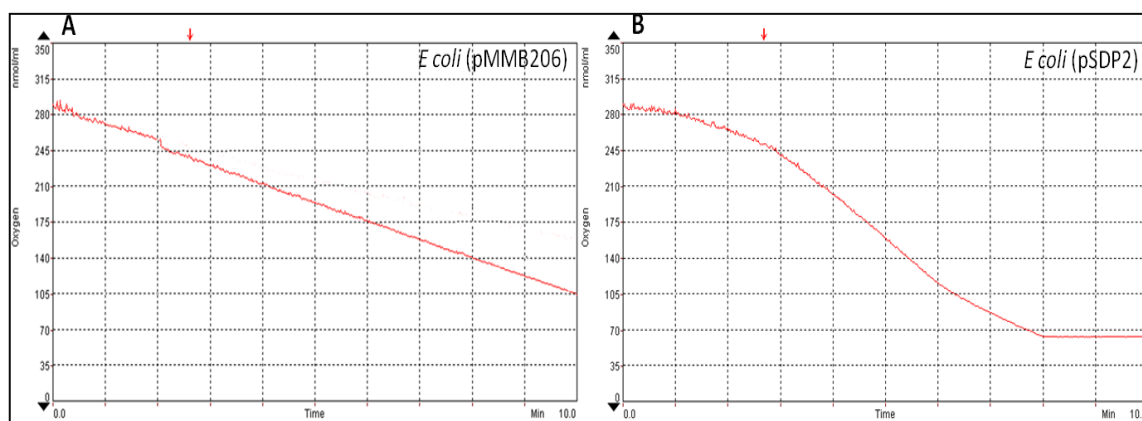


Fig 4-12| Oxygraph studies showing the increased uptake of O_2 during the conversion of PNP in *E. coli* (PSDP2) indicating the oxidation reactions

If this proposition is true, the mono-oxygenation at *para* position should contribute for stoichiometric release of nitrite from PNP. When PNP was estimated in the culture medium a stoichiometric release of nitrite was only observed in MfhA expressing induced culture of *E. coli* K-12 MG1655 (pSDP5) [Fig 4-13].

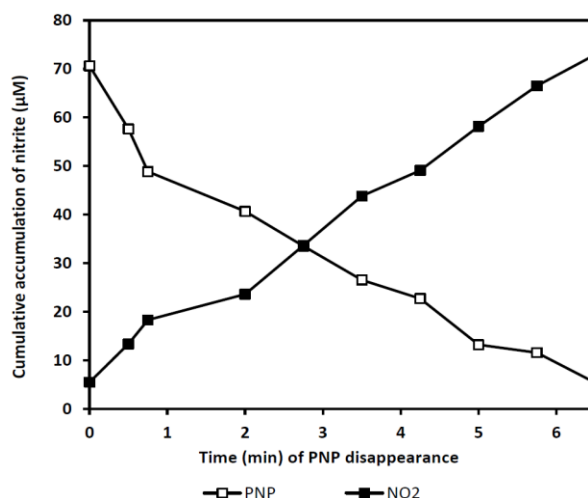


Fig. 4-13| Nitrite estimation studies showing the stoichiometric release of nitrite with PNP.

4.4.1.2 HPLC and LC-MS/MS analysis of PNP degradation products

After gaining convincing evidence on the involvement of mono-oxygenases and di-oxygenases in MfhA induced PNP degradation, a resting cell assay was carried out to identify PNP catabolic intermediates in MfhA induced *E. coli* K-12 MG1655(pSDP5). When the metabolites extracted from the MfhA expressing resting cells were analysed on LC-MS there was a time dependent decrease in PNP (Peak 11.4min). Simultaneously an increase in concentration of its degradation products was noticed in the medium. The height of the new peaks at RT 4.7 min (peak C) and RT 8.2 (peak B) increased with increase of incubation time [Fig 4-14].

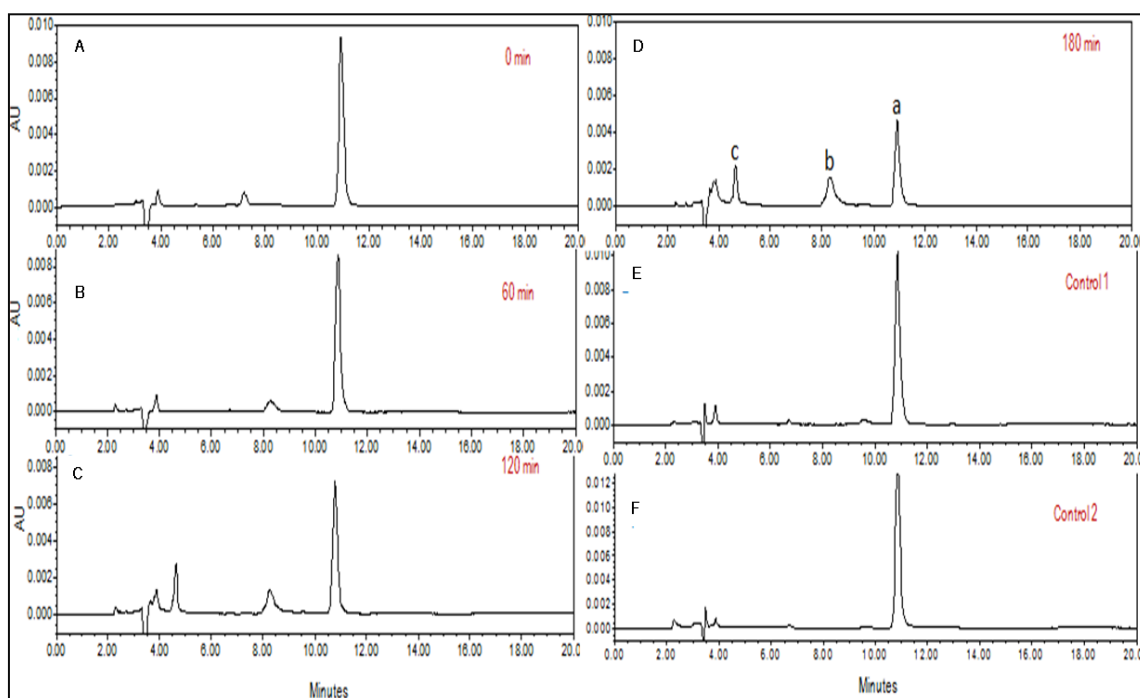


Fig. 4-14| RP-HPLC analysis of PNP degradation products are shown in panel A, B, C, and D respectively. The chromatograms of PNP degradation products prepared from *E. coli* (pSDP5) resting cells after incubating for 0, 60, 120 and 180 min respectively. Panel E and F represent chromatograms of PNP degradation product extracted from control *E. coli* and *E. coli* (pMMB206) resting cell assay after 180min.

These new peaks (peak B and C) were then subjected to mass spectral analysis using on-line LC-MS, (agilent 6500) work station operated in positive mode. HPLC grade Nitrocatechol and Hydroxy-benzoquinone were run under identical conditions and compared their retention time and mass patterns with these new peaks. The mass

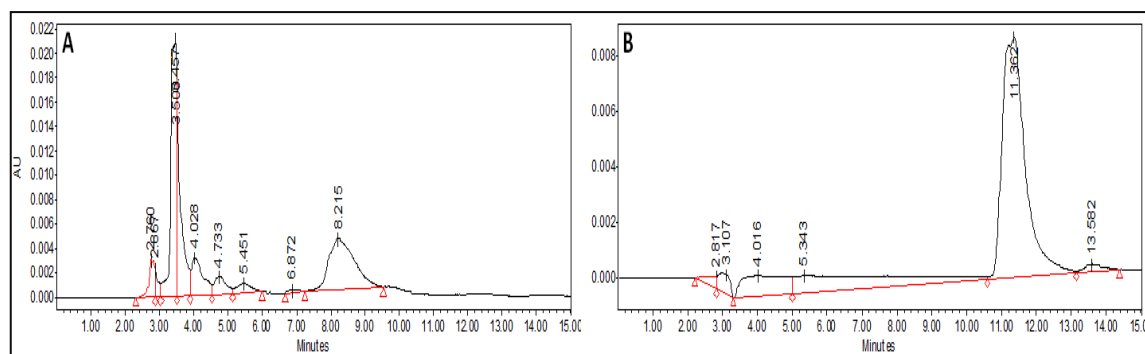


Fig. 4-15| RP-HPLC analysis of 2,3,5,6 Deuteriated 4-Nitrophenol degradation products. Panel A and B represent chromatogram of 2,3,5,6 Deuteriated 4-Nitrophenol extract prepared from *E. coli* (pSDP5) and *E. coli* (pMMB206) resting cell assay after 60 min of incubation respectively.

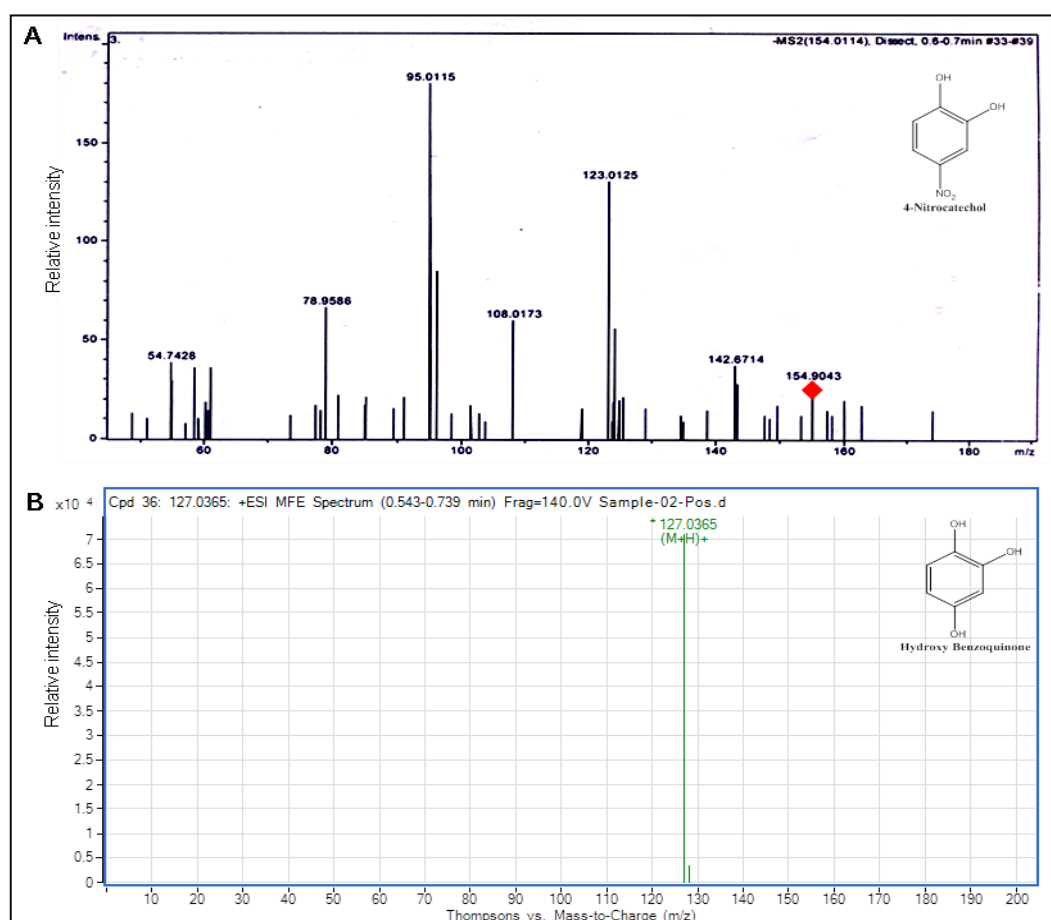


Fig. 4-16| LC-MS analysis of PNP degradation products. Panel A MS/MS fragmentation pattern of peakB which has shown identical mass fingerprint of 78.9, 95.2, 108, 123 and 142.4 generate during the LC-MS/MS of standard Nitrocatechol and Panel C represent MS pattern of peak C of HPLC chromatogram that has shown identical MS pattern of Hydroxy benzoquinone (BT).

fingerprints thus generated for these standards matched with the mass fingerprint of peak B (RT 4.7 min) and peak C (8.2 min) [Fig 4-16] indicating that PNP degradation in MfhA induced *E. coli* K-12 MG1655 cells proceeds via *ortho*-cleavage pathway, before entering

into TCA cycle. These results were further confirmed using stable PNP isotope, 2,3,5,6 Deuteriated 4-Nitrophenol and as shown in fig B and identical results were obtained [Fig 4-15].

4.4.1.3 Proteomic approach

After identifying the PNP catabolic products and obtaining evidence on the involvement of mono and di-oxygenases, an attempt was made to identify involvement of catabolic enzymes by performing proteomic analysis. As stated in materials and methods section, the total proteins extracted from MfhA induced *E. coli* were compared with the similar protein extracts prepared from control cultures [Fig 4-17]. Proteome analysis of IPTG induced culture of *E. coli* K-12 MG1655 (pSDP5) was compared with proteome of control maintained at similar conditions to examine differentially expressed proteins [Fig 4-17].

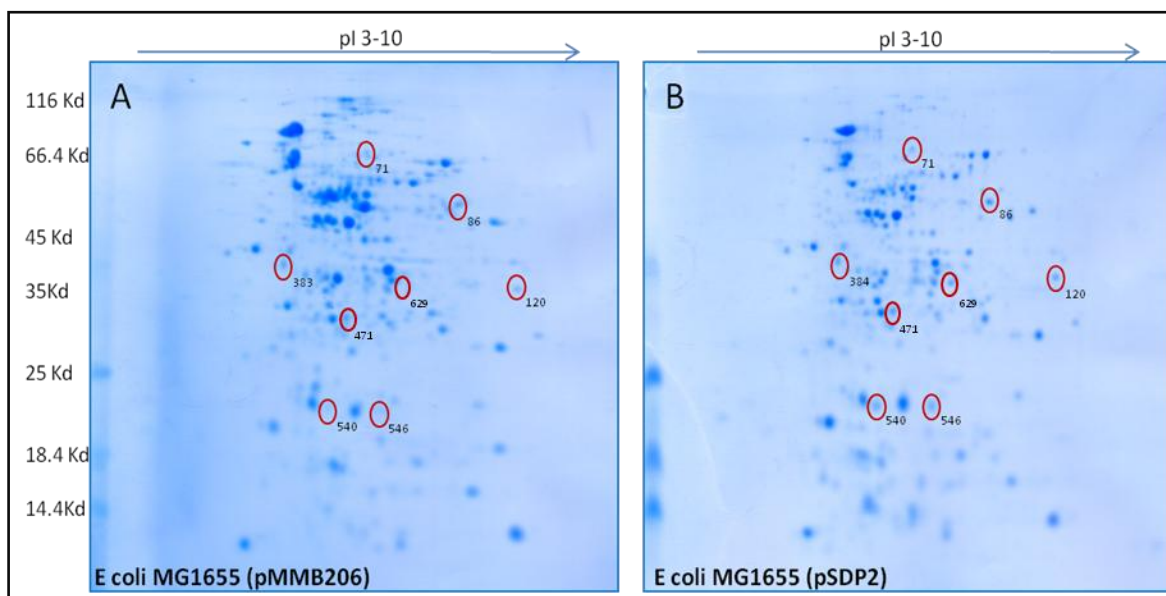
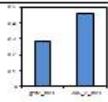
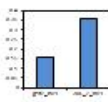
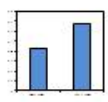
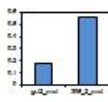
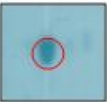
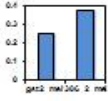
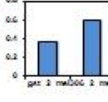
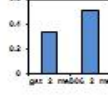


Fig. 4-17| Complete protein profile of *E. coli* K-12 MG1655 in the presence (Panel B) and absence (Panel A) of MfhA expression. The protein spots upregulated in presence of MfhA are shown in circles and were selected for MALDI-MS analysis.

The 2D gels obtained were subjected to image analysis using ImageMaster2D Platinum software. After performing normalization studies, protein spots that were shown up-regulated were selected for MALDI-TOF analysis. The up-regulated proteins showing

significant score and sequence coverage with the proteins found in database was presented in table 4-1. Out of the seven protein spots identified through MALDI-MS, two of them were shown to be involved in degradation of aromatic compounds. One of them was a mono-oxygenase (spot120), the second one was a DNA binding transcriptional regulator (HcaR) (spot540). The HcaR is involved in upregulation of *hca* operon involved in degradation of Phenyl propionates (PP). This data correlates well with the data obtained on, O₂ consumption and PNP degradation profile generated in MfhA induced *E.coli* cells. It also suggests that MfhA dependent upregulation of PP pathway. In addition to the aforementioned protein spots that are directly involved in catabolism of aromatic compound degradation, several TCA cycle specific enzymes got upregulated [Table 4-1].

Table 4-1| Magnified regions of 2D gel images in the region containing upregulated protein spots. The histograms are represented in panel A. The 1st and 2nd bars represent protein spot intensities in the absence and presence of MfhA.

Spot No	Histogram	E coli K-12 MG1655 (pMfMB206)	E coli K-12 MG1655 (pSDF5)	Protein ID	Mouse score	pI	Mass (Da)	Accession No.
86				NADH dehydrogenase I, subunit C	21	7.6	101148	NUOG_ECOLI
71				NADH dehydrogenase I, subunit nuof	16	8.0	58000	NUOF_ECOLI
384				Succinate dehydrogenase flavoprotein subunit	17	7.5	67000	gi 5822495
120				Monoxygenase	37	7.9	36000	Q7AAZ5_ECO57
540				DNA binding transcriptional regulator HcaR	36	5.29	24940	gi 297518100
629				Methylisocitrate lyase	48	5.33	32300	gi 260450477
471				DNA-binding transcriptional regulator GlcC	44	9.77	31284	gi 26249541

cycle intermediates during the course of aromatic compounds degradation is an established phenomenon (DIAZ *et al.* 2001). Therefore, increase in TCA cycle enzymes, especially succinate dehydrogenase is certainly an indication for assuming the conversion of PNP into TCA intermediates via dedicated degradation pathway, which is induced in *E. coli* K-12 MG1655 (pSDP5) in an MfhA dependent manner. Upregulation of a regulatory protein HcaR, which has positive influence on PP degradation pathway, that to in a MfhA dependent manner points its involvement in degradation of *p*-Nitrophenol. In the subsequent chapters detailed study was undertaken to gain further evidence on the mechanism involved in the upregulation of phenylpropionic acid pathway genes.. Basing on the metabolites identified during PNP degradation a tentative degradation pathway followed in *E. coli* K-12 MG1655 for PNP degradation is proposed [Fig 4-18].

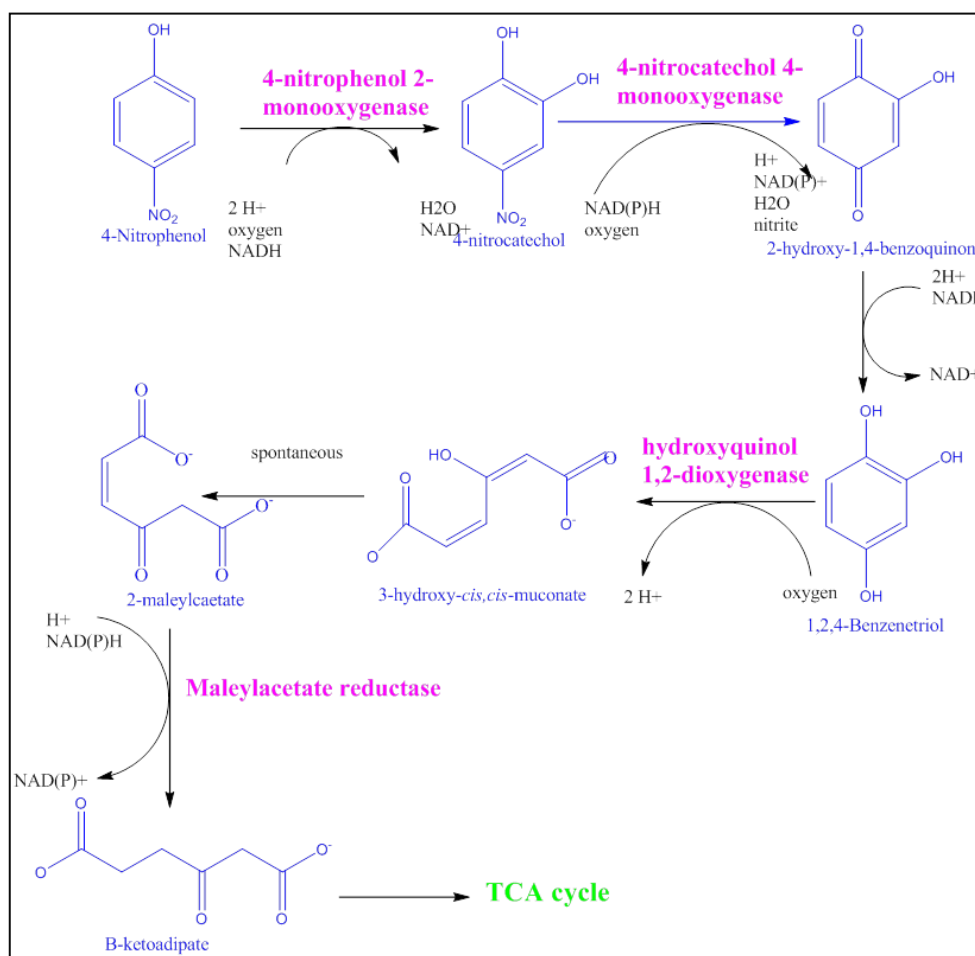


Fig 4-18| Proposed PNP degradation pathway in *E. coli* K-12 MG1655 (pSDP5).

4.5 OPH interacts with MfhA

The experimental evidence gathered from the aforementioned experiments described above clearly suggest that the MfhA mediated PNP utilization by *E. coli* K-12 MG1655 (pSDP5), is due to induction of Phenylpropionate (PP) operon. It also clearly suggests that the PNP catabolism in *E. coli* K-12 MG1655 (pSDP5) is proceeding via *ortho*-cleavage pathway. The OPH is a membrane associated enzyme (GORLA *et al.* 2009). The studies conducted in our lab clearly showed mechanism of membrane targeting of OPH in *B. diminuta*. The genetic organization of *opd*-cluster, in both *S. fuliginis* and *B. diminuta* suggest localization of *mfhA* adjacent to *opd* gene (PANDEETI *et al.* 2011; PANDEETI *et al.* 2012), that codes for membrane anchored OPH (GORLA *et al.* 2009). In *S. fuliginis* it is organized as an independent transcriptional unit and located downstream of *tnpA* [Fig 4-2] in the same transcriptional orientation. Such genetic organization and the similarity of MfhA with esterases, Aes, lipY which promote utilization of alternate carbon sources, to some extent indicate existence of similar mechanism in MfhA dependent PNP utilization in *E. coli*. Since OPH is a membrane protein, initially experiments were conducted to establish interactions between these proteins.

The interactions between OPH and MfhA were established by performing pull down assays as described in materials and methodology section. Two expression plasmids were generated to express OPH_{C-6His} and MfhA_{N-GST}. These two are compatible plasmids and hence were transformed in *E. coli*. The *E. coli* JM109DE3 having vector, pGEX-4T-1 and pPHLLC400 served as control. Induction of *E. coli* JM109DE3 (pSDP4/pPHLC400) with 1mM IPTG results in the simultaneous expression of MfhA_{N-GST} and OPH_{C-6His} proteins. To perform interaction studies, single colony of *E. coli* JM109DE3 (pSDP4/pPHLC400) was inoculated in 10mL of LB broth and grown to log phase. This culture was then induced with 1mM IPTG and incubated at 18°C for 4 h. Cells from

induced culture was harvested by centrifugation and used for GST pull down assay as described in the methodology. Cell lysates prepared from experimental and control cultures were incubated with Magne Glutathione beads and the thoroughly washed beads were analysed on 12.5% SDS-PAGE. A protein band corresponding to a size of 36KDa (OPH) was found to be co-purified along with the 54 KDa, MfhA_N-GST. Such co-purification of 36KDa protein was not identified in the Magne Glutathione beads prepared from the control sample [Fig 4-19A]. The 36 KDa protein band gave positive signal, when western blot was done using anti-OPH antibodies. The OPH_{C-6His} specific signal was seen only in the protein preparations isolated from *E. coli* JM109DE3 (pSDP4/pPHLC400). However, such signal was not obtained in the control culture *E. coli* JM109DE3 (pGEX-4T-1/pPHLC400) where GST and OPH_{C-6His} were co-expressed [Fig 4-19A]. This clearly indicates that OPH_{C-6His} association to the Magne Glutathione beads is due to MfhA_N-GST but not due to GST protein.

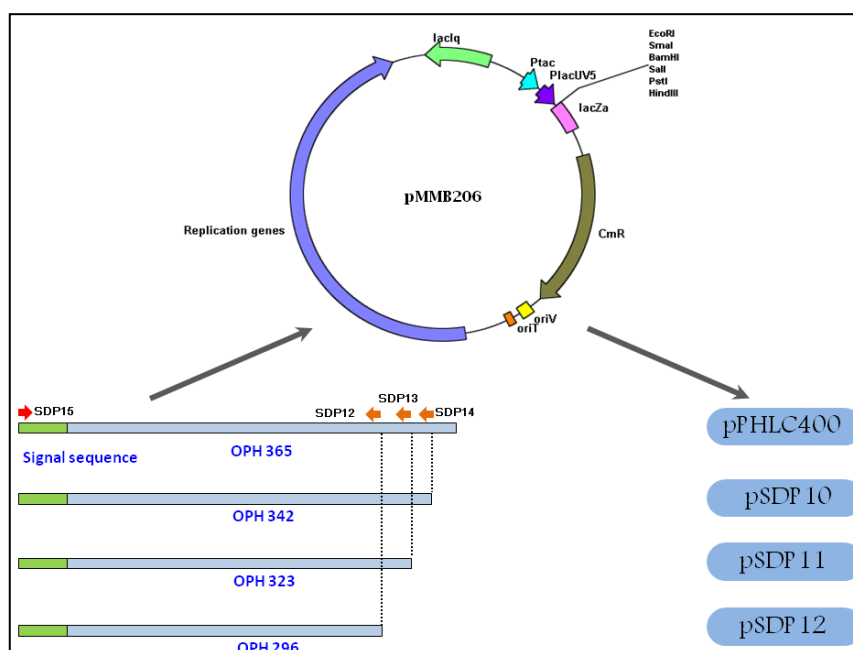


Fig 4-19| Diagrammatic representation of cloning strategy of *opd* expression plasmids coding OPH with C-terminal deletions. Using pPHLC400 as a template an amplicon was generated using SDP14/SDP15 primer set and cloned into pMMB206 to generate pSDP10, which codes for precursor form of OPH with C-terminal 13 amino acids deletion. Similarly pSDP11 and pSDP12 were generated using primer sets SDP13/SDP15 and SDP12/SDP15 respectively. pSDP11 and pSDP12 codes for precursor form of OPH with deletion of C-terminal 42 and 69 amino acids respectively.

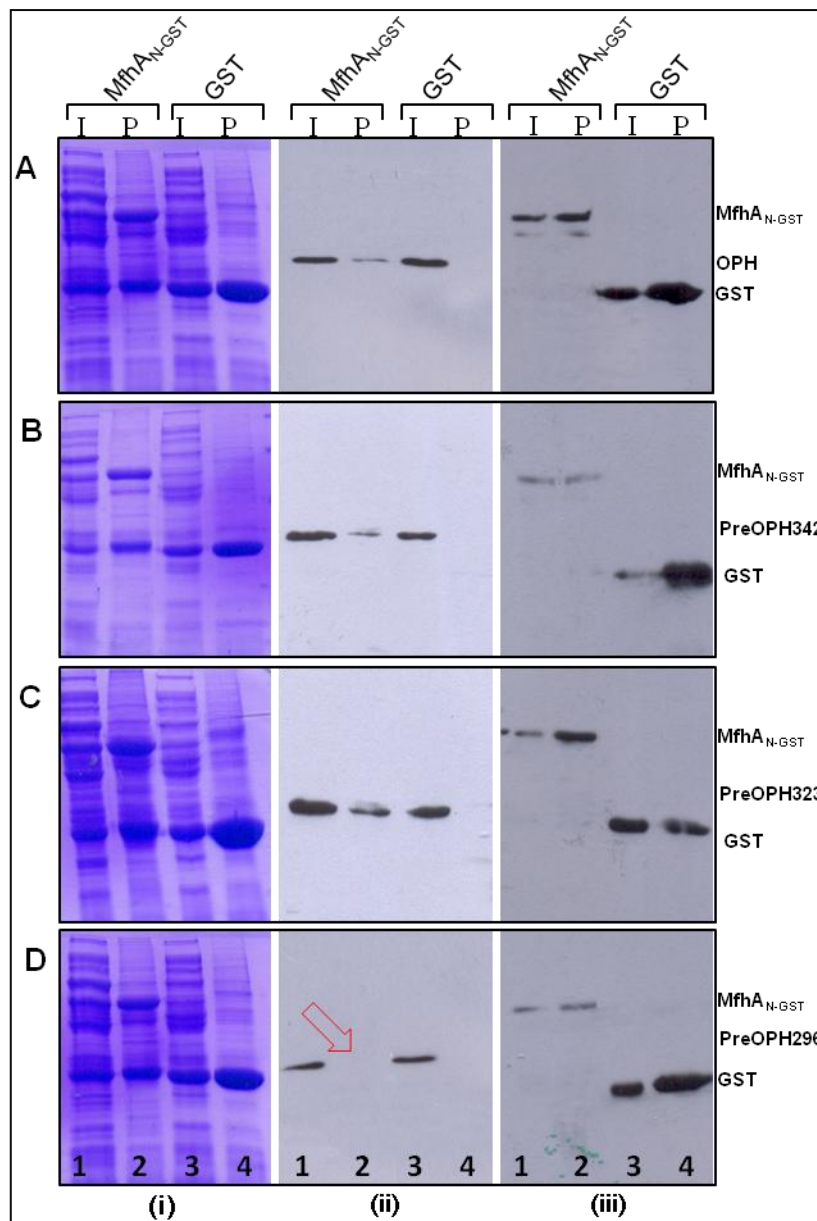


Fig 4-20| GST pull down assay showing interactions between OPH and MfhA_{N-GST}. Input (I) and pull down proteins (P) from *E. coli* (ppHLC400) expressing either MfhA_{N-GST} or GST are analysed on 12.5% SDS-PAGE (i). The corresponding immunoblots probed with anti-OPH (ii) or anti-GST antibodies (iii) indicate existence of only in MfhA_{N-GST} co-expressed cultures [Panel A, lane 2(ii)]. No OPH specific band is seen when only GST is expressed with OPH. Requirement of C-terminal position of OPH for MfhA interaction is shown in Panels B, C, and D. Deletion of 69 amino acids showed no OPH specific band even in the presence of MfhA_{N-GST} [Panel D, Lane 2(ii)].

Further, expression plasmids were also constructed to identify the OPH region interacting with MfhA. As shown in Fig 4-19, expression plasmids were constructed to express OPH with C-terminal deletions. These plasmids were then transformed in *E. coli* JM109DE3 (pSDP4) strain expressing MfhA_{N-GST}. The pull down assays performed indicates co-

elution of OPH along with MfhA_{N-GST} only when C-terminal region was found in OPH. The pull down assays performed from the clones expressing sequential C-terminal regions indicated that the last 69 amino acid residues from the C-terminal region of OPH are critical for interacting with MfhA.

4.5.1 Sub-cellular localization of MfhA_{N-6His} in *S. fuliginis*

The experiments described above gave clear indication on OPH and MfhA_{N-GST} interactions. Since OPH is a membrane associated protein (GORLA *et al.* 2009) an attempt was made to localize MfhA in *S. fuliginis*. The broad host range expression plasmid pSDP5 coding for MfhA_{N-6His} mobilized into *S. fuliginis* ATCC 27551. The *S. fuliginis* ATCC 27551 (pSDP5) cultures expressing MfhA_{N-6His} were used to prepare membrane and cytosolic fractions. The prepared membrane and cytosolic fractions were then analyzed on 12.5% SDS-PAGE and presence of MfhA_{N-6His} was detected by performing western blotting with anti-His antibodies. As shown in fig 4-21, a signal corresponding to the size of MfhA_{N-6His} was found in membrane fraction. These results gave a preliminary indication on localization of MfhA in membrane. As MfhA interactions with OPH were apparent it appears that the MfhA is transported and associated to the membrane in a OPH dependent manner.

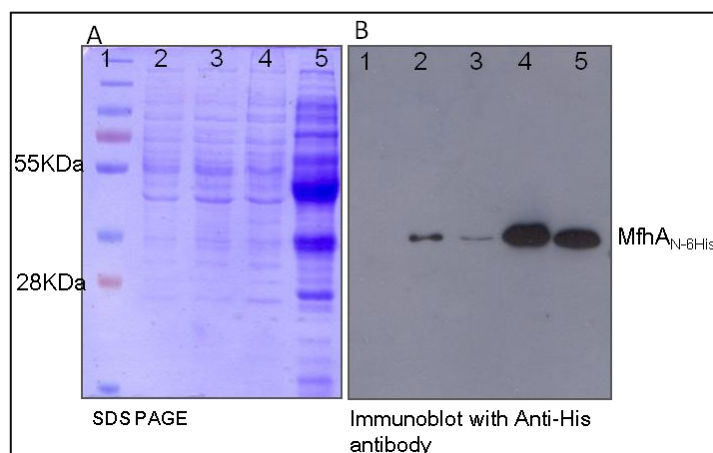


Fig 4-21| Subcellular localization of MfhA_{N-6His} in *S. fuliginis* ATCC 27551 (pSDP5). The total proteins extracted prepared from *S. fuliginis* is loaded in lane 2. Lane 3 and 4 represents cytosolic and membrane fraction protein extracts of *E. coli* BL21 DE3 (pSDP3) expressing MfhA_{N-6His} is shown in lane 5. Panel B represents western blots probed using anti-His antibodies.

Results and Discussion | Chapter 3

5.0 Background

In the first and second chapters the HGT of *opd*-island and indirect involvement of MfhA, in degradation of PNP, the recalcitrant metabolite generated during OPH mediated degradation of parathion and methyl parathion were studied. As stated in preceding chapters, expression of MfhA in *E. coli*, enabled it to degrade PNP added to the culture medium. The *E. coli* cells expressing MfhA have even grown using PNP as carbon source. The proteome analysis of MfhA induced *E. coli* K-12 MG1655 (pSDP5) cells, revealed upregulation of proteins/enzymes involved in degradation of aromatic compounds. Upregulation of a di-oxygenase, mono-oxygenase and PNP dependent oxygen consumption pointed towards existence of MfhA dependent upregulation of genes/operons involved in aromatic compound degradation. These observations have promoted us to undertake genome wide expression profiling in *E. coli* K-12 MG1655 (pSDP5) cells expressing MfhA. The genome expression profiling was done by performing microarray studies using probes corresponding to both coding and non-coding sequences. The total RNA extracted from glucose grown *E. coli* cells, with and without MfhA expression plasmids were hybridized with *E. coli* K-12 MG1655 microarray (Agilent control grid: IS-15744-8-V1_8x15K_Gx_EQC_ V20060608) chip. The differential expression thus obtained was recorded in a time dependent manner (0, 1.5 and 3.0 h respectively). Out of the 4115 genes, about 387 gene transcripts were up-regulated and about 389 were found down-regulated. Nearly expression of 3390 genes and 2096 out of 2326 non-coding sequences remained unaltered. As expected, the microarray data complemented proteomics data and provided better insights on MfhA dependent PNP degradation in *E. coli*. These differentially expressed genes were carefully analyzed to identify influence of MfhA on various metabolic pathways. Among aromatic compound catabolic pathways, the pathways involved in degradation of phenyl propionates (PP) and hydroxyl phenyl

propionates (HPP) were found upregulated [Fig 5-1A]. Similarly genes coding methyl citrate cycle I and glyoxalate shunt-TCA cycle enzymes were also found in the list of upregulated genes [Fig 5-1B]. In contrast the expression levels of glycolysis and glycolysis-TCA superpathway got down regulated. Down regulation of these two primary pathways involved in carbon metabolism, especially in *E. coli* cells grown in glucose, is an interesting observation. An increase in the transcript levels of the tryptophan degradation was also found upregulated. However no change is observed in transcript quantity of the genes coding for all three aromatic amino acid biosynthetic pathways. Reflecting the decreased metabolic activity, the transcripts of genes coding for aminoacid biosynthetic pathway enzymes got down regulated.

However, the transcriptome analysis of the whole genome of *E. coli* K-12 MG1655 revealed significant induction of PP, HPP operons, along with methyl citrate pathways and glyoxalate shunt pathways. Much difference in the nucleotide metabolism was not observed. An overview of the transcriptome data suggests that the presence of MfhA influences the carbon metabolism. To gain further insights into these observations, null mutants of *E. coli* were generated by deleting key genes coding for upregulated pathway genes and studied their influence on MfhA dependent degradation of *p*-nitrophenol. Further the transcript levels of the key genes coding for differentially regulated pathways were quantified by performing the real time q-PCR to assess if microarray data reflects the physiological status of the cell.

5. 1 MfhA dependent genome-wide expression profiling in *E. coli* K-12 MG1655

Microarray data was generated using commercially available *E. coli* K-12 MG1655 microarray (Agilent control grid: IS-15744-8-V1_8x15K_Gx_EQC_ V20060608) chip. As mentioned in methodology, *E. coli* K-12 MG1655 (pSDP5) was grown in MM

supplemented with glucose as sole carbon source. After inducing MfhA, the total RNA extracted at different time intervals (0, 1.5, and 3.0h) were hybridised to chip. Similarly total RNA extracted under identical conditions from *E.coli* K-12 MG1655 (pMMB206) having empty expression vectors were used to normalise the background. Care was taken to avoid the addition of *p*-Nitrophenol to the culture medium.

5.1.1 MfhA dependent upregulation of Phenyl propionate (PP) pathway

As described in the preceding chapter, the proteome analysis has revealed upregulation of mono-oxygenase, di-oxygenase and a transcriptional activator HcaR [Table 4-1, page No.76.]. It has given preliminary indication about MfhA dependent upregulation of enzymatic machinery involved in aromatic compound degradation. In *E.coli* K-12 there are four dedicated operons for degradation of a variety of aromatic compounds (DIAZ *et al.* 2001). All of them code for oxygenases. Under such a scenario the proteome analysis indicates upregulation of oxygenases, but fails to identify the operon coding for an oxygenase upregulated in an MfhA dependent manner. The genome-wide expression profiling has clearly shown down regulation of both glycolytic and TCA cycle enzymes [Fig 5-1]. In *E.coli* cells, especially when grown in glucose, down-regulation of enzymes/proteins involved in glucose metabolism is unusual (Fig 5-1B). Interestingly, when expression profile of aromatic compound degrading operons was examined, of all the four operons, the operon involved in phenylpropionate (PP) degradation is up regulated in MfhA dependent manner. Consistent of this observation, the transcription factor coding for HcaR is also up-regulated. HcaR is a transcriptional activator of PP operon. In *E.coli* cells both HcaR and PP operon specific transcripts got upregulated only in *E.coli* cells expressing MfhA [Fig 5-2]. The concentration of the transcripts increased in a time dependent manner [Fig 5-3].

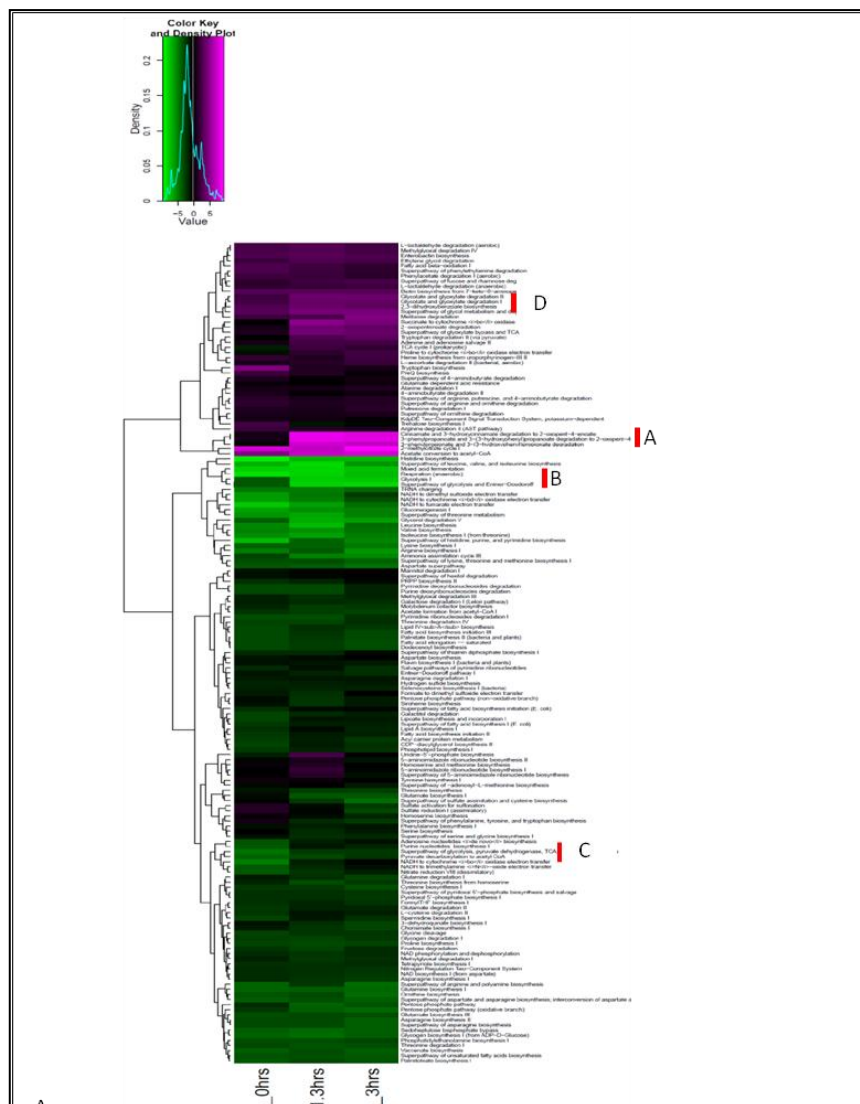


Fig 5-1| Heatmap generated for the differentially regulated pathways in *E.coli* K-12 MG1655 (pSDP5). MfhA was induced and the transcriptome analysis was done at 0h, 1.5h, and 3.0h time intervals. The upregulated/downregulated pathways are shown as A, B, C and D.

As seen in heat map at 0 minutes of MfhA induction no change is seen in the transcript concentration of *hca* operon. However, when induction time is increased, the expression levels got proportionally increased and reached a steady state level at 3.0h of MfhA induction. The cells were grown in glucose. There was no PNP in culture medium to implicate its direct role in induction of *hca* operon. In the absence of any aromatic compound, induction of PP pathway indeed speaks of existence of a novel mechanism for inducing *hca* operon in a MfhA dependent manner.

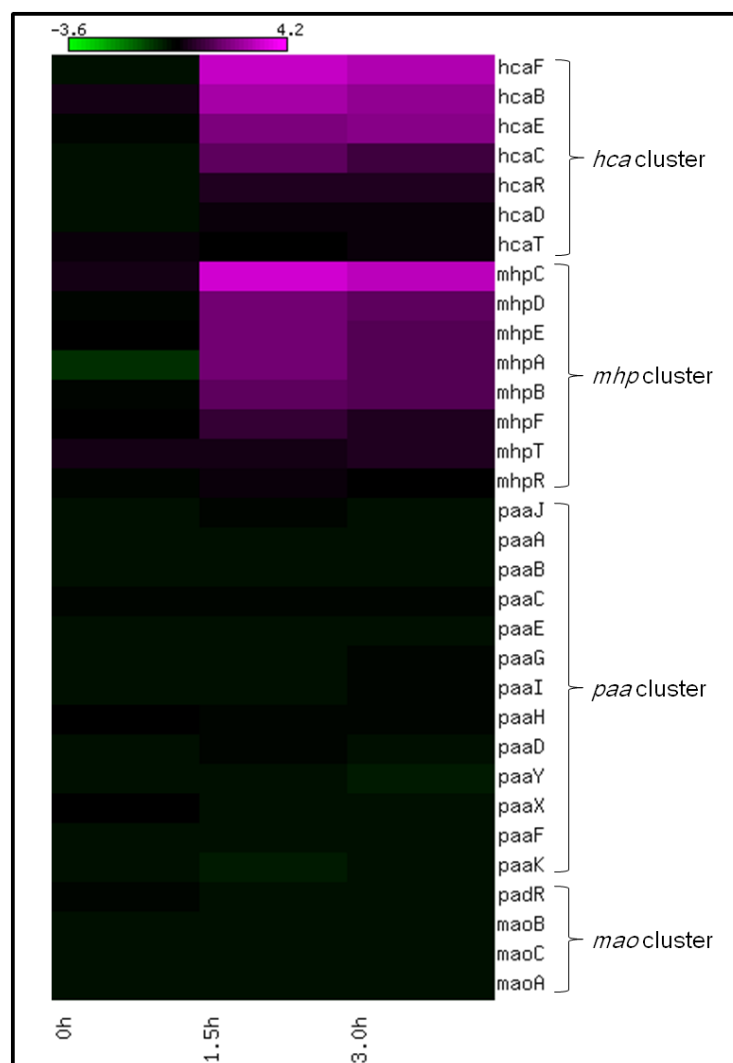


Fig 5-3| Heat map representing the MfhA influence on the transcript levels of four aromatic degradation pathway genes. 0h, 1.5h and 3.0h indicate duration after induction of MfhA.

In the light of this observation the proteomics data described in the previous chapter was revisited to identify if there are any biochemical similarities between upregulated oxygenases and PP specific oxygenases. The pI, mass of oxygenase and transcription activator identified in MfhA induced *E. coli* proteome perfectly matched with HcaR and mono-oxygenase of *hca* and *mhp* operons respectively [Table 4-1]. If these two independently generated results are taken into consideration, it certainly points towards involvement of PP and HPP operons in PNP degradation. Therefore, studies were conducted to gain role of *hca* operon in PNP degradation. Initially we have carefully observed microarray data pertaining to four operons involved in degradation of aromatic

compounds. As shown in fig 5-2 only *hca* and *mhp* operons were induced in a MfhA dependent manner [Fig 5-1]. The other two operons, such as *paa* and *mao* operons have not responded positively to MfhA expression. The microarray data was further validated by generating mutant strains of *E. coli* K-12 MG1655 by deleting key ORFs in each of these four operons. The *hcaE*, *mhpA*, *paaA* and *maoA* were deleted from the Phenyl propionate (PP), 3-Hydroxyphenyl propionate (HPP), Phenyl acetate (PA) and Monoaromatic amine degradation pathways respectively Fig 5-4.

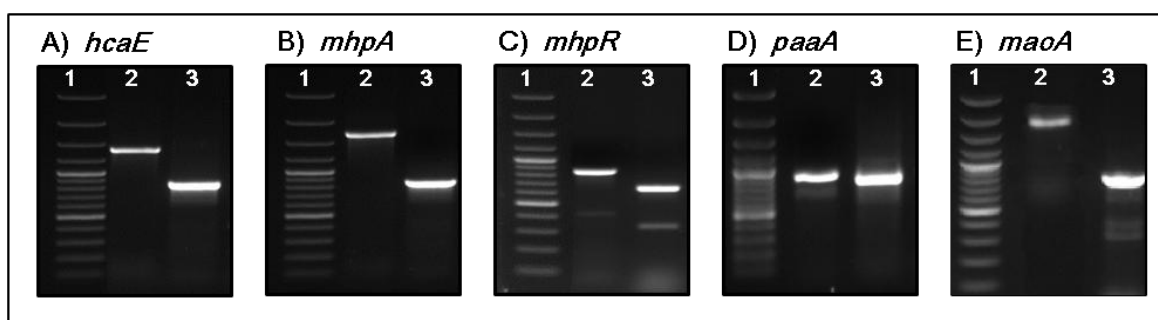


Fig 5-4| Generation of mutant strains of aromatic compound degradation pathway in *E. coli* K-12 MG1655. Panel A, B, C, D and E represent deletion of *hcaE*, *mhpA*, *mhpR*, *paaA*, and *maoA* respectively. Lane 1 molecular weight marker, Lane 2 and 3 represent amplicons of mutant and wild type genes of *E. coli* K-12 MG1655 cells.

The *hcaE* codes for PP-dioxygenase component of PP degradation pathway. Similarly, the *mhpR* and *mhpA* code for transcription factor and monooxygenase gene of HPP pathway respectively. Likewise, the *maoA* codes for monoamine oxidase of aromatic amine degradation pathway and *paaA* code for a subunit of multi-component monooxygenase involved in PA degradation pathway. In microarray data, the *hca* and *mhp* operons were significantly induced in a MfhA dependent manner and probably suggest their involvement in *p*-Nitrophenol degradation. If this proposition is true *E.coli* $\Delta hcaE$, $\Delta mhpA/\Delta mhpR$ mutants should not grow in PNP even in presence of MfhA. Similarly, there should not be any influence on MfhA assisted PNP growth in *E. coli* $\Delta maoA$ and $\Delta paaA$ mutant strains. Supporting this hypothesis, the *E.coli* $\Delta mhpA$, $\Delta mhpR$, $\Delta hcaE$ mutants failed to grow in PNP even in the presence of MfhA [Fig 5-5 D, E, and F].

However, the *E. coli* $\Delta maoA$, $\Delta paaA$ mutants have grown on PNP where MfhA was induced [Fig 5-5 B, C]. This data clearly shows involvement of only *hca* and *mhp* operons in degradation of *p*-Nitrophenol in a MfhA dependent manner [Fig 5-5].

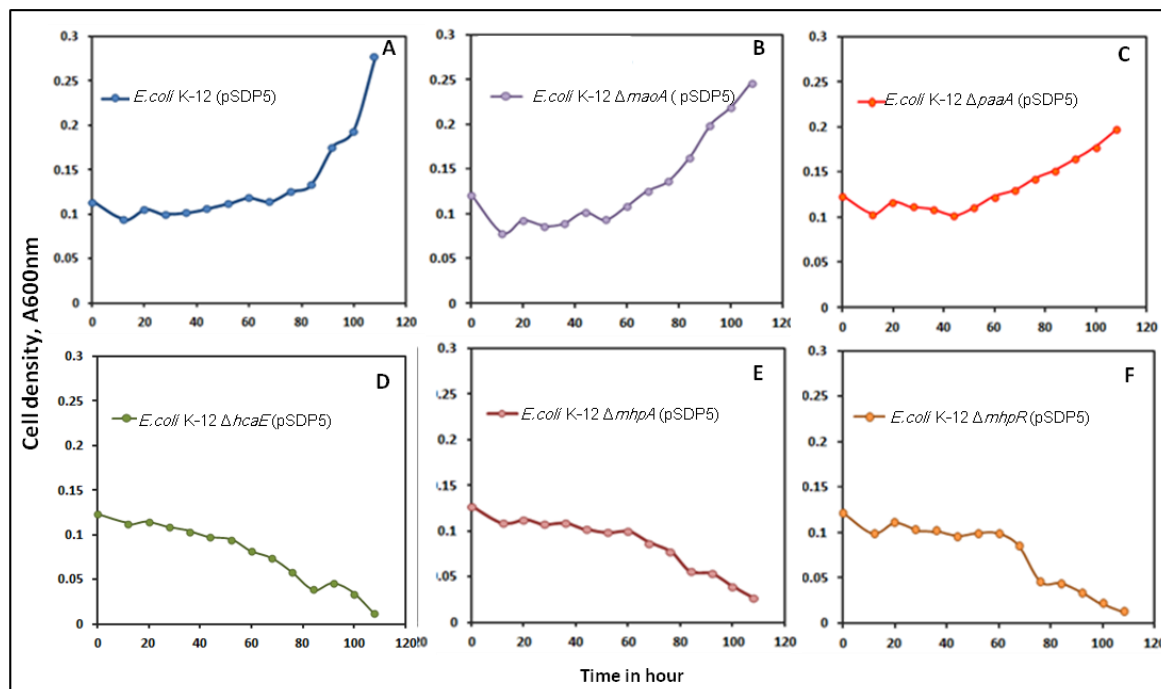


Fig 5-5| Growth studies of *E. coli* K-12 MG1655 (pSDP5) wild type and mutant strains in minimal medium supplemented with PNP as sole source of carbon. Growth is seen only in wild type (panel A), *E. coli* $\Delta maoA$ (pSDP5) [panel B], *E. coli* $\Delta paaA$ (pSDP5) [Panel C] mutants. No growth was observed in *E. coli* $\Delta hcaE$ (pSDP5) [Panel D], *E. coli* $\Delta mhpA$ (pSDP5) [Panel E], *E. coli* $\Delta mhpR$ (pSDP5) [Panel F].

5.1.2 Quantification of PP and HPP transcripts in presence of MfhA

Growth studies conducted with the deletion mutants of *E. coli* K-12 MG1655 clearly suggested the involvement of the PP and HPP pathways in the MfhA dependent degradation of PNP. This is indeed a good evidence to support the MfhA dependent induction of PP and HPP operons. While gaining the third level of evidence, the expression pattern of *hcaR*, *hcaE*, *mhpA*, and *mhpR* was observed by performing quantitative reverse transcription (qRT) PCR. The total RNA extracted from *E. coli* cells expressing MfhA was used as template to quantify the concentration of *hcaR*, *hcaE*, *mhpA*, and *mhpR* specific transcripts. As shown in fig 5-6, the transcript levels of *hcaE*, *hcaR* and *mhpA*, *mhpR* genes were found to be up-regulated in presence of MfhA. As

indicated in microarray data, the concentration got steadily increased with increase in the time of induction of MfhA. The results clearly suggest upregulation of PP and HPP operon in presence of MfhA.

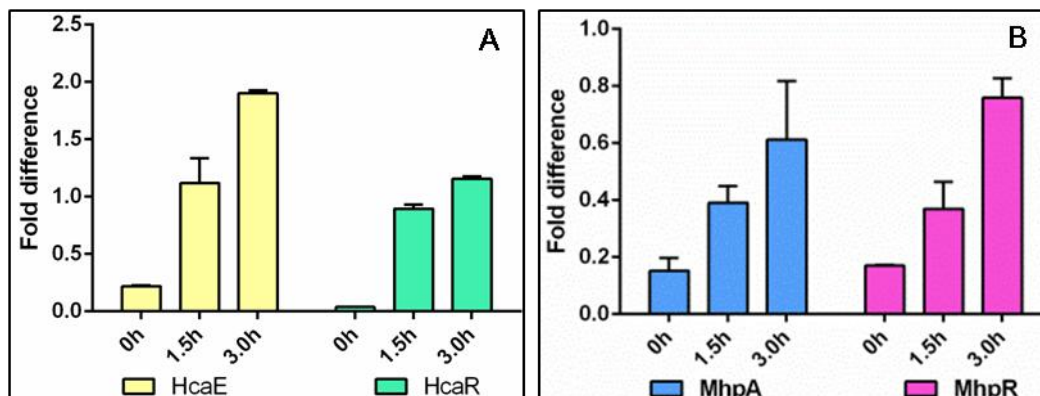


Fig 5-6| Real time q-PCR analysis of the *hcaE*, *hcaR* genes of PP pathway and *mhpA*, *mhpR* genes of HPP pathway in the presence of MfhA expression.

5.1.3 MfhA dependent promoter activity of MhpA

As mentioned before, in *E. coli* K-12 the genes responsible for mineralisation of aromatic compounds are organised in four different operons. The genes involved in degradation of Phenyl propionates (PP) are organised as *hca* cluster known as PP operon. HcaR, LysR family of transcriptional regulator, is the master regulator of the pathway (DIAZ *et al.* 1998; (PRIETO *et al.* 2004). The PP operon codes for HcaEFCD PP-dioxygenase which converts phenyl propionate into di-hydroxy phenyl propionate (DHPP). The DHPP is then channelled into 3-Hydroxyphenylpropionate (HPP) pathway. MhpR is the master regulator of the HPP pathway and it belongs to IclR family of transcriptional regulators (FERRANDEZ *et al.* 1997). Involvement of CRP-cAMP complex in the regulation of PP and HPP catabolic pathways is well studied in *E. coli* K-12 (Manso *et al.*, 2011). In HPP pathway, the regulatory gene *mhpR* and structural gene *mhpA* have opposite transcriptional orientation [Fig 5-7]. The class II and class III CRP binding regions were found upstream of both *mhpA* and *mhpR* promoter motifs. Unlike other IclR group of transcriptional regulators, the transcription of *mhpR* and *mhpA* are under the

control of CRP (DiMARCO and ORNSTON 1994; FERRANDEZ *et al.* 1997; DIAZ *et al.* 1998 GUO and HOUGHTON 1999). In the light of this information further experiments are conducted to know if MfhA mediated induction of HPP operon is CRP-cAMP dependent. Initially the *crp* negative mutants of *E.coli* K-12 MG1655 were generated and tested them by plating on McConkey plate. As expected the *crp* negative *E.coli* K-12 MG1655 Δ CRP cells have given colourless colonies on McConkey agar [Fig 5-7B]. In continuation of this observation, the *crp* specific PCR gave 0.8 Kb amplicon, instead of 0.63 Kb indicating insertion of 0.8 Kb kanamycin cassette. This clearly established generation of *E.coli* K-12 MG1655 Δ *crp* mutant.

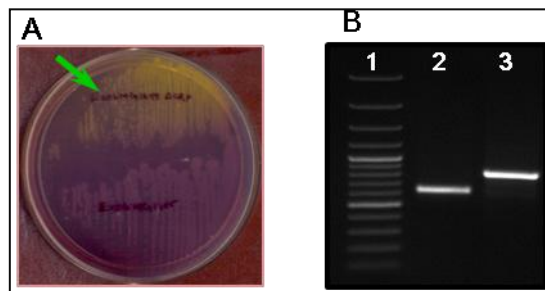


Fig 5-7| Generation of *E.coli* K-12 MG1655 Δ *crp*. Panel A represents growth of wild type and Δ *crp* mutant strains of *E.coli* K-12 MG1655 on MacConkey agar plate. Panel B represents agarose gel showing amplification of wild type (lane 2) and mutant *crp* (lane 3) gene.

After establishing generation of *crp* deletion in *E.coli* K-12 MG1655 the influence of MfhA was studied on the expression of *mhpA* and *mhpR* genes. Initially the promoter elements of *mhpA* and *mhpR* were amplified using the primer sets SDP27/SDP28 and SDP29/SDP30 and fused to a promoterless-*lacZ* gene of pMP220 (Spaink H. P 1987) to create pSDP14 and pSDP15 respectively. These constructs were then transformed into *E. coli* K-12 MG1655 wild type and *crp* negative mutants having expression plasmid pSDP5 coding MfhA. The promoter activity of the *mhpA* and *mhpR* were estimated by performing the β -galactosidase activity. As shown in Fig 5-7, CRP influence was not seen

on the activities of the *mhpA* and *mhpR* promoters, suggesting that the MfhA dependent activities of *mhpA* and *mhpR* promoters is independent of catabolite repression.

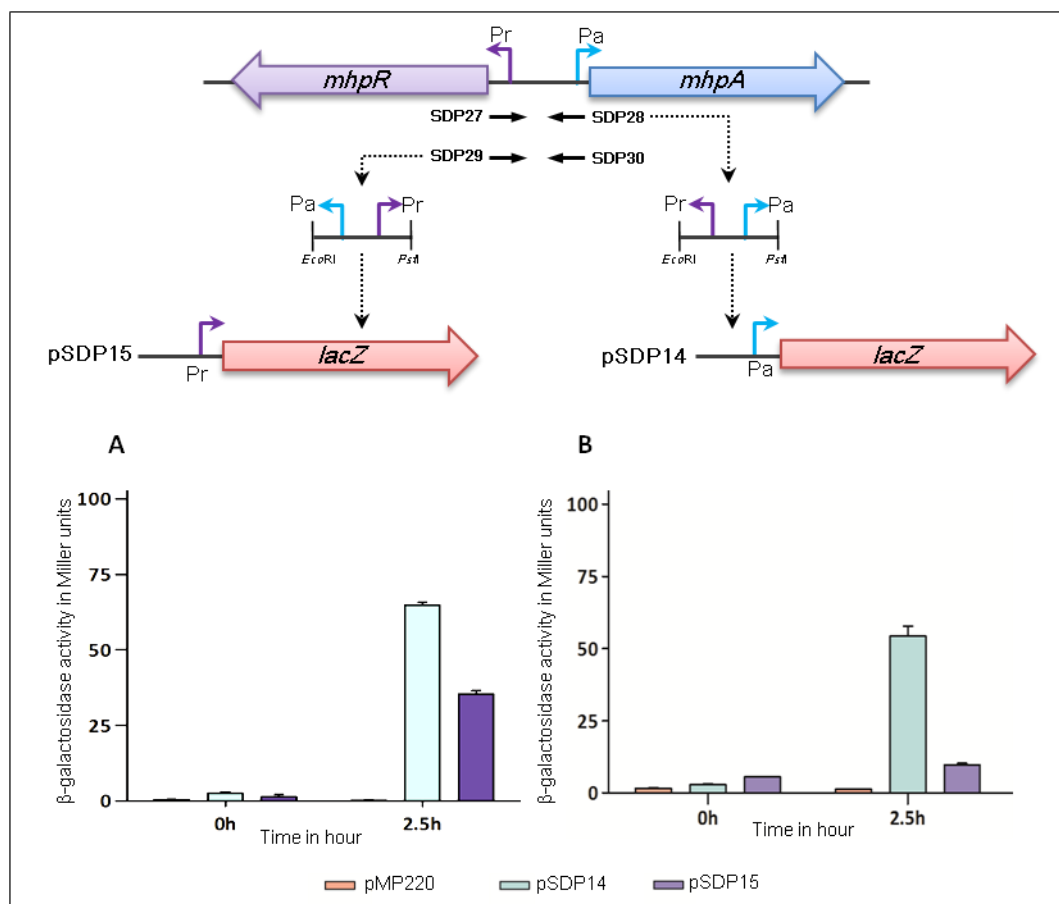


Fig 5-8| Assay of *mhpA* and *mhpR* promoters in the presence of MfhA. Panel A and B represent β -galactosidase activity obtained in wild type and Δ CRP mutants of *E. coli* K-12 MG1655 expressing MfhA.

The data presented until now clearly states the influence of MfhA on carbon metabolism. As MfhA specifically promotes utilization of aromatic compounds like PNP even in presence of glucose, the heat map generated for the transcriptome of *E. coli* K-12 MG1655 cells expressing MfhA was carefully analyzed. The heat map clearly indicates down regulation of primary pathways responsible for glucose catabolism. The glycolytic pathway genes and certain genes coding for TCA cycle enzymes are seen significantly downregulated when MfhA is expressed in *E. coli*. Especially, the genes coding for critical subunits of multimeric pyruvate dehydrogenase and α -ketoglutarate dehydrogenase got significantly downregulated [Fig 5-9].

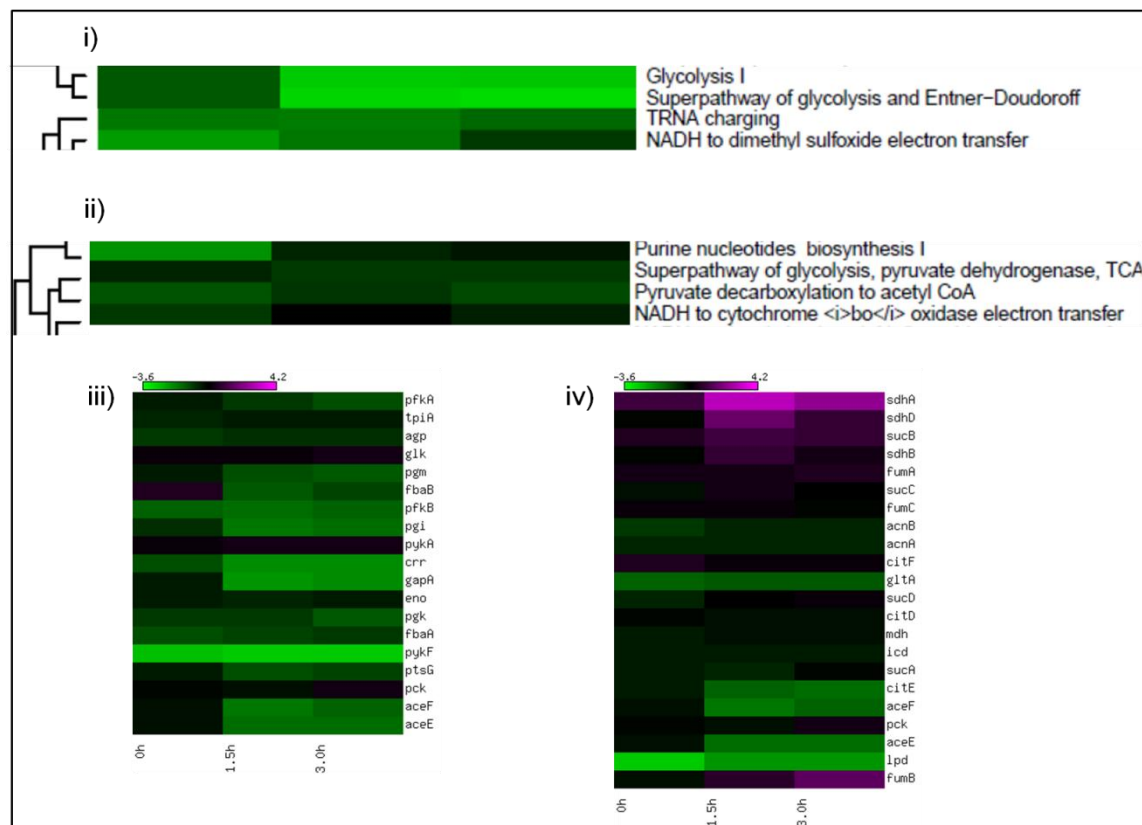


Fig 5-9| Influence of MfhA on certain key carbon metabolic pathways. Panel (i), A section of the heat map showing the down regulation of glycolytic pathway. Panel (ii), A section of the heat map showing the down regulation of glycolysis/TCA cycle superpathway, Panel (iii) and (iv) represent the heat maps generated for the gene transcripts coding for glycolytic pathway and TCA cycle enzymes.

This is rather an interesting observation. The RNA was extracted from glucose grown cells, the physiological conditions prevailed during extraction of RNA show no carbon limitation. Under such physiological conditions the reasons for downregulation of genes coding for glycolysis-TCA cycle superpathway is unrealistic. However, further analysis of the heat map showing genome wide expression gave valuable clues pertaining to carbon metabolism. Interestingly the methyl citrate cycle, glyoxalate pathway and the super pathway merging glyoxalate pathway with TCA cycle showed significant upregulation [Fig 5-10]

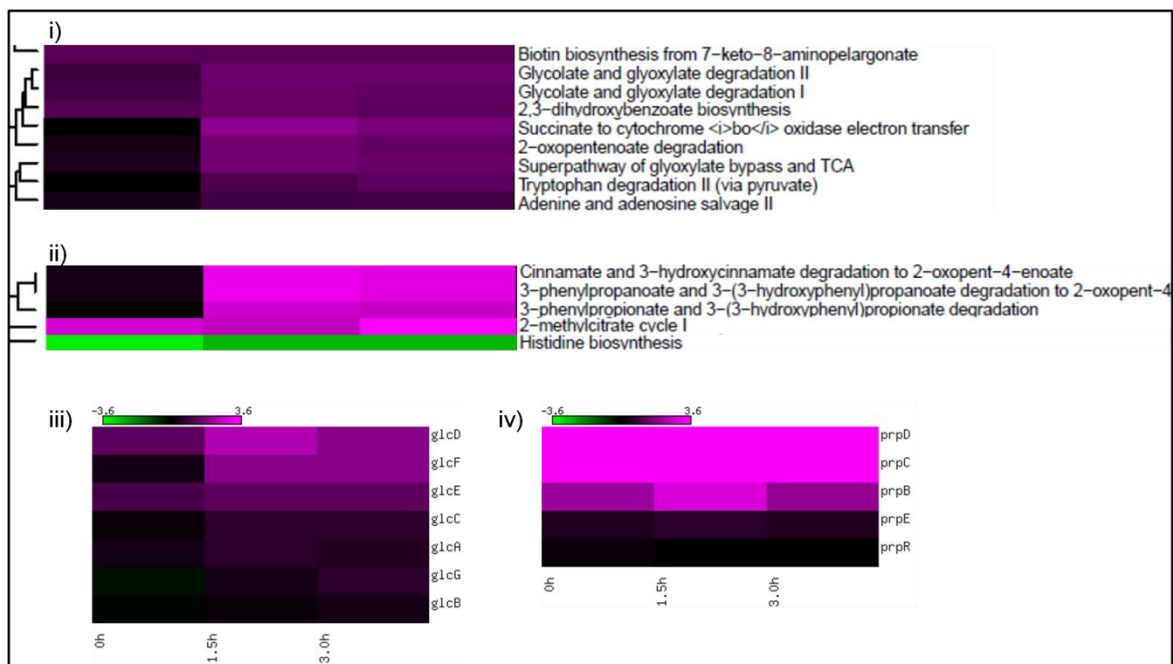


Fig 5-10| Influence of MfhA on carbon metabolic pathways. Panel (i), A section of the heat map showing the upregulation of glycolate pathway and Glycolate bypass/TCA superpathway. Panel (ii), A section of the heat map showing the upregulation of Methyl citrate cycle, Panel (iii) and (iv) represent the heat maps generated for the glyoxalate pathway and methyl citrate cycle gene transcripts.

Such differential expression speaks of existing metabolic diversion from conventional glycolytic, TCA cycle superpathway to glyoxalate, TCA cycle pathway, under the influence of MfhA. Such catabolic shift is only seen under certain unusual genetic/carbon limiting conditions. *E. coli* cells under *fadR* negative background have shown such metabolic shift (Peng et al., 2006). Similarly *lpdA* negative mutants have also shown such shift in carbon catabolic pathways. Lpd is a part of multi subunit regulatory enzymes coding for pyruvate dehydrogenase (PDH), α -ketoglutarate dehydrogenase (AKGDH). In the absence of Lpd both the TCA cycle and glycolytic pathway are downregulated (Shimizu et al., 2006). As Lpd subunit is required to make functional enzyme complex of both PDH and α -KGDH in the *lpd* null mutants of *E. coli* K-12 MG1655, glycolytic, TCA cycle superpathway is downregulated. The *lpd* is not an essential gene, the *lpd* null mutants of *E. coli* grow by operating glyoxalate, TCA cycle superpathway instead of glycolysis/TCA cycle superpathway (Shimizu et al., 2006). If microarray data is carefully

examined the MfhA expression is creating similar situation in *E. coli*. It mimics physiological state prevailed under *lpd* and *fadR* negative background. Interestingly in presence of MfhA both *fadR* and *lpd* show downregulation. In order to gain further evidence on this assumption, qRT-PCR was performed for the key genes coding for these two differentially regulated superpathways. The total RNA was extracted from *E.coli* K-12 MG1655 (pSDP5) cells after 0h, 1.5h, and 3.0h of MfhA induction was used while performing the q-PCR analysis. The quantity of key genes involved in glycolysis (*pfkA* codes for phosphofructo kinase, *eno* codes for enolase), TCA cycle (*acnA* aconitase hydratase), glyoxalate pathway (*glcC* codes dual transcriptional regulator of glyoxalate pathway, and *glcB* codes for malate synthase G), methyl citrate pathway (*prpR* codes for transcriptional activator of methyl citrate cycle and, *prpB* codes for 2-methylisocitrate lyase) and fatty acid metabolism (*fadR* codes for DNA-binding transcriptional dual regulator of fatty acid metabolism) were measured. Primers used for the qRT-PCR analysis are listed in Table A-3.

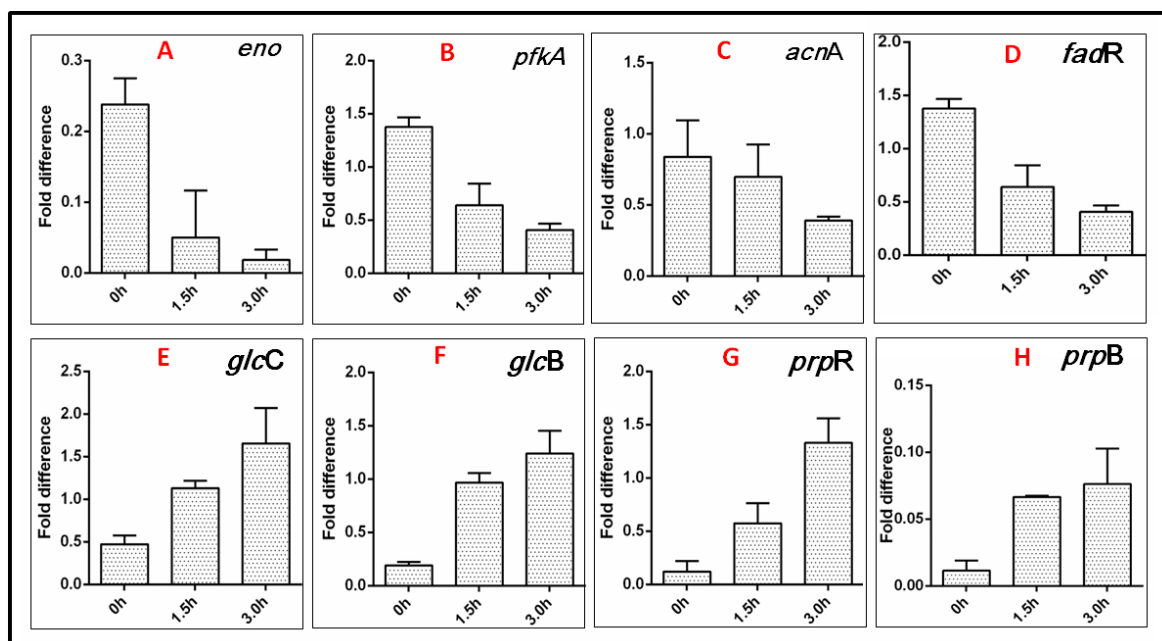


Fig 5-11| MfhA dependent repression of *eno* (panel A), *pfkA* (panel B) and *acnA* (panel C) genes coding for glycolysis-TCA cycle and *fadR* (panel D), involved in fatty acid metabolism. MfhA dependent induction of *glcC* (panel E), *glcB* (panel F) and *prpR* (panel G), *prpB* (panel H) coding for glyoxalate-TCA cycle superpathway. The transcript quantities were measured by performing qRT-PCR.

As shown in fig 5-11, the qRT-PCR analysis indicated reduced level of transcription of *eno*, *pfkA*, and *acnA* genes soon after induction of MfhA. Enolase (*eno*), phosphor fructo kinase (*pfkA*), aconitase (*acnA*) are the key enzymes that contribute both for operation and regulation of glycolysis and TCA cycle. Down regulation of these key enzymes in presence of MfhA speaks of metabolic diversion. Interestingly, the *glcC*, *glcB*, *prpR*, and *prpB* transcripts that code for glyoxalate-TCA cycle superpathway enzymes have shown steady increase. They recorded 1.5 fold upregulation in presence of MfhA. Increased expression levels of the glyoxalate pathway enzymes coding genes *glcC*, *glcB* and methyl citrate pathway enzyme coding genes *prpR* and *prpB* suggests operation of glyoxalate-TCA cycle superpathway in presence of MfhA. Down regulation of glycolysis and TCA cycle pathways in the presence of MfhA and the upregulation of glycolate/TCA cycle bypass pathway points towards existence of an unknown mechanism for diverting carbon metabolism for glycolysis-TCA cycle superpathway to glyoxalate-TCA cycle pathway. The data obtained till now indicates that MfhA, besides contributing for diversion in certain catabolisms, induces PP and HPP operons. The mutational analysis clearly indicated involvement of these two operons in *p*-Nitrophenol metabolism. The end products of the PP and HPP pathway [Fig 5-2] are Succinate and acetyl CoA [Fig 5-12].

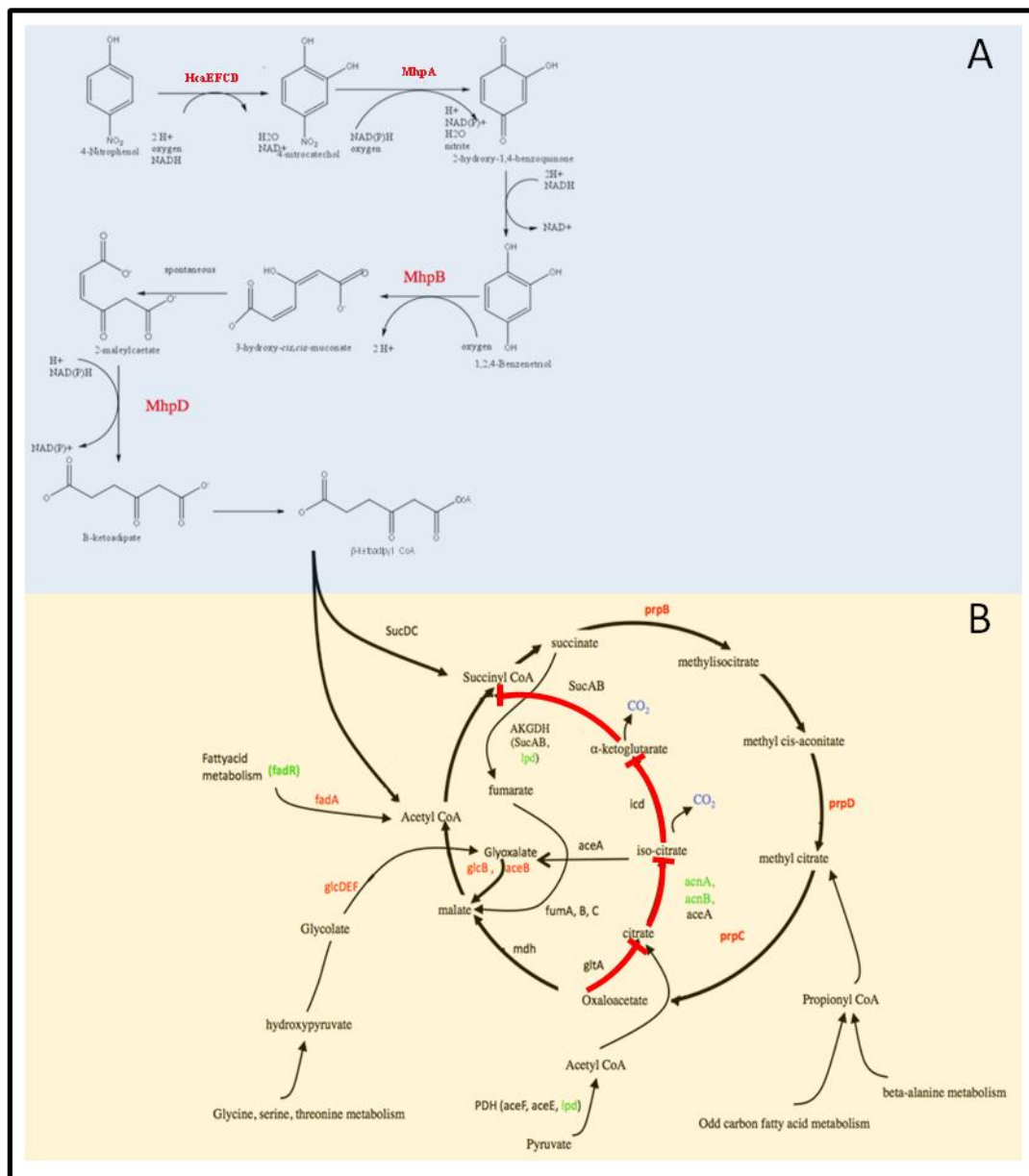


Fig 5-12| MfhA mediated changes on the carbon metabolism of *E. coli* K-12 MG1655 is shown in panel B. Red colour indicates the genes upregulated and down regulated genes were shown in green colour. Channelling of *p*-Nitrophenol degradation products into Glyoxalate-methyl citrate superpathway is shown in panel A.

The succinyl CoA thus generated was generated appears to join methyl citrate pathway which in turn is contributing for operation of glyoxalate-TCA cycle pathway. It is not clear why there is MfhA dependent shift from glycolysis-TCA cycle superpathway to glyoxalate-TCA cycle superpathway. One possible reason could be carbon conservation. In TCA cycle, isocitrate dehydrogenase (ICD), α -ketoglutarate dehydrogenase (AKGDH) contribute for elimination of carbon in the form of CO₂. If the glyoxalate-TCA cycle

superpathway is in operon there is no such elimination [Fig 5-12]. The *p*-Nitrophenol generated metabolic intermediates directly form carbon skeleton of the cell. Though the hypothesis is close to reality, experimental evidence needs to be gained to get acceptance.

5.2 Is non-coding RNA responsible for metabolic diversion ?

The transcriptome analysis revealed differential expression of non-coding RNAs (ncRNA) in presence of MfhA. While gaining insights on the data, bioinformatic tools were used to predict putative promoter and Rho-independent terminators using BPROM (<http://molbiol-tools.ca/Promoters.htm>) and ARNOLD (<http://rna.igmors.u-psud.fr/toolbox/arnold/>) software tools respectively. Such analysis is expected to provide validation to claim them as sRNA coding genes. Among those putative sRNAs coding genes, one of the *srna46* got significantly upregulated in presence of MfhA. Its product, sRNA46 was identified to have potential target interaction with free energy of -8.8 KJ/mole with the mRNA of *LpdA*, exactly at translational start site (TSS) [Fig 5-13].

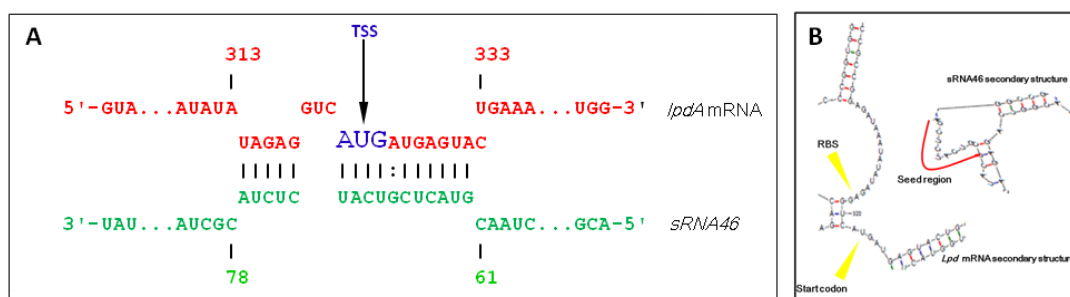


Fig 5-13| Predicted interactions between *lpdA* mRNA and sRNA46. Panel A Indicates *lpd* and sRNA46 duplex near translation start site (TSS). Panel B indicates the interaction regions shown in a two dimensional view.

Upregulation of a sRNA that strongly interacts with *lpd* mRNA in MfhA dependent manner gives a preliminary lead to show that MfhA dependent shift in carbon metabolism pathway is sRNA46 dependent. In order to understand the influence of MfhA on the expression of the novel sRNA, *srna-lacZ* fusions were constructed using pMP220, promoter probe vector. Using SDP63 (5' AGC TAC GAA TTC TCG CGT GGT CAG CAT TGA 3') and SDP64 (5' AGC TAC CTG CAG GGC TAC GGG CTT TAT CA 3')

as primers, the promoter region of *sRNA46* was amplified from *E. coli* K-12 MG1655 and cloned into pMP220 to generate pSDP16. The *srna46-lacZ* fusion was then transformed into *E. coli* K-12 MG1655 (pSDP5) and *E. coli* K-12 MG1655 (pMMB206) cells. The promoter activity of *srna46-lacZ* fusion was estimated by performing β -galactosidase activity. The promoter of the *sRNA46* gene was found to be active only in presence of MfhA.

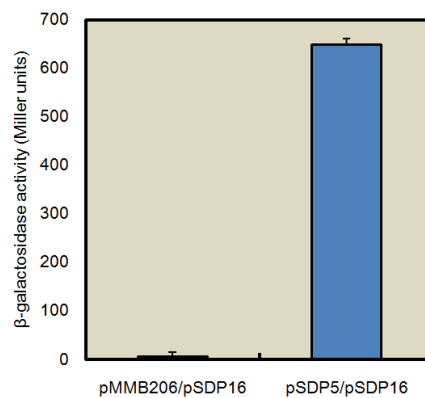


Fig 5-14| Influence of MfhA on the promoter activity of *srna46* gene.

No such activity was seen in its absence [Fig 5-14). This clearly states relationship between MfhA and *srna46*. How the upregulation is mediated is unknown. Further studies need to be conducted to gain conclusive evidence on MfhA influence on expression of small RNA, *srna46*.

Summary

Neurotoxic OPs have been used as insecticides to control various insect pests that damage economically important crops. Due to their increased usage, in many cases these chemicals are found as major contaminants of the environment posing challenge to the micro-flora living in soils. A number of soil bacteria have acquired ability to use these OPs as sole source of carbon and energy. These taxonomically diverse bacterial species isolated from different geographical regions, have been shown to contain phosphotriesterases (PTEs) capable of hydrolyzing triester linkage found in structurally diverse group of OP compounds. The bacterial PTEs have been classified into three major groups-The organophosphate hydrolases (OPH), methyl parathion hydrolases (MPH) and organophosphate acid anhydases (OPAA). Out of these three PTEs the physiological substrate is known only for OPAA. The OPH and MPH appears to have evolved from quorum quenching lactonases and β -lactamases. The *mpd* gene coding MPH have been shown to move horizontally among soil bacteria. Despite of having identical OPH coding *opd* genes on large indigenous plasmids, horizontal gene transfer of *opd* genes has not been demonstrated. The experiments conducted in this study have shown existence of multiple mechanisms in horizontal gene transfer of *opd* genes. In *Sphingobium fuliginis*, the *opd* cluster is organized as integrative mobilizable element (IME). It has also shown features of a catabolic transposon. The entire work related to HGT of *opd* is presented in first chapter.

The second and third chapters are devoted to assess the functional status of a novel esterase MfhA. The MfhA is coded by *mfhA* gene found as part of plasmid pPDL2-borne *opd* island. The MfhA is shown to induce the innate genetic capability for using PNP as source of carbon in *E.coli*. The molecular analysis described in the second and third chapters have clearly shown MfhA dependent induction of Phenyl propionate (PP) and

Hydroxy Phenyl Propionate (HPP) pathways. The mutational analysis, qRT-PCR studies and promoter assays have clearly shown existence of MfhA dependent induction of *hca* and *mhp* operons and their involvement in degradation of PNP in *E.coli*.

The genome-wide expression profiling revealed MfhA dependent metabolic diversion. The glycolytic pathway and TCA cycle specific enzymes got repressed in presence of MfhA. Instead, the glyoxalate-Methyl isocitrate super-pathway enzymes have shown upregulation. It clearly indicates MfhA dependent metabolic diversion from traditional glycolysis-TCA cycle to glyoxalate-methyl isocitrate shunt super pathway. The PNP catabolic intermediates generated through PP and HPP pathways appear to have channeled into the glyoxalate- methyl isocitrate TCA shunt pathway. The qRT-PCR experiments and promoter functional assays have confirmed such metabolic diversion in MfhA expressed *E. coli* cells. The non coding RNAs (ncRNAs) have also shown MfhA dependent differential expression. One of them designated as *srna46* is shown to have good seed region with mRNA coding for Lpd subunit. As the Lpd subunit is part of PDH and AKGDH. Inhibition of its synthesis is expected to generate a shift in carbon catabolic pathway. Though direct evidence is yet to be shown, the induction of *srna46* promoter in the presence of MfhA points towards existence of sRNA46 role in the observed diversion of carbon catabolic pathway.

Appendix

Table A-1| PCR primers used for construction of expression plasmids or transcriptional fusions.

S.No	Gene	Primer sequence(5'→3')
1	SDP01	GGACGCTATGGAGGGCAGCCGCTG
2	SDP02	GCCAAGAGCGATGAAGGCGTGCGCAACGG
3	SDP03	GAGCTGGATCCATGGAACACCCG
4	SDP04	GCCCTGCAGCTGTGACTAACCCGGGCGCGG
5	SDP05	GGACTGAATTCCGCCCTGCGCGAGG
6	SDP06	ATCTGGAATTCCCTCCGGTCTCAATC
7	SDP07	GGCTTTCTGCAGTCCAGCGATAGTC
8	SDP08	AACAAGATCTAGGGAGACCACAACGGTTTCCC
9	SDP09	CCTTAGATCTCTAGTTATTGCTCAGCGGTGGC
10	SDP10	AACAATAGATCTCAGGAAACAGTATTCATGTCC
11	SDP11	CGAGGCAGATCTTCAGACAGTCACGATGCGGCC
12	SDP12	GGCTGCCATCATCCCATGGGAACACCCGCTA
13	SDP25	GGGTGCGCGAGCGTGCATATGTCGATCGGCACAGGC
14	SDP26	GGATCCAGATGCTCGAGTGACGCCCGCAAGG
15	SDP27	CCGGAGAATTCATTAATTGACATTTCTAT
16	SDP28	CCGAGCTGCAGTTCAGTACCTCACGACTCGG
17	SDP29	CCGGAGAATTCCTCAGTACCTCACGAC
18	SDP30	CCGAGCTGCAGATTAATTGACATTTCTATA

Table A-2| PCR primers used to screen deletion mutants of *E. coli* K-12 MG 1655

S.No	Gene	Size of the gene (KB)	Primer name	Primer sequence(5'→3')
1	<i>hcaE</i>	1.362	SDP13	AT CTTTCAGGAT TAAAAAAT (F)
			SDP14	CTCTAGTGAAACTTGCGCAC (R)
2	<i>mhpA</i>	1.665	SDP15	GAACCGAGTC GTGAGGTACT (F)
			SDP16	AGTGAAGATAAGCGTGCATA (R)
3	<i>mhpR</i>	0.897	SDP17	ATTTTGTTGTTAAAAACATGTAA (F)
			SDP18	CCACCAGAAT AGCCTGCGAT (R)
4	<i>paaA</i>	0.863	SDP19	GCTATCGAGC CACAGGACTG (F)
			SDP20	ATTACTCATTTTGAATCTCC (R)
5	<i>maoA</i>	2.274	SDP21	AACATC TGACGAGGTT AATA (F)
			SDP22	CGTTTTTTTGTCTGAAACAA (R)
6	<i>crp</i>	0.633	SDP23	AT AACAGAGGAT AACCGCGC (F)
			SDP24	AACGCGCCACTCCGACGGGA (R)

Table A-3| PCR primers used for quantitative real time PCR

S.No	Gene	Primer name	Primer sequence(5'→3')
1	<i>16sRNA</i>	SDP31	AGTCGAACGGTAACAGGAAGA(F)
		SDP32	GCAATATTCCTCCACTGCTG(R)
2	<i>aceB</i>	SDP33	TGAAATCCTTCACGCGCTGC(F)
		SDP34	TTGCTCGGAATAAACGCCGC(R)
3	<i>aceK</i>	SDP35	GAAAGAGCACGATCGCGTGG(F)
		SDP36	GCAAGCTGGCGAATAGCGTT(R)
4	<i>acnA</i>	SDP37	TAAGGACACGTTGCAGGCCA(F)
		SDP38	GGCGGTAGGCAATTCACGG(R)
5	<i>eno</i>	SDP39	TGGTTCCCGTGAAGCTCTGG(F)
		SDP40	TGCAGCAGCTTTGGCGTTAG(R)
6	<i>pfkA</i>	SDP41	CAATTCGCGGGGTTGTTCGT(F)
		SDP42	GGTTTTCGATAGCCACGGCG(R)
7	<i>fadA</i>	SDP43	GCAGAAATGCTGGCGCGTAT(F)
		SDP44	ATGTGCCCGCCGTTACCATA(R)
8	<i>fadR</i>	SDP45	ACCGCTAATGAAGTGGCCGA(F)
		SDP46	CTGCACAACGCCGACAGTTT(R)
9	<i>glcB</i>	SDP47	TGCTCGGTATGGCACCGAAT(F)
		SDP48	GGCTTTGATCCAAGGCGTCG(R)
10	<i>glcC</i>	SDP49	TACTGAAGGTTCGGTCAGCCG(F)
		SDP50	CCTCCAGTAATGCGCGAACG(R)
11	<i>hcaE</i>	SDP51	CGAAGGCGGCACCGAAATTG(F)
		SDP52	CGGGCGGTTTGTCCATCACC(R)
12	<i>hcaR</i>	SDP53	CAGACAGCCAGACACCTTGA(F)
		SDP54	CGGATCGGTACTGACGAAA(R)
13	<i>mhpA</i>	SDP55	CCCGGTTGGGCTGATGATGG(F)
		SDP56	CGGCGTAGTGTGCGGCAGAA(R)
14	<i>mhpR</i>	SDP57	GCGGTACGGCGATAGAGGCG(F)
		SDP58	ACCTGGCTGGCCTTTTGCCC(R)
15	<i>prpB</i>	SDP59	CCACCGACGAATTACGCAGC(F)
		SDP60	TTCACCTGGCTACGGGCAAA(R)
16	<i>prpR</i>	SDP61	TATTTTGCCCGCCACGATGC(F)
		SDP62	GCGGCATTTCCGCAATCTCA(R)

Bibliography

- AFRIAT, L., C. ROODVELDT, G. MANCO and D. S. TAWFIK, 2006 The latent promiscuity of newly identified microbial lactonases is linked to a recently diverged phosphotriesterase. *Biochemistry* **45**: 13677-13686.
- ARBER, W., 1994 The Generation of Variation in bacterial genomes. *Journal of Molecular Evolution* **40**: 6.
- ARBER, W., 2000 Genetic variation: molecular mechanisms and impact on microbial evolution. *FEMS Microbiol Rev* **24**: 1-7.
- AZAD, R. K., and J. G. LAWRENCE, 2012 Detecting laterally transferred genes. *Methods Mol Biol* **855**: 281-308.
- BARNES H AND FOLKFARD A.R., 1951 The determination of nitrites. *Analyst*: 4.
- BARNIDGE, D. R., E. A. DRATZ, A. J. JESAITIS and J. SUNNER, 1999 Extraction method for analysis of detergent-solubilized bacteriorhodopsin and hydrophobic peptides by electrospray ionization mass spectrometry. *Anal Biochem* **269**: 1-9.
- BEIL, S., K. N. TIMMIS and D. H. PIEPER, 1999 Genetic and biochemical analyses of the *tec* operon suggest a route for evolution of chlorobenzene degradation genes. *J Bacteriol* **181**: 341-346.
- BENNING, M. M., S. B. HONG, F. M. RAUSHEL and H. M. HOLDEN, 2000 The binding of substrate analogs to phosphotriesterase. *J Biol Chem* **275**: 30556-30560.
- BIGLEY, A. N., and F. M. RAUSHEL, 2012 Catalytic mechanisms for phosphotriesterases. *Biochim Biophys Acta*.
- BLATTNER, F. R., G. PLUNKETT, 3RD, C. A. BLOCH, N. T. PERNA, V. BURLAND *et al.*, 1997 The complete genome sequence of *Escherichia coli* K-12. *Science* **277**: 1453-1462.
- BOYD, E. F., S. ALMAGRO-MORENO and M. A. PARENT, 2009 Genomic islands are dynamic, ancient integrative elements in bacterial evolution. *Trends Microbiol* **17**: 47-53.
- Bradford, M., 1976 A rapid and sensitive method for the quantitation of micrograms quantities of protein utilising the principles of protein dye binding. *Analytical Biochemistry* **72**: 248-254.
- BURGESS, R. R., 1996 Purification of overproduced *Escherichia coli* RNA polymerase sigma factors by solubilizing inclusion bodies and refolding from Sarkosyl. *Methods Enzymol* **273**: 145-149.
- CASES, I., and V. DE LORENZO, 2001 The black cat/white cat principle of signal integration in bacterial promoters. *EMBO J* **20**: 1-11.
- CHEN Y, Z. X., LIU H, WANG Y, XIA X, 2002 Study on *Pseudomonas* sp. WBC-3 capable of complete degradation of methylparathion. *Wei Sheng Wu Xue Bao* **42**: 490-497

- CHENG, T. C., S. P. HARVEY and A. N. STROUP, 1993 Purification and Properties of a Highly Active Organophosphorus Acid Anhydrolase from *Alteromonas undina*. *Appl Environ Microbiol* **59**: 3138-3140.
- CHENG, T. C., S. P. HARVEY and G. L. CHEN, 1996 Cloning and expression of a gene encoding a bacterial enzyme for decontamination of organophosphorus nerve agents and nucleotide sequence of the enzyme. *Appl Environ Microbiol* **62**: 1636-1641.
- CHENG, T., L. LIU, B. WANG, J. WU, J. J. DEFRAK *et al.*, 1997 Nucleotide sequence of a gene encoding an organophosphorus nerve agent degrading enzyme from *Alteromonas haloplanktis*. *J Ind Microbiol Biotechnol* **18**: 49-55.
- CHU, X., X. ZHANG, Y. CHEN, H. LIU and D. SONG, 2003 [Study on the properties of methyl parathion hydrolase from *Pseudomonas* sp. WBC-3]. *Wei Sheng Wu Xue Bao* **43**: 453-459.
- COPLEY, S. D., 2000 Evolution of a metabolic pathway for degradation of a toxic xenobiotic: the patchwork approach. *Trends Biochem Sci* **25**: 261-265.
- CURRIER, T. C., and E. W. NESTER, 1976 Isolation of covalently closed circular DNA of high molecular weight from bacteria. *Anal Biochem* **76**: 431-441.
- DATSENKO, K. A., and B. L. WANNER, 2000 One-step inactivation of chromosomal genes in *Escherichia coli* K-12 using PCR products. *Proc Natl Acad Sci U S A* **97**: 6640-6645.
- DAVIES, J. H. M., T. A.; SALGADO, V. L.; LITCHFIELD, M. H.; HILL, I. R.; HERVÉ, J. J. (Editor), 1985 *The pyrethroid insecticides*. Taylor & Francis, London, UK.
- DE LA CRUZ, F., and J. DAVIES, 2000 Horizontal gene transfer and the origin of species: lessons from bacteria. *Trends Microbiol* **8**: 128-133.
- DEB, C., J. DANIEL, T. D. SIRAKOVA, B. ABOMOELAK, V. S. DUBEY *et al.*, 2006 A novel lipase belonging to the hormone-sensitive lipase family induced under starvation to utilize stored triacylglycerol in *Mycobacterium tuberculosis*. *J Biol Chem* **281**: 3866-3875.
- DEFRAK, J. J., and T. C. CHENG, 1991 Purification and properties of an organophosphorus acid anhydrase from a halophilic bacterial isolate. *J Bacteriol* **173**: 1938-1943.
- DEFRAK, J. J., W. T. BEAUDRY, T. C. CHENG, S. P. HARVEY, A. N. STROUP *et al.*, 1993 Screening of halophilic bacteria and *Alteromonas* species for organophosphorus hydrolyzing enzyme activity. *Chem Biol Interact* **87**: 141-148.
- DEL SOLAR, G., and M. ESPINOSA, 1992 The copy number of plasmid pLS1 is regulated by two trans-acting plasmid products: the antisense RNA II and the repressor protein, RepA. *Mol Microbiol* **6**: 83-94.
- DEL SOLAR, G., P. ACEBO and M. ESPINOSA, 1997 Replication control of plasmid pLS1: the

- antisense RNA II and the compact rnaII region are involved in translational regulation of the initiator RepB synthesis. *Mol Microbiol* **23**: 95-108.
- DIAZ, E., A. FERRANDEZ and J. L. GARCIA, 1998 Characterization of the hca cluster encoding the dioxygenolytic pathway for initial catabolism of 3-phenylpropionic acid in *Escherichia coli* K-12. *J Bacteriol* **180**: 2915-2923.
- DIAZ, E., A. FERRANDEZ, M. A. PRIETO and J. L. GARCIA, 2001 Biodegradation of aromatic compounds by *Escherichia coli*. *Microbiol Mol Biol Rev* **65**: 523-569, table of contents.
- DIAZ, E., S. ORDONEZ, A. VEGA and J. COCA, 2004 Characterization of Co, Fe and Mn-exchanged zeolites by inverse gas chromatography. *J Chromatogr A* **1049**: 161-169.
- DIMARCO, A. A., and L. N. ORNSTON, 1994 Regulation of p-hydroxybenzoate hydroxylase synthesis by PobR bound to an operator in *Acinetobacter calcoaceticus*. *J Bacteriol* **176**: 4277-4284.
- DING, Z., K. ATMAKURI and P. J. CHRISTIE, 2003 The outs and ins of bacterial type IV secretion substrates. *Trends Microbiol* **11**: 527-535.
- DOBRINDT, U., B. HOCHHUT, U. HENTSCHEL and J. HACKER, 2004 Genomic islands in pathogenic and environmental microorganisms. *Nat Rev Microbiol* **2**: 414-424.
- DONG, Y. J., M. BARTLAM, L. SUN, Y. F. ZHOU, Z. P. ZHANG *et al.*, 2005 Crystal structure of methyl parathion hydrolase from *Pseudomonas* sp. WBC-3. *J Mol Biol* **353**: 655-663.
- DRAGUN, L., KUFFNER, A. C., AND SCHNEITTER, R. W. , 1984 Ground water contamination. 1. Transport and transformation of organic chemicals. *Chemical engineering* **91**: 65-70.
- DUMAS, D. P., S. R. CALDWELL, J. R. WILD and F. M. RAUSHEL, 1989 Purification and properties of the phosphotriesterase from *Pseudomonas diminuta*. *J Biol Chem* **264**: 19659-19665.
- EFREMENKO, E. N. A. S., V. S. , 2001 Organophosphate hydrolase- an enzyme catalyzing degradation of phosphorus containing toxins and pesticides., pp. 1826-1832. *Russ. Chem. B+*
- ELIAS, M., and D. S. TAWFIK, 2012 Divergence and convergence in enzyme evolution: parallel evolution of paraoxonases from quorum-quenching lactonases. *J Biol Chem* **287**: 11-20.
- ELIAS, M., J. DUPUY, L. MERONE, L. MANDRICH, E. PORZIO *et al.*, 2008 Structural basis for natural lactonase and promiscuous phosphotriesterase activities. *J Mol Biol* **379**: 1017-1028.

- FERRANDEZ, A., J. L. GARCIA and E. DIAZ, 1997 Genetic characterization and expression in heterologous hosts of the 3-(3-hydroxyphenyl)propionate catabolic pathway of *Escherichia coli* K-12. *J Bacteriol* **179**: 2573-2581.
- FIGURSKI, D. H., and D. R. HELINSKI, 1979 Replication of an origin-containing derivative of plasmid RK2 dependent on a plasmid function provided in trans. *Proc Natl Acad Sci U S A* **76**: 1648-1652.
- FONG, K. P., C. B. GOH and H. M. TAN, 2000 The genes for benzene catabolism in *Pseudomonas putida* ML2 are flanked by two copies of the insertion element IS1489, forming a class-I-type catabolic transposon, Tn5542. *Plasmid* **43**: 103-110.
- FRANKLIN, F. C., M. BAGDASARIAN, M. M. BAGDASARIAN and K. N. TIMMIS, 1981 Molecular and functional analysis of the TOL plasmid pWWO from *Pseudomonas putida* and cloning of genes for the entire regulated aromatic ring meta cleavage pathway. *Proc Natl Acad Sci U S A* **78**: 7458-7462.
- FU, G., Z. CUI, T. HUANG and S. LI, 2004 Expression, purification, and characterization of a novel methyl parathion hydrolase. *Protein Expr Purif* **36**: 170-176.
- GHANEM, E., and F. M. RAUSHEL, 2005 Detoxification of organophosphate nerve agents by bacterial phosphotriesterase. *Toxicol Appl Pharmacol* **207**: 459-470.
- GHANEM, E., Y. LI, C. XU and F. M. RAUSHEL, 2007 Characterization of a phosphodiesterase capable of hydrolyzing EA 2192, the most toxic degradation product of the nerve agent VX. *Biochemistry* **46**: 9032-9040.
- GOMIS-RUTH, F. X., M. SOLA, P. ACEBO, A. PARRAGA, A. GUASCH *et al.*, 1998 The structure of plasmid-encoded transcriptional repressor CopG unliganded and bound to its operator. *EMBO J* **17**: 7404-7415.
- GORKE, B., and J. STULKE, 2008 Carbon catabolite repression in bacteria: many ways to make the most out of nutrients. *Nat Rev Microbiol* **6**: 613-624.
- GORLA, P., J. P. PANDEY, S. PARTHASARATHY, M. MERRICK and D. SIDDAVATTAM, 2009 Organophosphate hydrolase in *Brevundimonas diminuta* is targeted to the periplasmic face of the inner membrane by the twin arginine translocation pathway. *J Bacteriol* **191**: 6292-6299.
- GRINSTED, J., F. DE LA CRUZ and R. SCHMITT, 1990 The Tn21 subgroup of bacterial transposable elements. *Plasmid* **24**: 163-189.
- GUO, Z., and J. E. HOUGHTON, 1999 PcaR-mediated activation and repression of *pca* genes from *Pseudomonas putida* are propagated by its binding to both the -35 and the -10 promoter elements. *Mol Microbiol* **32**: 253-263.
- HACKER, J., and E. CARNIEL, 2001 Ecological fitness, genomic islands and bacterial

- pathogenicity. A Darwinian view of the evolution of microbes. *EMBO Rep* **2**: 376-381.
- HALDIMANN, A., L. L. DANIELS and B. L. WANNER, 1998 Use of new methods for construction of tightly regulated arabinose and rhamnose promoter fusions in studies of the *Escherichia coli* phosphate regulon. *J Bacteriol* **180**: 1277-1286.
- HANAHAN, D., 1983 Studies on transformation of *Escherichia coli* with plasmids. *J Mol Biol* **166**: 557-580.
- HAO, W., and G. B. GOLDING, 2006 The fate of laterally transferred genes: life in the fast lane to adaptation or death. *Genome Res* **16**: 636-643.
- HARPER, L. L., C. S. MCDANIEL, C. E. MILLER and J. R. WILD, 1988 Dissimilar plasmids isolated from *Pseudomonas diminuta* MG and a *Flavobacterium* sp. (ATCC 27551) contain identical *opd* genes. *Appl Environ Microbiol* **54**: 2586-2589.
- HARWOOD, C. S., and R. E. PARALES, 1996 The beta-ketoadipate pathway and the biology of self-identity. *Annu Rev Microbiol* **50**: 553-590.
- HAUGLAND, R. A., U. M. SANGODKAR and A. M. CHAKRABARTY, 1990 Repeated sequences including RS1100 from *Pseudomonas cepacia* AC1100 function as IS elements. *Mol Gen Genet* **220**: 222-228.
- HAYASHI, K., N. MOROOKA, Y. YAMAMOTO, K. FUJITA, K. ISONO *et al.*, 2006 Highly accurate genome sequences of *Escherichia coli* K-12 strains MG1655 and W3110. *Mol Syst Biol* **2**: 2006 0007.
- HORNE, I., T. D. SUTHERLAND, R. L. HARCOURT, R. J. RUSSELL and J. G. OAKESHOTT, 2002 Identification of an *opd* (organophosphate degradation) gene in an *Agrobacterium* isolate. *Appl Environ Microbiol* **68**: 3371-3376.
- HORNE, I., X. QIU, R. J. RUSSELL and J. G. OAKESHOTT, 2003 The phosphotriesterase gene *opdA* in *Agrobacterium radiobacter* P230 is transposable. *FEMS Microbiol Lett* **222**: 1-8.
- HUBNER, A., C. E. DANGANAN, L. XUN, A. M. CHAKRABARTY and W. HENDRICKSON, 1998 Genes for 2,4,5-trichlorophenoxyacetic acid metabolism in *Burkholderia cepacia* AC1100: characterization of the *tftC* and *tftD* genes and locations of the *tft* operons on multiple replicons. *Appl Environ Microbiol* **64**: 2086-2093.
- HUGGINS, C., AND J. LAPIDES, 1947 Chromogenic substrates. IV. Acyl esterases of p- Nitro phenol as substrates for the colorimetric determination of esterase. *Journal of Biological chemistry*: 16.
- JU, K. S., and R. E. PARALES, 2010 Nitroaromatic compounds, from synthesis to biodegradation. *Microbiol Mol Biol Rev* **74**: 250-272.

- JUHAS, M., J. R. VAN DER MEER, M. GAILLARD, R. M. HARDING, D. W. HOOD *et al.*, 2009 Genomic islands: tools of bacterial horizontal gene transfer and evolution. *FEMS Microbiol Rev* **33**: 376-393.
- KADIYALA, V., and J. C. SPAIN, 1998 A two-component monooxygenase catalyzes both the hydroxylation of p-nitrophenol and the oxidative release of nitrite from 4-nitrocatechol in *Bacillus sphaericus* JS905. *Appl Environ Microbiol* **64**: 2479-2484.
- KARLIN, S., A. M. CAMPBELL and J. MRAZEK, 1998 Comparative DNA analysis across diverse genomes. *Annu Rev Genet* **32**: 185-225.
- KAWAHARA, K., A. TANAKA, J. YOON and A. YOKOTA, 2010 Reclassification of a parathione-degrading *Flavobacterium* sp. ATCC 27551 as *Sphingobium fuliginis*. *J Gen Appl Microbiol* **56**: 249-255.
- KHAJAMOHIDDIN, S., P. S. BABU, D. CHAKKA, M. MERRICK, A. BHADURI *et al.*, 2006 A novel meta-cleavage product hydrolase from *Flavobacterium* sp. ATCC27551. *Biochem Biophys Res Commun* **351**: 675-681.
- KHOLODII, G. Y., O. V. YURIEVA, Z. GORLENKO, S. Z. MINDLIN, I. A. BASS *et al.*, 1997 Tn5041: a chimeric mercury resistance transposon closely related to the toluene degradative transposon Tn4651. *Microbiology* **143** (Pt 8): 2549-2556.
- KRISCH, K., 1966 Reaction of a microsomal esterase from hog-liver with diethyl p-nitrophenyl phosphate. *Biochim Biophys Acta* **122**: 265-280.
- LAWRENCE, J. G., and H. OCHMAN, 1997 Amelioration of bacterial genomes: rates of change and exchange. *J Mol Evol* **44**: 383-397.
- LIU, H., J. J. ZHANG, S. J. WANG, X. E. ZHANG and N. Y. ZHOU, 2005 Plasmid-borne catabolism of methyl parathion and p-nitrophenol in *Pseudomonas* sp. strain WBC-3. *Biochem Biophys Res Commun* **334**: 1107-1114.
- MASATAKA TSUDA, H. M. T., AKITO NISHI, KENSUKE FURUKAWA, 1999 Mobile catabolic gene in bacteria. *Journal of Bioscience and bioengineering* **87**: 10.
- MERLIN, C., D. SPRINGAEL and A. TOUSSAINT, 1999 Tn4371: A modular structure encoding a phage-like integrase, a *Pseudomonas*-like catabolic pathway, and RP4/Ti-like transfer functions. *Plasmid* **41**: 40-54.
- MILLER, J. H., 1972 *Experiments in molecular genetics*.
- MONAD, J., 1942 *Recherches sur la Croissance des Cultures Bacteriennes*, pp., Paris.
- MORALES, V. M., A. BACKMAN and M. BAGDASARIAN, 1991 A series of wide-host-range low-copy-number vectors that allow direct screening for recombinants. *Gene* **97**: 39-47.

- MULBRY, W. W., J. S. KARNS, P. C. KEARNEY, J. O. NELSON, C. S. MCDANIEL *et al.*, 1986 Identification of a plasmid-borne parathion hydrolase gene from *Flavobacterium* sp. by southern hybridization with *opd* from *Pseudomonas diminuta*. *Appl Environ Microbiol* **51**: 926-930.
- MULBRY, W. W., P. C. KEARNEY, J. O. NELSON and J. S. KARNS, 1987 Physical comparison of parathion hydrolase plasmids from *Pseudomonas diminuta* and *Flavobacterium* sp. *Plasmid* **18**: 173-177.
- MUTO, A., and S. OSAWA, 1987 The guanine and cytosine content of genomic DNA and bacterial evolution. *Proc Natl Acad Sci U S A* **84**: 166-169.
- NUNES-DUBY, S. E., H. J. KWON, R. S. TIRUMALAI, T. ELLENBERGER and A. LANDY, 1998 Similarities and differences among 105 members of the *Int* family of site-specific recombinases. *Nucleic Acids Res* **26**: 391-406.
- OCHMAN, H., J. G. LAWRENCE and E. A. GROISMAN, 2000 Lateral gene transfer and the nature of bacterial innovation. *Nature* **405**: 299-304.
- ORNSTON, L. N., 1966 The conversion of catechol and protocatechuate to beta-ketoadipate by *Pseudomonas putida*. II. Enzymes of the protocatechuate pathway. *J Biol Chem* **241**: 3787-3794.
- PAKALA, S. B., P. GORLA, A. B. PINJARI, R. K. KROVIDI, R. BARU *et al.*, 2007 Biodegradation of methyl parathion and p-nitrophenol: evidence for the presence of a p-nitrophenol 2-hydroxylase in a Gram-negative *Serratia* sp. strain DS001. *Appl Microbiol Biotechnol* **73**: 1452-1462.
- PANDEETI, E. V., D. CHAKKA, J. P. PANDEY and D. SIDDAVATTAM, 2011 Indigenous organophosphate-degrading (*opd*) plasmid pCMS1 of *Brevundimonas diminuta* is self-transmissible and plays a key role in horizontal mobility of the *opd* gene. *Plasmid* **65**: 226-231.
- PANDEETI, E. V., T. LONGKUMER, D. CHAKKA, V. R. MUTHYALA, S. PARTHASARATHY *et al.*, 2012 Multiple mechanisms contribute to lateral transfer of an organophosphate degradation (*opd*) island in *Sphingobium fuliginis* ATCC 27551. *G3 (Bethesda)* **2**: 1541-1554.
- PAO, S. S., I. T. PAULSEN and M. H. SAIER, JR., 1998 Major facilitator superfamily. *Microbiol Mol Biol Rev* **62**: 1-34.
- PEIST, R., A. KOCH, P. BOLEK, S. SEWITZ, T. KOLBUS *et al.*, 1997 Characterization of the *aes* gene of *Escherichia coli* encoding an enzyme with esterase activity. *J Bacteriol* **179**: 7679-7686.
- PRIETO, M. A., B. GALAN, B. TORRES, A. FERRANDEZ, C. FERNANDEZ *et al.*, 2004 Aromatic metabolism versus carbon availability: the regulatory network that controls

- catabolism of less-preferred carbon sources in *Escherichia coli*. *FEMS Microbiol Rev* **28**: 503-518.
- QUANDT, J., and M. F. HYNES, 1993 Versatile suicide vectors which allow direct selection for gene replacement in gram-negative bacteria. *Gene* **127**: 15-21.
- RAGAN, M. A., and R. G. BEIKO, 2009 Lateral genetic transfer: open issues. *Philos Trans R Soc Lond B Biol Sci* **364**: 2241-2251.
- RAUSHEL, F. M., 2002 Bacterial detoxification of organophosphate nerve agents. *Curr Opin Microbiol* **5**: 288-295.
- RAUSHEL, F. M., and H. M. HOLDEN, 2000 Phosphotriesterase: an enzyme in search of its natural substrate. *Adv Enzymol Relat Areas Mol Biol* **74**: 51-93.
- RAVATN, R., A. J. ZEHNDER and J. R. VAN DER MEER, 1998 Low-frequency horizontal transfer of an element containing the chlorocatechol degradation genes from *Pseudomonas* sp. strain B13 to *Pseudomonas putida* F1 and to indigenous bacteria in laboratory-scale activated-sludge microcosms. *Appl Environ Microbiol* **64**: 2126-2132.
- RAVATN, R., S. STUDER, A. J. ZEHNDER and J. R. VAN DER MEER, 1998 Int-B13, an unusual site-specific recombinase of the bacteriophage P4 integrase family, is responsible for chromosomal insertion of the 105-kilobase *clc* element of *Pseudomonas* sp. Strain B13. *J Bacteriol* **180**: 5505-5514.
- RAVATN, R., S. STUDER, D. SPRINGAEL, A. J. ZEHNDER and J. R. VAN DER MEER, 1998 Chromosomal integration, tandem amplification, and deamplification in *Pseudomonas putida* F1 of a 105-kilobase genetic element containing the chlorocatechol degradative genes from *Pseudomonas* sp. Strain B13. *J Bacteriol* **180**: 4360-4369.
- RIDDLE, R. R., P. R. GIBBS, R. C. WILLSON and M. J. BENEDIK, 2003 Purification and properties of 2-hydroxy-6-oxo-6-(2'-aminophenyl)hexa-2,4-dienoic acid hydrolase involved in microbial degradation of carbazole. *Protein Expr Purif* **28**: 182-189.
- RITTER, L., K. SOLOMON, P. SIBLEY, K. HALL, P. KEEN *et al.*, 2002 Sources, pathways, and relative risks of contaminants in surface water and groundwater: a perspective prepared for the Walkerton inquiry. *J Toxicol Environ Health A* **65**: 1-142.
- ROODVELDT, C., and D. S. TAWFIK, 2005 Directed evolution of phosphotriesterase from *Pseudomonas diminuta* for heterologous expression in *Escherichia coli* results in stabilization of the metal-free state. *Protein Eng Des Sel* **18**: 51-58.
- ROULLAND-DUSSOIX, D., and H. W. BOYER, 1969 The *Escherichia coli* B restriction endonuclease. *Biochim Biophys Acta* **195**: 219-229.

- SAMBROOK, J., E.F. FRITSCH, AND T. MANIATIS (Editor), *Molecular cloning: a laboratory manual, 1st ed.* Cold Spring Harbor Laboratory Press, Cold Spring Harbor. Cold Spring Harbor Laboratory Press.
- SCHMIDT, H., and M. HENSEL, 2004 Pathogenicity islands in bacterial pathogenesis. *Clin Microbiol Rev* **17**: 14-56.
- SENTCHILO, V. S., A. N. PEREBITUK, A. J. ZEHNDER and J. R. VAN DER MEER, 2000 Molecular diversity of plasmids bearing genes that encode toluene and xylene metabolism in *Pseudomonas* strains isolated from different contaminated sites in Belarus. *Appl Environ Microbiol* **66**: 2842-2852.
- SENTCHILO, V., K. CZECHOWSKA, N. PRADERVAND, M. MINOIA, R. MIYAZAKI *et al.*, 2009 Intracellular excision and reintegration dynamics of the ICE_{clc} genomic island of *Pseudomonas knackmussii* sp. strain B13. *Mol Microbiol* **72**: 1293-1306.
- SENTCHILO, V., R. RAVATN, C. WERLEN, A. J. ZEHNDER and J. R. VAN DER MEER, 2003 Unusual integrase gene expression on the *clc* genomic island in *Pseudomonas* sp. strain B13. *J Bacteriol* **185**: 4530-4538.
- SERDAR, C. M., D. T. GIBSON, D. M. MUNNECKE and J. H. LANCASTER, 1982 Plasmid Involvement in Parathion Hydrolysis by *Pseudomonas diminuta*. *Appl Environ Microbiol* **44**: 246-249.
- SETHUNATHAN, N., and T. YOSHIDA, 1973 A Flavobacterium sp. that degrades diazinon and parathion. *Can J Microbiol* **19**: 873-875.
- SIDDAVATTAM, D., S. KHAJAMOHIDDIN, B. MANAVATHI, S. B. PAKALA and M. MERRICK, 2003 Transposon-like organization of the plasmid-borne organophosphate degradation (*opd*) gene cluster found in *Flavobacterium* sp. *Appl Environ Microbiol* **69**: 2533-2539.
- SILVIA RUSSI, R. B. A. M. C. (Editor), 2008 *Molecular Machinery for DNA Translocation in Bacterial Conjugation*, Germany.
- SIMON, R., PRIEFER AND PUHLER, 1983 A broad host range mobilization system for in vivo genetic engineering: transposon mutagenesis in gram negative bacteria. *Bio/Technology*: 784-791.
- SINGH, B. K., and A. WALKER, 2006 Microbial degradation of organophosphorus compounds. *FEMS Microbiol Rev* **30**: 428-471.
- SINGH, G., and D. KHURANA, 2009 Neurology of acute organophosphate poisoning. *Neurol India* **57**: 119-125.
- SINGH, S., and N. SHARMA, 2000 Neurological syndromes following organophosphate poisoning. *Neurol India* **48**: 308-313.

- SOMARA, S., and D. SIDDAVATTAM, 1995 Plasmid mediated organophosphate pesticide degradation by *Flavobacterium balustinum*. *Biochem Mol Biol Int* **36**: 627-631.
- SOMARA, S., B. MANAVATHI, C. C. TEBBE and D. SIDDAVATAM, 2002 Localisation of identical organophosphorus pesticide degrading (opd) genes on genetically dissimilar indigenous plasmids of soil bacteria: PCR amplification, cloning and sequencing of opd gene from *Flavobacterium balustinum*. *Indian J Exp Biol* **40**: 774-779.
- SPAIN, J. C., 1995 Biodegradation of nitroaromatic compounds. *Annu Rev Microbiol* **49**: 523-555.
- SPAINK H. P, R. J. H. O., CAREL A. WIJFFELMAN, ELLY PEES AND BEN J. J. LUGTENBERG, 1987 Promoters in the nodulation region of the *Rhizobium leguminosarum* sym plasmid pRL1J1. *Plant molecular biology*: 13.
- SPRINGAEL, D., A. RYNGAERT, C. MERLIN, A. TOUSSAINT and M. MERGEAY, 2001 Occurrence of Tn4371-related mobile elements and sequences in (chloro)biphenyl-degrading bacteria. *Appl Environ Microbiol* **67**: 42-50.
- SPRINGAEL, D., and E. M. TOP, 2004 Horizontal gene transfer and microbial adaptation to xenobiotics: new types of mobile genetic elements and lessons from ecological studies. *Trends in Microbiology* **12**: 53-58.
- SPRINGAEL, D., K. PEYS, A. RYNGAERT, S. VAN ROY, L. HOOYBERGHS *et al.*, 2002 Community shifts in a seeded 3-chlorobenzoate degrading membrane biofilm reactor: indications for involvement of in situ horizontal transfer of the *clc*-element from inoculum to contaminant bacteria. *Environ Microbiol* **4**: 70-80.
- SPRINGAEL, D., S. KREPS and M. MERGEAY, 1993 Identification of a catabolic transposon, Tn4371, carrying biphenyl and 4-chlorobiphenyl degradation genes in *Alcaligenes eutrophus* A5. *J Bacteriol* **175**: 1674-1681.
- STUDIER, F. W., and B. A. MOFFATT, 1986 Use of bacteriophage T7 RNA polymerase to direct selective high-level expression of cloned genes. *J Mol Biol* **189**: 113-130.
- SUEOKA, N., 1962 On the genetic basis of variation and heterogeneity of DNA base composition. *Proc Natl Acad Sci U S A* **48**: 582-592.
- TAN, H. M., 1999 Bacterial catabolic transposons. *Appl Microbiol Biotechnol* **51**: 1-12.
- TAN, H. M., and J. R. MASON, 1990 Cloning and expression of the plasmid-encoded benzene dioxygenase genes from *Pseudomonas putida* ML2. *FEMS Microbiol Lett* **60**: 259-264.
- TAN, H. M., and K. P. FONG, 1993 Molecular analysis of the plasmid-borne *bed* gene cluster from *Pseudomonas putida* ML2 and cloning of the *cis*-benzene dihydrodiol

- dehydrogenase gene. *Can J Microbiol* **39**: 357-362.
- TATUM, J. L. A. E. L., 1946 Gene recombination in *Escherichia coli*. *Nature* **158**.
- THOMAS, C. M., and K. M. NIELSEN, 2005 Mechanisms of, and barriers to, horizontal gene transfer between bacteria. *Nat Rev Microbiol* **3**: 711-721.
- TIAN, J., X. GUO, X. CHU, N. WU, J. GUO *et al.*, 2008 Predicting the protein family of methyl parathion hydrolase. *Int J Bioinform Res Appl* **4**: 201-210.
- TOP, E. M., and D. SPRINGAEL, 2003 The role of mobile genetic elements in bacterial adaptation to xenobiotic organic compounds. *Curr Opin Biotechnol* **14**: 262-269.
- TSUDA, M., and T. IINO, 1987 Genetic analysis of a transposon carrying toluene degrading genes on a TOL plasmid pWW0. *Mol Gen Genet* **210**: 270-276.
- VAN DER MEER, J. R., A. J. ZEHNDER and W. M. DE VOS, 1991 Identification of a novel composite transposable element, Tn5280, carrying chlorobenzene dioxygenase genes of *Pseudomonas* sp. strain P51. *J Bacteriol* **173**: 7077-7083.
- VAN DER MEER, J. R., A. R. VAN NEERVEN, E. J. DE VRIES, W. M. DE VOS and A. J. ZEHNDER, 1991 Cloning and characterization of plasmid-encoded genes for the degradation of 1,2-dichloro-, 1,4-dichloro-, and 1,2,4-trichlorobenzene of *Pseudomonas* sp. strain P51. *J Bacteriol* **173**: 6-15.
- VANHOOKE, J. L., M. M. BENNING, F. M. RAUSHEL and H. M. HOLDEN, 1996 Three-dimensional structure of the zinc-containing phosphotriesterase with the bound substrate analog diethyl 4-methylbenzylphosphonate. *Biochemistry* **35**: 6020-6025.
- WEI, M., J. J. ZHANG, H. LIU, S. J. WANG, H. FU *et al.*, 2009 A transposable class I composite transposon carrying mph (methyl parathion hydrolase) from *Pseudomonas* sp. strain WBC-3. *FEMS Microbiol Lett* **292**: 85-91.
- WELLS, T., JR., and A. J. RAGAUSKAS, 2012 Biotechnological opportunities with the beta-ketoadipate pathway. *Trends Biotechnol* **30**: 627-637.
- WERLEN, C., H. P. KOHLER and J. R. VAN DER MEER, 1996 The broad substrate chlorobenzene dioxygenase and cis-chlorobenzene dihydrodiol dehydrogenase of *Pseudomonas* sp. strain P51 are linked evolutionarily to the enzymes for benzene and toluene degradation. *J Biol Chem* **271**: 4009-4016.
- WILLIAMS, K. P., 2002 Integration sites for genetic elements in prokaryotic tRNA and tmRNA genes: sublocation preference of integrase subfamilies. *Nucleic Acids Res* **30**: 866-875.
- WILLIAMS, P. A., and J. R. SAYERS, 1994 The evolution of pathways for aromatic hydrocarbon oxidation in *Pseudomonas*. *Biodegradation* **5**: 195-217.

- WOZNIAK, R. A., and M. K. WALDOR, 2010 Integrative and conjugative elements: mosaic mobile genetic elements enabling dynamic lateral gene flow. *Nat Rev Microbiol* **8**: 552-563.
- WYNDHAM, R. C., A. E. CASHORE, C. H. NAKATSU and M. C. PEEL, 1994 Catabolic transposons. *Biodegradation* **5**: 323-342.
- YANISCH-PERRON, C., J. VIEIRA and J. MESSING, 1985 Improved M13 phage cloning vectors and host strains: nucleotide sequences of the M13mp18 and pUC19 vectors. *Gene* **33**: 103-119.
- ZHANG, R., Z. CUI, X. ZHANG, J. JIANG, J. D. GU *et al.*, 2006 Cloning of the organophosphorus pesticide hydrolase gene clusters of seven degradative bacteria isolated from a methyl parathion contaminated site and evidence of their horizontal gene transfer. *Biodegradation* **17**: 465-472.
- ZHANG, S., W. SUN, L. XU, X. ZHENG, X. CHU *et al.*, 2012 Identification of the para-nitrophenol catabolic pathway, and characterization of three enzymes involved in the hydroquinone pathway, in *Pseudomonas* sp. 1-7. *BMC Microbiol* **12**: 27.
- ZHONGLI, C., L. SHUNPENG and F. GUOPING, 2001 Isolation of methyl parathion-degrading strain M6 and cloning of the methyl parathion hydrolase gene. *Appl Environ Microbiol* **67**: 4922-4925.